A VIRAL VECTOR APPROACH TO FRAGILE X SYNDROME

By

ZANE ZEIER

A DISSERTATION PRESENTED TO THE GRADUATE SCHOOL
OF THE UNIVERSITY OF FLORIDA IN PARTIAL FULFILLMENT
OF THE REQUIREMENTS FOR THE DEGREE OF
DOCTOR OF PHILOSOPHY

UNIVERSITY OF FLORIDA

2007

ACKNOWLEDGMENTS

First, I must thank my family: Pamela, Sterling, Michelle, and Scott who have been unwavering in their love and support of me. Because of them, I have never felt alone, unloved, or misunderstood for a day of my life and I sincerely thank them for that gift. Second, I thank my colleagues and mentors at the University of Florida who have provided me with the immense honor of working and studying among them. In particular, I thank my mentor Dr. Davic C. Bloom for his kindness, humor, unpretentiousness, and intellectual guidance over the years. Also, I thank Dr. Henry Baker and Dr. Cecilia Lopez for providing invaluable expertise in microarray analysis; Dr. Tom Foster and Dr. Ashok Kumar for their considerable contribution of conducting electrophysiological experiments; and Dr. Feller for her cloning expertise. Also, I would like to thank my fellow graduate students in Dr. Bloom's laboratory for making it a fun and wonderfully inappropriate place of work. Finally, I would like to thank my close friends for their love, levity, and for making my life incredibly fun.

TABLE OF CONTENTS

LIST OF TABLES

LIST OF FIGURES

Abstract of Dissertation Presented to the Graduate School
of the University of Florida in Partial Fulfillment of the
Requirements for the Degree of Doctor of Philosophy

A VIRAL VECTOR APPROACH TO FRAGILE X SYNDROME

By

Zane Zeier

August 2007

Chair: David C. Bloom
Major: Medical Sciences--Neurosciences

Fragile X syndrome (FXS) is the most common inherited form of mental retardation. It is caused by a mutation that silences the *FMR1* gene which encodes the Fragile X mental retardation protein (FMRP). FMRP is an RNA binding protein that is expressed in neurons and is required for normal synaptic signaling. Since FXS results from an absence of FMRP, we wished to determine if FMRP replacement using viral vectors is therapeutic when delivered post-developmentally to specific regions of the brain. To this end, we constructed herpes simplex virus type 1 (HSV-1) and adeno-associated virus (AAV)-based viral vectors that express the major murine isoform of FMRP and tested their ability to rescue phenotypic deficits in an *Fmr1* knockout (KO) mouse model of FXS. Analyses of the expression characteristics of these two vectors revealed that while the AAV vector continued to express FMRP over the course of the study, expression of FMRP by the HSV-1 vector was negligible by three weeks. Microarray analyses of the host response to the HSV-1 vector suggested that limited expression of the HSV-1 transgene was due to transgene silencing rather than a host immune response. Based on these analyses, we chose to use the AAV vector to determine if FMRP replacement can rescue the *Fmr1* KO phenotype of enhanced long-term-depression (LTD). LTD is a form of synaptic plasticity that weakens the connectivity between neurons and may be linked to cognitive

impairments associated with FXS. Analyses of hippocampal function in *Fmr1* mice that received hippocampal injections of vector showed that the paired pulse low frequency stimulated LTD in the CA1 region of the hippocampus was restored to wild-type levels. Our results show that expression of the major isoform of FMRP alone is sufficient to rescue this phenotype. Our ability to reverse this phenotype suggests that post-developmental protein replacement may improve cognitive function in FXS and that other neurological deficits associated with FXS may be treatable by a gene therapy approach. Therefore, we assessed the feasibility of rescuing another KO phenotype which is susceptibility to audiogenic seizures (AGS). We found that *Fmr1* KO mice in the FVB/NJ (FVB) background strain demonstrate a robust AGS phenotype, providing a testable model for the *Fmr1* vector, whereas C57BL/6J (C57) *Fmr1* KO mice do not. We suggest that FMRP's role in neuronal plasticity dictates that post-developmental FMRP replacement can only rescue KO phenotypes resulting from a disruption of neuronal plasticity such as LTD, and not sensory signal transduction processes such as audition in the inferior colliculus.

CHAPTER 1
INTRODUCTION

The goal of gene therapy is to safely and effectively replace or manipulate gene expression *in vivo* for the purpose of treating human diseases. While the potential of such genetic-based treatments is undeniable, practical success has been meager. Currently, the most feasible way to alter gene expression *in vivo* is to utilize the natural ability of viruses to gain access to cells and deposit their genetic material. Strategies for viral vector gene therapy include replacement of mutant genes or the expression of growth factors or immune modulatory genes to reverse disease pathology. In addition, viral vectors can be used to express "knock-down" genes that encode ribozyme or siRNA molecules capable of reducing the expression of an endogenous gene (Kijima et al., 1995; Ryther et al., 2005). In the central nervous system (CNS) several unique challenges to successful gene transfer exist. First, the blood-brain-barrier (BBB) limits access of therapeutic agents to the tissue necessitating an invasive delivery strategy. Secondly, neurons are inefficiently transduced by some vectors as they are terminally differentiated.

Despite these obstacles, the CNS is amenable to vector therapy in that priming of the adaptive immune system is limited which reduces the risk of vector induced immunopathology. However, innate immunity still poses a formidable obstacle to efficient vector gene expression. Indeed, silencing of vectored genes is a major obstacle in gene therapy and, although the mechanism of silencing is not well understood, aspects of the immune response likely play a role. Well thought-out gene therapy strategies must consider the limitations viral vectors such as transient expression, limited payload capacity, limited dissemination, and safety. In addition, the basis of the disease itself must be considered. Ideally, one therapeutic gene is all that is required for treatment, and only in a particular region of tissue. Finally, testable paradigms in an animal model aid in the establishment of proof of principal and prompt clinical trials.

The overall goal of this dissertation project was to examine the therapeutic potential of gene replacement to rescue phenotypes in a mouse model of Fragile X syndrome (FXS). FXS is the most common form of inherited mental retardation, results from a single gene loss of function mutation, and has a well characterized animal model providing an appropriate test-bed for viral vector mediated gene replacement. A secondary goal of the project was to investigate the issue of gene silencing and toxicity associated with current HSV-1 vectors.

To achieve these goals, we constructed both HSV-1 and AAV vectors capable of restoring *Fmr1* gene expression, which is absent in FXS. Furthermore, we examined the host response to HSV-1 vectors in the CNS using microarray technology. Both herpes simplex virus type I (HSV-1) and adeno-associated virus (AAV) based vector systems are well established and have amenable properties for applications in the CNS, where FXS manifests.

The following chapters will discuss aspects of gene therapy in the CNS in more detail, focusing on HSV-1 and AAV based vector systems. Also, an overview of FXS will be given followed by how the vectors were constructed and what the host responses to HSV-1 vectors are. Finally, experiments that were conducted demonstrating phenotypic rescue in an animal model of FXS will be presented. The work represents a significant contribution to our understanding HSV-1 vectors, and provides needed information as to potential mechanisms that lead to transgene silencing. Furthermore, the data indicate that a gene therapy approach to FXS may be successful, at least with respect to some of the cognitive deficits associated with the disease.

CHAPTER 2
FRAGILE X SYNDROME

Introduction

Fragile X syndrome (FXS) affects nearly 1 in 4,500 males and 9,000 females, representing the most common form of inherited mental retardation (O'Donnell and Warren, 2002; Bagni and Greenough, 2005). Neuro-behavioral symptoms include mental retardation, decreased IQ, anxiety, hyperactivity, and autistic-like behaviors such as repetitive motor and speech patterns, impaired socialization, and gaze aversion. Physical characteristics include macroorchidism (enlarged testicles), large ears, a prominent jaw, and elongated face (Kaufmann and Reiss, 1999). The name of the syndrome stems from early diagnostic testing that revealed dislocated, "fragile" long arm of the X chromosome. Further investigations determined that the abnormality results from a CGG repeat expansion in a gene that was coined the Fragile X mental retardation (*FMR1*) gene (Verkerk et al., 1991). *FMR1* encodes the RNA binding protein Fragile X mental retardation protein (FMRP) absent in FXS due to methylation-dependent silencing of the CGG expansion and CpG islands of the promoter (Pieretti et al., 1991; Kaufmann and Reiss, 1999; O'Donnell and Warren, 2002; Bagni and Greenough, 2005). A *FMR1* knock-out (KO) mouse was created which shares biochemical, morphological, and behavioral similarities to the human condition providing a relevant model for testing potential treatment strategies (D-B-C, 1994). KO phenotypes include long, thin dendritic spines similar to those seen in FXS, reduced dendritic polyribosome aggregates, and reduced protein synthesis in synaptoneurosome preparations (a subcellular fraction of connected pre and post synaptic terminals) (Greenough et al., 2001).

The Mutation

Positional cloning of the *FMR1* gene led to the identification of a CGG repeat expansion in the 5' untranslated region (UTR) (Verkerk et al., 1991). While normal individuals typically have up to 50 repeats, unaffected premutation (PM) carriers can have up to 200, and full mutations (FM) can grow to 1000 copies. A FM facilitates methylation of the repeat, and CpG islands in the promoter. This results in transcriptional silencing of the *FMR1* gene and FXS (Pieretti et al., 1991).

Expansion

The mechanism of repeat expansion is the thought to involve formation of secondary structure in single strand flaps that are formed during lagging strand DNA synthesis of repetitive sequences. Such secondary structures inhibit 5' flap endonuclease (FEN-1), which mediates the removal of the displaced intermediates (flaps), and leads to expansion (Gordenin et al., 1997). Longer repeats, capable of forming more stable secondary structures are more likely to expand leading to more severe pathology, a process known as genetic anticipation (Henricksen et al., 2000). FXS bears some similarities to other triplet repeat disorders such as Huntington's disease and myotonic dystrophy in that expansion, somatic mosaicism, and genetic anticipation are observed (Kaufmann and Reiss, 1999). In the case of heterozygous females, mosaicism results from X chromosome inactivation and is the reason that females demonstrate a moderate FXS phenotype and reduced prevalence compared to men. Males only have one X chromosome and do not undergo X inactivation. Therefore, the existence of mosaic males suggests that post zygotic expansion of the premutation occurs in some cells but not others (Rousseau et al., 1991). Proponents of this model argue that the rarity of full mutations (FM) in male gametes suggests that expansion occurs following germ line differentiation. However, this model predicts that the degree of mosaicism should be proportional to the premutation size, a trend that is not observed.

An alternative model suggests that pre-zygotic expansion is followed by constriction of somatic FM alleles (Moutou et al., 1997). In contrast to the post zygotic expansion model, the pre-zygotic expansion and somatic constriction model accounts for the lack of FM containing sperm. The idea is that sperm are unable to accommodate such a large expansion and are therefore selected against (O'Donnell and Warren, 2002).

Silencing

Allelic expansion leads to methylation-dependent silencing of the repeat mutation and CpG islands that are located within the promoter (Pieretti et al., 1991). Such silencing occurs when cytosine residues are methylated then bound by methylated-DNA binding proteins such as Methyl-C binding protein (MeCP2) that recruit histone deacetylases (El-Osta, 2002). Lending support to this model of silencing, it was shown that acetylation of *FMR1* chromatin in Fragile X patients is decreased (Coffee et al., 1999). Addition of the cytidine analogue 5-aza-2'-deoxycytidine (5adC) (a methyl transferase inhibitor) restores the chromatin to a normal, acetylated state. Unfortunately, the compound globally perturbs methylation-mediated gene regulation and is therefore toxic *in vivo* preventing its utility as a therapeutic agent.

Diagnostic Testing

PCR and Southern blotting techniques provide powerful diagnostic tools for detecting the CGG repeat mutation. Southern blotting has been the most common test and provides information on the expansion size and methylation state of the mutation, when used in conjunction with the methylation sensitive restriction enzymes (Oostra and Willemsen, 2001). However, Southern blots require large amounts of DNA, and are laborious. PCR can also be used to detect the methylation of specific cytosines following treatment of the target DNA with sodium bisulfite which converts unmethylated cytosines to uracil. Sequence analysis of PCR product can then detect the specific nucleotide changes and reveal the methylation state of a

mutation (Frommer et al., 1992). One drawback of PCR is that accuracy is compromised due to an averaging affect in mosaic males and heterozygous females. Another type of diagnostic test, immunodetection of FMRP in hair roots, provides a non invasive method of diagnostic testing (Crawford et al., 2001).

The *FMR1* Gene

The mouse *FMR1* gene contains 17 exons, several of which are subject to alternative splicing (Figure 2-1) (Ashley et al., 1993; Huang et al., 1996). The gene encodes a 3.9 Kb mRNA and spans 40 Kb of the X chromosome. Exclusion of exon 12 is most common in testes and that of exon 14 leads to a frame shift conferring a unique carboxy terminal end. The largest cDNA clone is characterized by an ATTAAA poly (A) addition sequence followed by a poly (A) tract. Eight CGG repeats were present in the 5' terminus, and a putative translational initiation site (ATG codon) was identified 66 base pairs downstream. Without alternative splicing, a 614 amino acid (68,912 Da protein) is predicted (Ashley et al., 1993).

Sequence comparison of the mouse, dog, monkey, and human *FMR1* promoter reveal four conserved motifs. They include Pal and Nrf transcription factor binding sites, two GC boxes (CpG islands), an Ebox, and an initiation like element. The promoter has an initiation like element but lacks a traditional TATA box. Interaction with Pal, USF1, and USF2 in PC-12 cells up-regulates gene expression but only when the gene is unmethylated (Kumari and Usdin, 2001).

The Fragile X Mental Retardation Protein (FMRP)

Fragile X syndrome is caused by methylation dependent silencing of the *FMR1* gene, which encodes FMRP. The protein is marked by increased expression developmentally and in the adult brain and testes, corresponding to the primary FXS phenotypes of mental retardation and macroorchidism (Devys et al., 1993). Alternative splicing is possible at several splice donor and acceptor sites and can result in the absence of exons 12 and 14. Although several isoforms

are predicted only 11 have been confirmed by cloning and sequencing of cDNAs, and fewer by Western blot and immunodetection. Furthermore, one isoform seems to be the dominant form and accounts for about 40% of total FMRP in the CNS (Huang et al., 1996). To date it has not been determined if different isoforms have essential functions or if the dominant isoform is also functionally dominant.

Functional domains of FMRP include two coiled-coils (involved in protein-protein interactions) and three RNA binding motifs (two ribonucleoprotein K homology domains [KH] domains) and one RGG box [Arg Gly Gly triplet]) (Ashley et al., 1993; Kooy et al., 2000). The importance of FMRP's RNA binding capability is exemplified by an individual with severe FXS found to posses a point mutation (1304N) in the second KH domain (De Boulle et al., 1993). Some have suggested that the severity of this individual's phenotype is due to mutant FMRP sequestering mRNA thereby blocking its translation through divergent pathways (O'Donnell and Warren, 2002). FMRP also contains nuclear localizing (NLS) and nuclear export signals (NES), co-fractionates with rough endoplasmic reticulum, and associates with polyribosomes in dendritic spines (Feng et al., 1997a). FMRP co-immunoprecipitates with mRNP particles and its homologues (FXR1 and FXR2) in an mRNA dependent manner (Feng et al., 1997b; Tamanini et al., 1999). Taken together, the evidence suggests that FMRP shuttles mRNA from the nucleus to polyribosomes in the cell body and in dendritic spines as part of an mRNP particle (O'Donnell and Warren, 2002). Therefore, it is an important goal among researchers to elucidate the RNA ligands of FMRP and to identify messages that are differentially expressed in FXS. Each technique that has been used to identify the mRNA targets of FMRP has caveats and the disparity among their findings is significant.

Neuronal Implications

One of the first neuronal phenotypes to be identified was that individuals with FXS demonstrate long, thin dendritic spines (Rudelli et al., 1985), a phenotype also seen in the *Fmr1* knock-out (KO) mouse, an animal model (D-B-C, 1994; Comery et al., 1997; Nimchinsky et al., 2001; Irwin et al., 2002; Galvez and Greenough, 2005; Restivo et al., 2005; Grossman et al., 2006). Immature spines similar to those observed in FXS exist early in development and in animals reared in sensory deprivation (Greenough et al., 1973; Turner and Greenough, 1985). Therefore, the presence of similar spine structure in FXS dendrites may reflect aberrant pruning or maturation, a problem that would have profound effects on brain development and cognition. This has been demonstrated in an "experience-expected synaptogenesis" model of dendritic development in the barrel cortex of mouse somatosensory cortex where whisker sensory information is processed. In the cortex, dendrites initially extend both outwardly toward the septae, and inwardly, toward the hollow. The septae-oriented dendrites are then selectively pruned and hollow-oriented dendrites mature by becoming shorter and thicker in wild type but not KO mice (Greenough et al., 2001).

In addition to developmental pruning, FMRP is required for normal synaptic plasticity: a long-term change in synaptic strength after stimulation. Specifically, group 1 metabotropic glutamate receptor (mGluR) mediated, protein synthesis dependent, long-term depression (LTD) is enhanced in hippocampal preparations from KO mice (Huber et al., 2002; Nosyreva and Huber, 2006). Long-term potentiation (LTP) and LTD represent the most widely accepted models of learning and memory in which synapses are strengthened and weakened, respectively. Electrophysiologically, LTP and LTD can be induced with stimulation bursts of high or low frequency and are robust in the hippocampus, a structure known to be involved in learning and memory. Long-term maintenance of LTP and LTD requires protein synthesis, a portion of which

occurs near synapses (Steward and Schuman, 2001). Such local protein synthesis (LPS) is thought to confer synaptic specificity to plasticity occurring in dendritic spines. FMRP localizes to dendritic polyribosomes, levels of FMRP increase following synaptic stimulation, and FMRP is an mRNA binding protein suggesting a role in LPS (Weiler et al., 1997). Both protein synthesis dependent LTP and LTD have been linked to mGluR activation during synaptic activation. This corresponds with work demonstrating increased polyribosomal-associated mRNA protein synthesis in synaptoneurosomes following stimulation with a specific group 1 mGluR agonist (Weiler and Greenough, 1993). In addition, levels of FMRP are elevated following mGluR stimulation in synaptoneurosome preparations (Weiler and Greenough, 1999). The signaling cascade responsible for this increase involves G protein-linked activation of phospholipase C, which hydrolyzes membrane phosphatidyl inositol into inositol triphosphate (liberating Ca+ from stores in the endoplasmic reticulum) and diacyglycerol, which activates protein kinase C (Greenough et al., 2001).

These events may represent the molecular processes that underlie "experience-dependant synaptogenesis", which increases the number of synapses seen in the visual cortex of animals reared in enriched environments, and in the motor cortex of animals after learning (Greenough et al., 2001). They may also underlie the protein synthesis dependant modality of LTP and LTD.

One proposed model suggests that FMRP negatively regulates protein synthesis following mGluR activation, which is consistent with evidence that FMRP inhibits the translation of its mRNA ligands (Li et al., 2001; Huber et al., 2002). The model suggests that mGluR mediated protein synthesis dependent LTD is down regulated by FMRP, and involves the protein synthesis dependent, long-term internalization of AMPA receptors (α-amino-3-hydroxy-5-methylisoxazoleproprionic acid). AMPA receptors are ionotropic glutamate receptors that are

inserted into the postsynaptic density during LTP and removed during LTD. The model accounts for the observation that LTD is enhanced in *Fmr1* KO mice and has relevance to the morphological and behavioral phenotypes of FXS. The authors suggest that the long, thin spines seen in FXS are due to improper maturation of synapses rather than overactive sprouting (Huber et al., 2002). Therefore, reduced protein synthesis and polyribosomal aggregation in KO synaptoneurosomal preparations from KO mice may be secondary to enhanced LTD, which limits the metabolic might of synapses. Taken together, these findings suggest that FMRP plays a role in protein synthesis-mediated synaptic plasticity by transporting its mRNA payload to the dendritic spine and/or regulating their translation in response to synaptic activity.

The *FMR1* Knock Out Behavioral Phenotype

The degree of mouse *Fmr1* and human *FMR1* homology has been reported to be as high as 95% (Ashley et al., 1993). FMRP localization and expression patterns are also very similar (Hinds et al., 1993). In light of these findings, a relevant mouse model has been developed by inserting a neomycin cassette into exon 5 of *Fmr1* using homologous recombination in transgenic embryonic stem cells (D-B-C, 1994). The model has been essential in characterizing molecular aspects of the syndrome and provides an important tool for testing possible treatments.

Macroorchidism is readily observed in the KO mouse, but cognitive phenotypes are more modest. The Morris water maze, a well-known paradigm that requires an animal to find a submerged platform in a circular pool of water was one of the first tests of cognitive function in the KO mouse. The task is dependent upon hippocampal LTP where *FMR1* expression is high, and is a test of spatial learning (Morris, 1984; Morris et al., 1986). The KO mouse performes similar to WT animals in spatial learning as well as spatial memory as measured by escape latency and probe trails respectively. Furthermore, visible platform trials do not identify strategy, motivational, or motor deficits in the KO mouse. During reversal trials where the platform is

moved to a new location, a significant effect is seen suggesting a subtle impairment (D-B-C, 1994). However, this may also be an indication of hyperactivity, a trait found in human FXS.

Further behavioral abnormalities are found in exploratory behavior and motor activity, as measured by a light dark transition paradigm and cage activity respectively (D-B-C, 1994). In another study, an open field test confirmed an increase in exploratory behavior as measured by total distance traveled, but also demonstrated a significantly higher center to distance ratio, suggesting a reduced anxiety level (Peier et al., 2000). The study also examined YAC transgenic mice which over-express FMRP and demonstrated an opposite phenotype than the KO mouse. Transgenic mice were more likely to stay near the walls, and traveled less distance compared to WT mice. An abnormal response in auditory startle paradigms was reported although habituation and pre-pulse anxiety levels appeared normal (Nielsen et al., 2002). Others have demonstrated hyperactivity in pre-pulse experiments and susceptibility to auditory induced seizures (Chen and Toth, 2001). No abnormalities have been observed in conditioned fear or contextual fear paradigms, suggesting that FMRP is not involved in punishment-based learning. The *FMR1* KO mouse appears to demonstrate hyperactive behavior consistant with the prevalence of attention deficit and hyperactivity disorder (ADHD) in FXS. Furthermore, hyperactivity to sensory stimulation is observed in FXS, however open-field, and light to dark transition paradigms, which measure anxiety in isolation, may not relate to social anxiety seen in FXS (Peier et al., 2000). In summary, the KO mouse model has provided invaluable data as to the biochemical and physiological characterization of FXS, shares many similarities to the human disease, and demonstrates strong phenotypic characteristics amenable to testing prospective treatments.

Treatment

Since the CGG repeat expansion occurs in the 5' UTR region of the *FMR1* gene, a functional protein could exist if DNA methylation mediated silencing could be reversed. This has

been demonstrated *in vitro* using DNA methylation inhibitors to restore the *FMR1* locus to a transcriptionally active state. (Coffee et al., 1999). However, application of this strategy *in vivo* is not possible due to the toxicity of these agents. Furthermore, some premutation carriers develop Fragile X tremor/ataxia syndrome (FXTAS) which suggests that expanded mRNA is pathological and may not be translated properly even if such agents could reverse silencing *in vivo* (Feng et al., 1997b; Hagerman and Hagerman, 2002; Oostra and Willemsen, 2003).

Pharmaceutical strategies are being explored following the observation that mGluR dependent LTD is enhanced in the hippocampus of mice (Huber et al., 2002). Activation of mGluRs also leads to FMRP synthesis at dendritic polyribosomes (Weiler and Greenough, 1999), and AMPA receptor internalization (Snyder et al., 2001). Therefore, it has been proposed that FMRP acts as a negative feedback inhibitor of mGluR dependent protein synthesis (Huber et al., 2002). In light of these findings pharmacological agents such as ampakines (AMPA agonists) or 2-methyl-6- (phenylethynyl)-pyridine (MPEP), an mGluR5 agonist, may prove useful for the treatment of FXS.

The lack of alternative treatment methods for FXS has prompted interest in viral vector delivery of *FMR1* for restoration of FMRP expression. Advantages to this approach include the relatively short time required for the genesis of vectors and the ability to alter expression characteristics, as promoters of varying potency can be employed to regulate expression levels. Vectors also allow separation of developmental effects of FXS from the learning consequences. This is an important aspect because FXS is rarely diagnosed until early childhood necessitating a post-developmental treatment strategy. Furthermore, there is much to be learned about the biochemical properties of FMRP, and the ability to quickly manipulate the protein in an *in vivo* system will be useful.

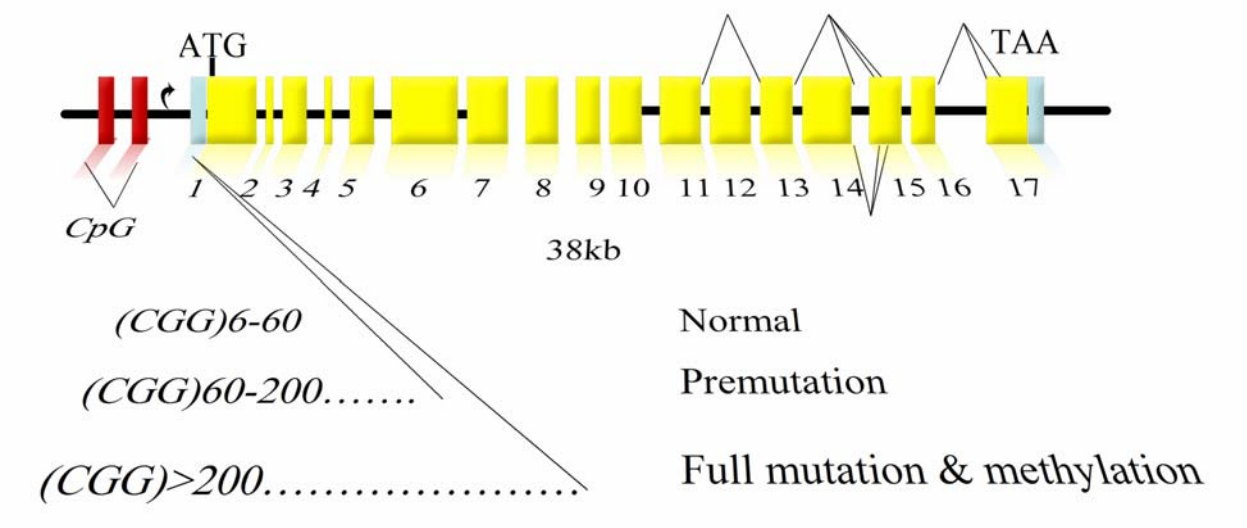

Figure 2-1. The *FMR1* gene contains 17 exons that are alternatively spliced to produce several isoforms. The CGG triplet repeat expansion occurs in the 5' UTR. An expansion beyond 200 repeats leads to methylation of CpG islands in the promoter which abrogates transcription.

CHAPTER 3
VIRAL VECTOR GENE THERAPY IN THE CENTRAL NERVOUS SYSTEM (CNS)

Application of Viral Vectors in the CNS

Viral vectors based on both HSV-1 and AAV have advantageous properties for use in gene transfer in the CNS (Burton et al., 2005; Mandel et al., 2006). Perhaps the most important factor is that both viruses can be attenuated offering a high degree of safety. Furthermore, production of both AAV and HSV-1 amplicon vectors has been improved so that contamination with helper virus is negligible. Another advantage is that neither vector integrates into the host genome, avoiding potentially harmful mutagenesis. In addition to their high degree of safety, both vectors are efficacious because they readily access neurons which are typically the target of therapy in the CNS. Furthermore, both vectors can be produced in very high titers although for HSV-1 there is a tradeoff between the degree of attenuation and production capacity.

Given their high degree of safety and efficacy HSV-1 and AAV vectors have been utilized for studying and treating neurological diseases. One strategy of treating neurodegenerative diseases such as Parkinson's disease (PD), Huntington's disease (HD), Alzheimer's disease (AD), and amyotrophic lateral sclerosis is to express neuroprotective molecules such as anti-apoptotic factors, growth factors, anti-oxidant, or immune modulatory molecules (Costantini et al., 2000; Mandel et al., 2006). More direct therapeutic strategies target specific biological pathways associated with the disease. For example, PD may be treatable by expression of molecules that directly enhance dopamine production and/or efficacy. Other examples include reduction of amyloid plaques in AD, knock-down of Huntington for treatment of HD, and restoration of enzymatic activity absent in lysosomal storage disorders (Mandel and Burger, 2004; Burger et al., 2005a).

Another slightly different application of viral vectors to treat human disease is their use as "oncolytic" or anti-cancer therapy. For treatment of deadly malignant glioblastoma multiforme, therapeutic strategies include the use of viral vectors to express anti-angiogenic, immune-modulatory, or pro-apoptotic molecules. Furthermore, several neuro-attenuated HSV-1 vectors that preferentially replicate in tumors have shown therapeutic promise. To improve efficacy, these vectors often incorporate suicide genes such as thymidine kinase that lead to lysis of tumor cells upon administration of ganciclovir (Marconi et al., 2000). These anti-tumor vector therapy strategies aim to improve successful treatment when surgical and irradiation therapies are insufficient.

Herpes Simplex Virus Type 1 Vectors

Relevant HSV-1 Biology and its Advantages as a Vector

Payload capacity

HSV-1 is an enveloped icosahedral virus with a large (150 Kb) double stranded DNA genome (Fields et al., 2001). Many of the genes encoded by the virus are non-essential to replication *in vitro*, and can therefore be replaced with potentially therapeutic transgenes (Burton et al., 2002). This confers a large payload capacity to HSV-1 vectors and represents an important advantage over other vector systems. Eventually, this property may allow for an entire gene locus to be incorporated into an HSV-1 vector rather than non-native cDNA transgenes.

Cellular entry

The HSV-1 virion gains access to a variety of host cells including terminally differentiated cells such as neurons. This is an attractive property for most applications of viral vectors and is due to the binding and entry of HSV-1 mediated by several glycoproteins that protrude from the viral envelope, and the ubiquity of their cellular receptors. Initial viral attachment of viral glycoprotein C (gC) and/or B (gB) to cellular heparin sulfate receptors is followed by the viral

glycoprotein D interacting with cellular herpes viral entry mediators (Hve) receptors (Fields et al., 2001). Subsequent fusion of the viral envelope and the cellular membrane completes the process of entry. The efficiency of this process and the involvement of common cellular receptors confer a potent transduction capacity to HSV-1 vectors.

Latency

A hallmark of the HSV-1 life cycle is the establishment of latency in sensory ganglion following lytic infection of the mucosal epithelium and transport of virus along afferent neuronal tracts (Wagner and Bloom, 1997; Sandri-Goldin, 2006). During latency the viral genome exists as a circular episome and all viral transcription is halted with the exception of the latency associated transcript (LAT) (Stevens et al., 1987). No protein is known to be encoded by LAT, but the transcript is spliced, producing two long lasting introns (Farrell et al., 1991; Thomas et al., 2002). HSV-1 latency and reactivation is not fully understood, nor is the mechanism by which LAT transcription is maintained during latency. However, epigenetic factors associated with histone modifications and boundary elements likely provide a permissive chromatin structure in the LAT region during latency and may determine the propensity for reactivation (Kubat et al., 2004; Amelio et al., 2006b; Amelio et al., 2006a).

Relevant to HSV-1 vectors is the fact that attenuation is easily achieved by strategically mutating essential viral genes which relegates the virus to a non-replicating state similar to latency. This is especially appropriate for applications in the nervous system where HSV-1 latency naturally occurs. The fact that HSV-1 possesses an inherent ability to avoid clearance, and maintain expression of a viral gene for the life of the host makes it extremely attractive as a gene therapy vector. Understanding the mechanisms behind these abilities is critical for improving safety and efficacy of HSV-1 vectors.

Attenuation of HSV-1 Viral Vectors

Amplicons

The most attenuated HSV-1 vectors contain only the desired transgenes and the minimum amount of HSV-1 sequence that is necessary for *in vitro* DNA replication and packaging. These "Amplicons" can be constructed by co-transfection with a bacterial artificial chromosome (BAC) that provides necessary viral genes in *trans* (Olschowka et al., 2003). In practice, high titer Amplicon preparations needed for vector applications have been difficult to obtain, as well as avoiding contamination by the helper BAC. Amplicons benefit from the high payload capacity of HSV-1 vectors, as well as their efficient transduction properties, but removal of some viral proteins such as ICP0 and ICP47 may reduce their efficacy (Samaniego et al., 1998; Jackson and DeLuca, 2003). Furthermore, any advantage of mimicking the long-term latent HSV-1 expression of the LAT may be lost since little HSV-1 sequence remains. Furthermore, prokaryotic DNA in the Amplicon genome may actually be more immunogenic than HSV-1 DNA itself.

Another method of attenuating HSV-1 is to abrogate the expression of viral genes that are necessary for replication while maintaining most of the viral genome (Wolfe et al., 1999; Burton et al., 2002). These recombinants can be rendered replication incompetent by disrupting essential viral genes, or replication conditional by mutating accessory genes such as γ34.5 (Chou et al., 1990). Mutants of γ34.5 replicate in dividing cells, but are severely restricted in non-dividing neurons, a property which makes them a candidate anti-tumor agent in the CNS (Markovitz et al., 1997; Burton et al., 2005).

Infected cell protein 4 mutants

Non-replicating HSV-1 recombinants are constructed by mutagenesis of one or more immediate early (IE) genes (Lilley et al., 2001). The IE genes ICP4 and ICP27 are essential for

replication; therefore, mutation of either one of these genes prevents HSV-1 from entering the lytic infection cycle. ICP4 is the key viral transactivator that ushers in early and late viral gene expression (Fields et al., 2001). Therefore, ICP4 mutants are non-replicating due to the lack of progression from immediate early viral gene expression, to early and late phases of infection. One aspect of ICP4 mutant biology is that other IE genes demonstrate a small degree of expression. For many years it was suggested that these mutants are toxic to cells due to the various IE gene functions. However, many of these studies were carried out *in vitro* under extremely high multiplicities of infection, and may not translate to the *in vivo* condition (Johnson et al., 1992; Johnson et al., 1994). Determining the toxicity of ICP4 mutant vectors *in vivo* is of critical importance for the assessment of their safety and efficacy. Chapter 5 of this document describes in detail the host response to an ICP4 mutant in the CNS and discusses the repercussions of IE gene expression *in vivo*.

Multiple IE gene mutants

Recombinant HSV-1 vectors with multiple IE gene deletions have been created in order to reduce the potential for IE induced toxicity (Lilley et al., 2001). However, these mutants are difficult to obtain in high titers because IE genes are toxic to complementary cell lines that provide them in *trans*. Furthermore, the vectors are typically less efficacious than ICP4 mutants, presumably due to the lack of ICP0. ICPO is a promiscuous transactivator that enhances transgene expression possibly by dictating how the viral genome is maintained (Jackson and DeLuca, 2003), or by limiting the interferon response to vectors (Eidson et al., 2002). In addition, some IE genes such as ICP47 which inhibits MHC I antigen presentation may be advantageous. Therefore, the most sophisticated HSV-1 recombinant vectors have multiple IE gene mutations but maintain ICP0 and ICP47 expression (Burton et al., 2005). Maximizing

attenuation to improve vector safety is desirable, but whether or not attenuation and efficacy are correlated is a matter of contention.

Transgene Expression Strategies

Stable expression of transgenes from replication incompetent HSV-1 vectors in the CNS has been very difficult to achieve. Almost every promoter that has been employed, including the LAT promoter itself, is silenced after only a few weeks (Scarpini et al., 2001; Burton et al., 2002). However, some success has been achieved by combining a strong viral core promoter and enhancer, namely, the Moloney murine leukemia long terminal repeat promoter (LTR) with the LAT promoter in order to mimic the sustained LAT expression that is seen from the native latent HSV-1 genome (Dobson et al., 1990; Lokensgard et al., 1994; Bloom et al., 1995; Tabbaa et al., 2005). Subsequently, an enhancer element dubbed the LTE that exists downstream of the transcriptional start site of LAT was shown to improve LAT promoter expression during latency (Lokensgard et al., 1997). Furthermore, this LTE, which may also contain a promoter element itself is capable of biologically active expression for 6 months in an animal model of Parkinson's disease (Puskovic et al., 2004).

Transgene Silencing

Many factors could contribute to the transgene silencing which occurs in almost every viral vector system. Strong hybrid promoters have helped overpower silencing but do not address the root of the problem. In the context of HSV-1 as discussed above, LAT promoter elements can improve expression, but ultimately they too are silenced. Perhaps the presence of viral double stranded RNA, methylated DNA, or repeat sequences in viral DNA induces a cellular defense response that precludes extended vector transcription. The complement arm of the immune system can certainly recognize foreign microbes, including HSV-1, and limit the efficacy of vector expression. Or perhaps expression of viral proteins or the transgene itself induces antigen

presentation leading to immune mediated transcriptional silencing. In the context of HSV-1, using LAT promoter elements and maintaining ICP0 expression improves transgene expression, but silencing could result from any number of host defense immune responses, or epigenetic silencing that may or may not be linked to immunity. Perhaps IE gene toxicity reduces cell viability, or marks it for immune mediated destruction or silencing. What is evident is that while vector genomes are maintained for essential the life of the host, robust transgene expression is transient (Bloom et al., 1994). This suggests that the lack of long-term expression by HSV-1 vectors is not due to immune elimination of transduced cells, but instead silencing of transgene expression from the latent vector episomes.

Adeno-Associated Viral Vectors

Relevant AAV Biology

Adeno-associated virus (AAV) is a naked, icosahedral virus able to infect a range of cell types, including terminally differentiated neurons (Berns and Giraud, 1996). Cellular attachment is mediated primarily by heparin sulfate proteoglycan receptors. The viral genome is 4.7 Kb, composed of single stranded DNA, and contains two open reading frames (rep and cap) which are flanked by inverted terminal repeats (ITRs). Rep encodes non-structural regulatory proteins (Rep 78/68 and Rep 52/40), and cap encodes three structural capsid proteins (VP 1-3). The ITR sequences are essential for replication and integration into the host genome. Approximately 90% of the adult human population is seropositive for AAV with no known associated pathology. Although AAV is not a defective virus, it requires helper functions provided by co-infection with adenovirus (Ad) or HSV-1 for replication. In the absence of helper functions, the AAV genome is inserted site specifically into chromosome 19 where it remains quiescent.

Adeno-Associated Viral Vectors

To construct AAV vectors, only the ITR and adjacent 45 base pairs are required for replication and production (Samulski et al., 1987). The deleted viral sequences can be replaced with desirable therapeutic gene cassettes, although only about 4.7 Kb of DNA (roughly the same size as the native genome) can be packaged into the small virion, limiting the utility of AAV vectors in some applications (Dong et al., 1996). AAV vectors lacking rep functions do not integrate into the host genome and are instead maintained as episomes, which is a desirable property for most gene therapy applications. Transduction efficiency and host cell specificity of AAV vectors can vary depending on the serotype from which the cap proteins are derived. Pseudo typed vectors with ITR sequence from serotype 2 packaged into serotype 5 capsids efficiently and preferentially transduce hippocampal CA1 and CA3 pyramidal neurons although serotype 2 capsids have been commonly used in the CNS (Burger et al., 2004). Current AAV vectors are not capable of utilizing endogenous promoters due to a shutdown mechanism that is not fully understood, although in some cases DNA methylation is thought to be responsible (Lo et al., 1999). Instead, to achieve long-term expression, artificial promoters have been engineered to overcome this silencing. Several promoters have been constructed that are capable of long-term transgene expression (Burger et al., 2005a; Mandel et al., 2006). One example is the chicken β-actin core promoter with elements from the Cytomegalovirus immediate-early enhancer (Doll et al., 1996; Xu et al., 2001). Vector re-administration can increase expression duration but is inherently hazardous and can induce vector neutralizing immune responses (Peden et al., 2004). In addition to promoters, other elements such as splice donor/acceptor sites and post-transcriptional regulatory elements can increase expression efficiencies (Xu et al., 2001). High titer recombinant vectors ($1 \times 10^{12\text{-}13}$ genomes/mL) can be purified using packaging/helper plasmids in combination with complementing cell lines that eliminates the risk

of contamination by helper virus (Grimm et al., 1998; Zolotukhin et al., 1999; Hauswirth et al., 2000; Zolotukhin et al., 2002). Perhaps the greatest asset of AAV vectors is the high degree of safety. This is because the virus is naturally non-pathogenic, all viral genes can be removed, little immune induction occurs, and vector preparations are essentially free of helper virus contamination

CHAPTER 4
CONSTRUCTION OF VIRAL VECTORS THAT EXPRESS THE FRAGILE X MENTAL RETARDATION PROTEIN

Abstract

Fragile X syndrome (FXS) is the most common inherited form of mental retardation. It is caused by the silencing of the *FMR1* gene encoding the Fragile X mental retardation protein (FMRP). To determine the ability of gene therapy vectors to rescue phenotypes of the *Fmr1* knockout (KO) mouse, we have constructed two different non-replicating viral vector systems, one based on Herpes simplex virus type 1 (HSV-1) and the other on Adeno-associated virus (AAV). The HSV-1 vector backbone used was ICP4(-) and the AAV vector backbone was gutted, containing only the AAV serotype 2 terminal repeats. The AAV-*Fmr1* vector was packaged in a type 5 virion to give broad transduction efficiency in CNS neurons (Burger et al., 2004). Both HSV-1 and AAV vectors contained the cDNA for the major murine CNS isoform of *Fmr1*. Identification of transduced cells is made possible utilizing the reporter genes *lacZ* (HSV-1 vectors) or green fluorescent protein (GFP) (rAAV vectors), as well as by immunohistochemical detection of vector-expressed FMRP. Expression of FMRP by both of these vectors was assessed in the CNS of the *Fmr1* KO mouse, the primary model for FXS following stereotaxic inoculation. These vectors provide useful tools for the study of FXS and will provide essential information for the potential use of viral gene therapy in FXS. This chapter will describe the general principals of vector construction and the strategies for construction and characterizing the *Fmr1* vectors used in subsequent chapters of this dissertation. For clarity, detailed protocols are not provided in this chapter, but instead are included in Appendices A (HSV-1) and B (AAV).

Herpes Simplex Virus Type 1 Vectors

Construction of Recombinant HSV-1 Vectors

The most straight forward way of creating a non-replicating HSV-1 vector is by co-transfection of HSV-1 genomic DNA and a recombination plasmid that contains homologous sequence to ICP4 that abrogates the essential IE gene upon recombination with the HSV-1 genomic DNA in an ICP4-complementing cell line (Bloom and Jarman, 1998). Multiple IE gene mutants can also be constructed to reduce cellular toxicity (Lilley et al., 2001).

Since the entire sequence of HSV-1 is known, a recombination plasmid can be easily cloned that contains a reporter gene cassette flanked by HSV-1 recombination arms that facilitate homologous recombination between the plasmid and the corresponding viral sequence (the ICP4 gene). The result is insertion of the reporter cassette and disruption of the viral ICP4 gene, precluding replication.

The transfection method most often employed for the construction of HSV-1 vectors is the calcium phosphate ($CaPO_4$) DNA precipitation and hypotonic shock method. Since HSV-1 DNA is infectious, virus will be produced following successful transfection of the genome and in the presence of a recombination plasmid DNA (10 fold molar excess) a subset of the progeny will be recombinant ICP4 deleted mutants.

Once viral plaques have formed on the cellular monolayers due to productive viral infection, the cell lysate is obtained and used to infect confluent 60mm dishes, which are over laid with agarose. The resulting plaques are picked, and amplified in confluent 96 well plates to increase the amount of viral DNA. Next, the material from infected 96 well plates is applied to DNA binding membranes (dot-blotted) and a radioactive isotope labeled DNA probe specific for a portion of the reporter gene is used to identify recombinants. Once a recombinant is identified it is purified by several rounds of plaque purification.

One advantage of HSV-1 recombinant vectors that have a minimum number of IE genes deleted is that very high titer preparations can be obtained by simple centrifugation of infected cell lysates, which can be further purified using iodixanol gradient centrifugation. Southern blot analysis is a common method of determining that the reporter gene has been inserted into the correct viral location and that it is of expected size. ICP4 mutants can also be characterized in vitro by titration on permissive and non-permissive cell lines. Viral neurovirulence can be examined following stereotactic injection into the CNS of mice or rats to ensure the virus is replication incompetent. Detection of the transgene expression and assay for its functionality in the CNS is the ultimate test for vector function (see appendix A for protocols).

In the present work, two HSV-1 vectors were utilized. The ICP4 minus 8117/43 control vector (Dobson et al., 1990) and the F81 vector. The later contains cDNA encoding the major murine isoform of FMRP, driven by a LAT/LTR promoter inserted into the intergenic UL 43/44 region of 8117/43. Both vectors contain a *lacZ* reporter gene (Figure 4-1).

Characterization of the HSV-1 Vectors

Previously, it has been demonstrated that ICP4 defective, non-replication competent HSV-1 vectors efficiently transduce neurons in the hippocampus (HC) as well as other regions of the CNS (Bloom and Jarman, 1998; Tabbaa et al., 2005). However, expression characteristics had not been examined in the inferior colliculus (IC), an important structure in the propagation of audiogenic seizures which is a major behavioral phenotype of *Fmr1* KO mice. Therefore, we confirmed efficient expression of the reporter gene *lacZ* following sterotactic delivery of 8117/43 into the HC and IC (Figure 4-2).

The ability of the F81 vector to express *Fmr1* RNA in the IC was analyzed by real-time reverse-transcription PCR (RT-PCR). Relative quantities of *Fmr1* RNA one week, or three weeks post injection (PI) were compared to wild type (WT) and knockout (KO) levels.

Significantly higher expression levels were observed one week following injection of F81 but not at three weeks PI. Levels were much lower than WT at both time points (Figure 4-3). Conventional RT-PCR indicates that the F81 vector expresses *Fmr1* RNA at levels similar to wild type, although the assay is not as quantitative as real time RT-PCR (Figure 4-7). Expression of *Fmr1* RNA was not observed in tissue injected with the control vector 8117/43, as expected.

Expression of FMRP was confirmed in the IC of KO mice by immunohistochemistry following injection of F81 (Figure 4-4). The staining was consistent with the RT-PCR analysis in that expression was apparent at early times (5 days) PI, but not at three weeks PI. Expression of FMRP at 5 days appeared to be more robust than RT-PCR indicated, although the levels were not quantitated.

Adeno-Associated Viral Vectors

Construction of AAV Viral Vectors

Protocols developed at the University of Florida Powell Gene Therapy core facility (see Appendix B) were used for purification of vectors. In addition, some of the vectors used in this study were constructed by the core facility itself. All AAV vectors contained ITRs from serotype 2 (ITR2) packaged in serotype 5 capsids. ITRs from serotype 2 are preferred because they are well characterized, and their integration properties have been established. In some cases the Rep proteins of one serotype do not bind ITRs from another serotype abrogating packaging; therefore, attention must be paid when such pseudo-typing is employed (Zolotukhin et al., 2002).

In recent years, the production of AAV vectors has been improved by transiently supplying the Ad helper functions from cell lines or plasmids which improves cell viability over the use of helper viruses. Also, it was discovered that decreasing the ratio of Rep 78/68 to 52/40 and capsid proteins can increase the amount of ssDNA genomes which improves the infectious unit to particle ratio (IU:P) (Li et al., 1997). Purification methods using heparin affinity resins (AAV2)

or Q Sepharose ion exchange (AAV5) have also contributed to improved IU:P ratios. In addition, iodixanol density gradients are an improvement over traditional CsCl gradients because they efficiently separate empty capsids from genome containing particles and such vector preparations are more suitable for introduction into tissue without the need to remove the iodixanol. Quantification of AAV2 can be done by an infectious center assay in a complementing cell line, but the low transduction of such cell lines by AAV5 prevents accurate quantification. Instead, a dot blot assay is used to determine the IU:P ratio of AAV5 vectors (Zolotukhin et al., 2002).

Two rAAV vectors containing the *Fmr1* gene were constructed: UFMTR and FAAV. Also, the UF11 vector was employed as a GFP-expressing control vector. UFMTR contains the CMV promoter and *Fmr1* gene, as well as a reporter GFP gene separated by an internal ribosomal entry site (IRES). FAAV contains the chicken-β-actin (CBA) promoter and the *Fmr1* gene which has been modified by insertion of a flag-tag for potential protein purification and detection (Figure 4-5).

Characterization of AAV Vectors

GFP expression in the hippocampus (HC) by UF11 was much more robust than by UFMTR (Figure 4-6). This is not surprising given the increased strength of the CBA promoter relative to the CMV promoter, and the smaller packaging size of UF11 which improves the IU:P ratio of vector preparations. Despite lower levels of expression, UFMTR expressed substantial *Fmr1* RNA as detected by conventional RT-PCR (Figure 4-7).

Following injection of FAAV into the IC of KO mice, real-time RT-PCR demonstrated a significant and robust increase (~12 fold relative to WT) in *Fmr1* RNA expression (Figure 4-8).

Robust staining for FMRP was observed in the IC (Figure 4-9) and HC (Figure 4-10) of KO mice injected with FAAV, supporting real-time RT-PCR data which indicates that injection

of this dose of FAAV vector into the IC of KO mice results in more *Fmr1* RNA than is expressed in the IC of WT mice.

Discussion

Vectors based on both HSV-1 and AAV systems containing the *Fmr1* gene have been constructed. Characterization of these vectors revealed that although the gene was expressed by all the vectors, the FAAV vector demonstrated the most robust FMRP expression in the CNS. Both *Fmr1* RNA and FMRP levels were much higher than WT levels in KO mice treated with the FAAV vector.

The F81 HSV-1 based vector demonstrated obvious FMRP staining at 5 days, but not at a 3 weeks PI; limiting the utility of F81 to applications where transient expression is desired. However, this vector may be useful if immediate expression is desired, as HSV-1 vectors require less time to express transgenes than their AAV counterparts. Transient expression characteristics of HSV-1 based vectors limits their utility in gene therapy applications.

The UFMTR vector expresses both *Fmr1* RNA and the reporter protein GFP. However, levels of GFP expression are substantially less that that of the UF11 vector which has a stronger promoter, does not rely on an IRES, and has a more efficiently packaged genome. Expression of FMRP by UFMTR was not quantitatively measured; however, experiments where reduced FMRP expression is desired could employ UFMTR.

Inclusion of a flag-tag epitope into the vectored FMRP allows for experiments aimed at determining FMRP's biochemical role in the CNS to be conducted. Furthermore, the vectored protein can be identified and isolated without the problem of antibody cross-reactivity of the FMRP homologues.

In summary, we have constructed two AAV vectors capable of expressing either low (UFMTR), or high (FAAV) levels of *Fmr1* in KO mice, as well as an HSV-1 vector capable of

moderate, but transient expression. The FAAV vector was tested for its ability to rescue phenotypes associated with the *Fmr1* KO mouse, an animal model of FXS (Chapter 6). Due to its transient level of *Fmr1* expression the HSV-1 vector (F81) was not used in the studies attempting to rescue the *Fmr1* KO mouse. However, the effects of the parent of this vector on the mouse CNS was examined by microarray analysis in an attempt to determine its level of safety and define mechanisms by which HSV-1 vectors are silenced (Chapter 5).

Materials and Methods

Herpes Simplex Virus Type 1 Vector Construction

8117/43

8117/43, a non-replicating, ICP4 deleted, HSV-1 recombinant vector was created previously (Dobson et al., 1990). Briefly, the pATD43 plasmid and KOS8117 viral DNA (Izumi et al., 1989) were co-transfected into ICP4 complementing E5 cells (DeLuca et al., 1985) and the recombinant virus was isolated and purified. pATD43 contains ICP4 homologous recombination arms and a Moloney murine leukemia virus long terminal repeat (MoMLV-LTR) promoter driving a β-galactosidase reporter gene (Price et al., 1987). Some contamination with replication competent virus occurs due to recombination with ICP4 gene within the E5 cell line, although at a very low rate (Dobson et al., 1990).

F81

An HSV-1 upstream recombination arm was generated by amplification of HSV-1 DNA (17+) (from base pairs 95,441 to 96,090) with DB112: (5'GAG CTC ATC ACC GCA GGC GAG TCT CTT3') and DB113: (5'GAG CTC GGT CTT CGG GAC TAA TGC CTT3'). The product was digested with SacI and inserted into the SacI restriction site of pBluescript to create pUP. An HSV-1 downstream recombination arm was generated using primers DB115-KpnI: (5'GGG GTA CCG GTT TTG TTT TGT GTG AC3') and DB120-KpnI: (5'GGG GTA CCG

GTG TGT GAT GAT TTC GC3') to amplify HSV-1 (17+ strain) genomic DNA sequence between base pairs 96,092 and 96,538. The PCR product was digested with KpnI, and cloned into KpnI digested pUP to create pIN994, which recombines with HSV-1 at the intergenic UL43/44 region, it was created by Robert Tran and Nicole Kubat.

To create the LAT/LTR promoter, a DraI-StyI fragment of the HSV-1 (17+) LAT promoter was taken from the pAAT2 plasmid (provided by Jack Stevens) and combine with a ScaI-BamHI fragment of the MoMuLV-LTR promoter obtained from the pBAG vector (Price et al., 1987) similar to previous studies (Lokensgard et al., 1994). For the construction of a FMRP expressing vector, the promoter was removed from pLAT/LTR GFP by EcoRI/SpeI digest and inserted into the SmaI restriction site of the MC2.17 plasmid (Ashley et al., 1993) containing the murine *Fmr1* cDNA encoding the major isoform of FMRP to create pLLF. Subsequently, the LAT/LTR FmrI cassette was removed from pLLF by BstXI/XhoI digestion and inserted into the EcoRV restriction site of pIN994 to create the final recombination plasmid pFIN. To create the F81 vector the pFIN plasmid was co-transfected with 8117/43 into E5 cells.

Recombinant AAV Vector Construction

UFMTR

The UFMTR rAAV plasmid was constructed by first removing the BclI/MfeI fragment (Neomycin resistance gene) from the pUF3 plasmid (Zolotukhin et al., 1996). Next, the HaeIII fragment (1984 base pairs) of *Fmr1* from the MC2.17 (Ashley et al., 1993) plasmid was inserted into the gutted gUF3 plasmid at the BspEI site to create pUFMTR. Cloning was conducted in Sure cells to maintain ITR sequences, which was confirmed by SmaI digestion prior to vector packaging. Essential features include a CMV promoter, *Fmr1* cDNA (not including 3' or 5' untranslated regions), splice donor/acceptor site, internal ribosomal entry site (IRES), a GFP

open reading frame, and SV40 and βGH poly A signals. Together 4884 base pairs are inserted into virions, which is near the maximum packaging size.

FAAV

The *Fmr1* cDNA for the major murine CNS isoform of FMRP was obtained from the MC2.17 plasmid, a gift from Dr. Nelson (Ashley et al., 1993). The cDNA included 123 bp upstream of the ATG start codon, all 17 exons, 2288 bp of 3' untranslated region (UTR) and a polyA signal (ATTA). To facilitate cloning, a multiple cloning site (MCS) was inserted upstream of the *Fmr1* translational start codon. Subsequently, a flag epitope tag was inserted between the 2nd and 3rd amino acid similar to (Brown et al., 1998), except that the NdeI restriction site located within the MCS was used instead of EcoNI. To improve translation of the *Fmr1* mRNA, a Kozak sequence (CCACCATG) was inserted at the start codon of *Fmr1*, as well as a HindIII site to aid in cloning.

Due to the limited packaging capacity of AAV vectors, only the coding sequence from HindIII to NsiI of the modified *Fmr1* gene was inserted into the pTR2 MCS AAV packaging plasmid, kindly provided by Dr. Nick Muzyczka. Essential features of this plasmid include AAV(2) terminal repeat elements required for packaging, the chicken β-actin core promoter with elements from the Cytomegalovirus immediate-early enhancer (Xu et al., 2001), and a polyA signal. Cloning of these plasmids was carried out in recombination-restricted Sure cells to prevent the loss of repeat ITR sequences. Before packaging a SmaI digest was performed to confirm ITR conservation.

Vector packaging was performed by the University of Florida Powell Gene therapy center. Briefly, the rAAV vector plasmid containing the *Fmr1* coding sequence (pTR2flag-*Fmr1*) was transfected into 293 cells (Graham et al., 1977) along with the pXYZ5 plasmid providing AAV (serotype 2) rep and AAV (serotype 5) cap, and essential Adenovirus helper functions (E4, VA,

E2a) in trans (Zolotukhin et al., 1999; Zolotukhin et al., 2002). Crude cell lysates were obtained from the vector core, and purified using an iodixanol gradient and Q sepharose column, then quantified by dot blot titration as described (Zolotukhin et al., 2002) (see appendix b for protocols).

UF11

The control AAV vector (UF11) containing a GFP reporter gene driven by the same promoter (CBA) as the FAAV vector was kindly provided by Dr. Muzyczka (Burger et al., 2004). The same packaging and purification methods were used for both vectors.

Stereotaxic Injection

KO mice were anesthetized, an incision made along the midline of the scalp, and holes burred in the skull, allowing for an injector to be inserted into the CNS using a stereotactic frame. 2 µL injections were delivered bilaterally into the IC (AP –5.02, L+/- 1.25, V 2mm, from Lambda) or hippocampus (-0.19mm AP, +/-0.15mm Lat, -0.17mm DV, from Bregma) via a glass micropipette fitted to a 10 µL Hamilton syringe at an infusion rate of 0.35µL/min.

RNA Isolation and Quantification

RNA was isolated from the CNS of mice by the guanidine isothiocyanate (GTC) extraction method and reverse transcribed. *Fmr1* cDNA was amplified by real-time PCR using TaqMan Universal PCR Master Mix, No AmpErase UNG (Applied Biosystems) and FAM-labeled TaqMan target-specific primer/probe (forward primer: 5'AGG GTG AGT TTT ATG TGA TAG AAT ATG CAG3', reverse primer: 5'TCG TAG ACG CTC AAT TGT GAC AA3', probe: 5'GTG ATG CTA CGT ATA ATG3'). PCR reactions were run in triplicate and analyzed using Applied Biosystems 7900HT Sequence Detection Systems. Cycle conditions used were as follows: 50°C for 2 min. (1 cycle), 95°C for 10 min. (1 cycle), 95°C for 15 sec., and 60°C for 1 min. (40 cycles). Threshold values used for PCR analysis were set within the linear range of PCR

target amplification. Relative values of *Fmr1* cDNA in each sample was determined by normalization with the cellular cDNA for adenene phosphoribosyltransferase (APRT). For conventional RT-PCR, *Fmr1* cDNA was amplified using the primers S1: (GTG GTT AGC TAA AGT GAG GAT GAT) and S2: (CAG GTT TGT TGG GAT TAA CAG ATC) (D-B-C, 1994). The cellular control APRT cDNA was amplified using the DB510: (GGC ATT AGT CCC GAA GAC C) and DB511: (GGC GAA ATC ATC ACA CAC C). HotStar Taq was used to amplify cDNA for 15 min. 95°C (1 cycle); 94°C 3 min., 65°C 3 min. 72°C 3 min. (1 cycle); 94°C 1min., 65°C 1min., 72°C 1min., (30 cycles).

Fragile X Mental Retardation Protein Immunohistochemistry

Following vector injection, animals were deeply anesthetized with xylene (8mg/kg) ketamine (24mg/kg) acepromazine (80mg/kg) and perfused with 4% paraformaldehyde. The brains were blocked and post-fixed overnight. The following day the tissue was transferred to 70% ethanol, paraffin embedded and sectioned at 5 microns. Sections were then deparafinized and hydrated. Epitope unmasking was performed for 25 minutes at 95˚C in citrate buffer (pH 6.0). Non-specific antibody binding was blocked with horse serum (Vector laboratories) diluted in Tris buffered saline with Tween 20 (TBS-T) (Dako). Endogenous avidin and biotin activity was blocked using the Vector labs kit. FMRP was detected with the IC3 antibody from Chemicon. A 1:500 dilution was applied for 1 hour in Zymed antibody diluent and washed for 5 minutes in TBS-T. Biotinylated anti-mouse secondary antibody was applied at 1:1500 in TBS-T with horse serum (15uL/mL) for 30 minutes. Vector labs Elite ABC detection kit in conjunction with the DAB substrate kit was used to visualize FMRP. Sections were counterstained with haematoxylin, dehydrated, and cover-slipped in Xylamount. Images of staining were captured on a Zeiss light microscope fitted with a digital camera

Green Fluorescent Protein Expression Analysis

For visualization of GFP reporter gene expression, animals were perfused with 4% paraformaldehyde, their brains removed, blocked, and post-fixed overnight. The tissue was then cryoprotected by placing them in 30% sucrose for 2 days, or until the tissue sank. The tissue was then flash frozen in embedding medium, and cryosectioned at 20 microns. Sections were mounted on glass slides, and cover-slipped using Vectamount (Vector Laboratories). The fluorescence was visualized and documented using a UV microscope fitted with a digital camera.

X-gal Staining

Utilizing the *lacZ* reporter genes in 8117/43 to visualize viral dissemination, X-gal staining was performed. Animals were deeply anesthetized with xylene (8mg/kg) ketamine (24mg/kg) acepromazine (80mg/kg) and perfused with 4% paraformaldehyde. Brains were blocked and placed in x-gal fixation solution (0.1% Sodium deoxycholate [NaDOC], 0.02% NP-40, 2% formaldehyde, 0.2% glutaraldehyde, 0.1 M HEPES [pH 7.4], 0.875% NaCl) for 1 hr at 4° C. Tissue samples were then washed 2x in PBS and 1x in PBS/DMSO (3%) and transferred to x-gal staining solution (0.15 M NaCl, 100mM HEPES [pH 7.4], 2mM MgCl2, 0.01% NaDOC, 0.02% NP-40, 5mM potassium ferricyanide, 5mM potassium ferrocyanide, 1mg/mL x-gal [from a 20mg x-gal/mL dimethylformamide stock]) overnight at 31°C. Samples were washed with PBS and images were captured using a dissection microscope fitted with a digital camera.

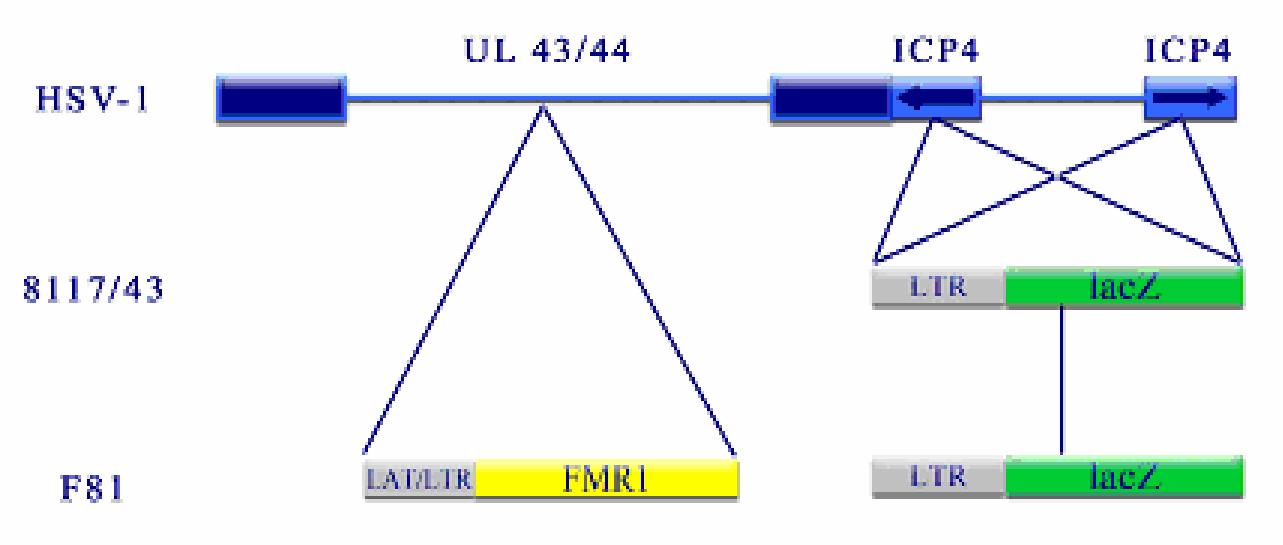

Figure 4-1. Herpes simplex virus type 1 vector constructs. Shown is the HSV-1 genome including the unique-long (UL) and unique-short regions flanked by long (dark blue) and short (light blue) repeats, respectively. The *E. coli lacZ* gene, driven by the MoMuLV LTR promoter/enhancer has been inserted into the ICP4 IE gene to construct the 8117/43 control vector (Dobson et al., 1990). The *Fmr1* gene, driven by LAT/LTR promoter was inserted into the UL43/UL44 region to construct the F81 vector. Both vectors were prepared as previously described (Bloom and Jarman, 1998) (see Appendix A for protocols). Titers were determined by plaque assay in an ICP4 complementing cell line, and determined to be 1.5 x 10^9 particle forming units (PFU)/mL and 1.25 x 10^9 PFU/mL for 8117/43 and F81 respectively.

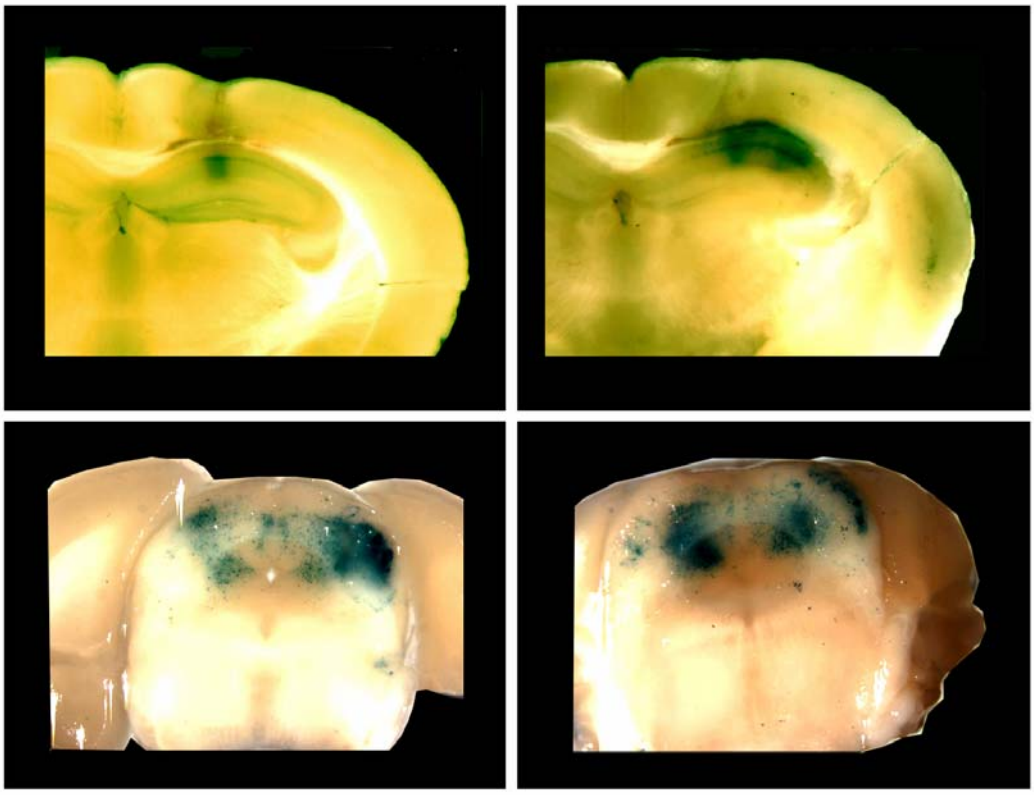

Figure 4-2. X-gal staining. To visualize vector transduction and expression of the *lacZ* reporter gene, mouse brains were X-gal stained 2 days (left panels) or 3 days (right panels) following stereotactical injection with $3x10^6$ PFU of the F81 vector into the hippocampus (top panels) or inferior colliculus (bottom panels).

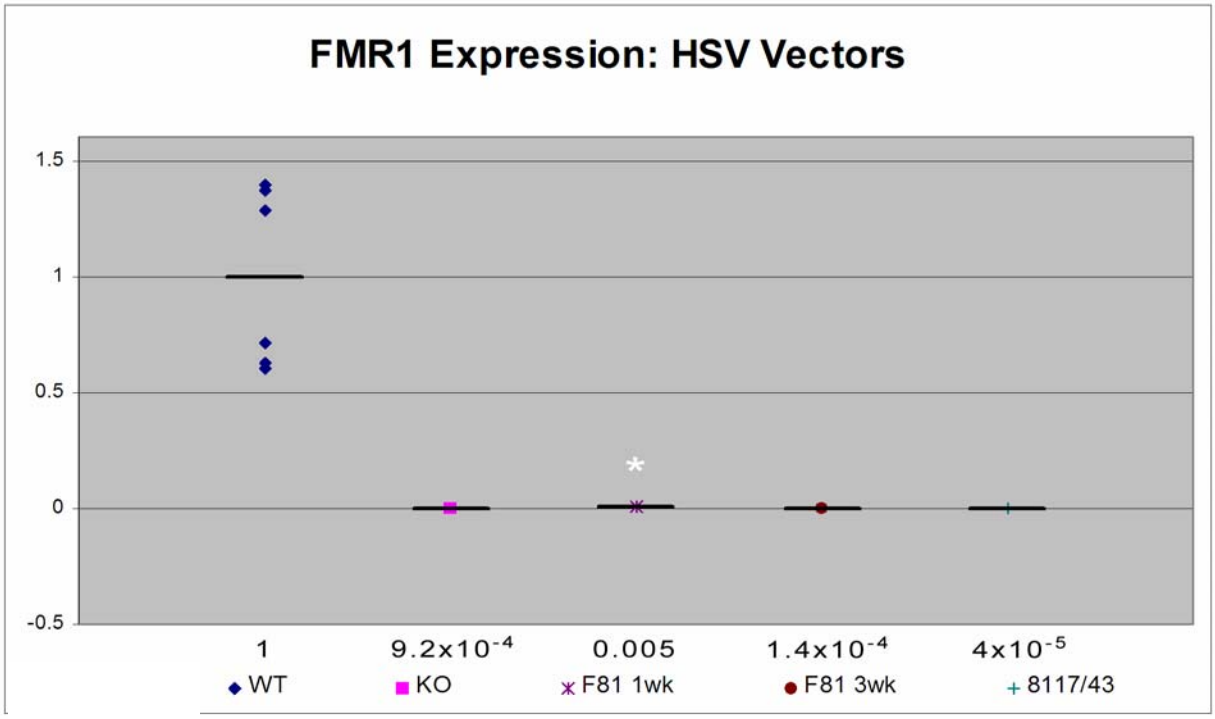

Figure 4-3. *Fmr1* RNA expression by the F81 vector. Real time RT-PCR analysis of tissue from mice injected with the F81 vector reveals significantly higher expression (*p< 0.05) of *Fmr1* RNA compared to uninjected mice one week post-injection, but not at three weeks or following injection of the control vector 8117/43.

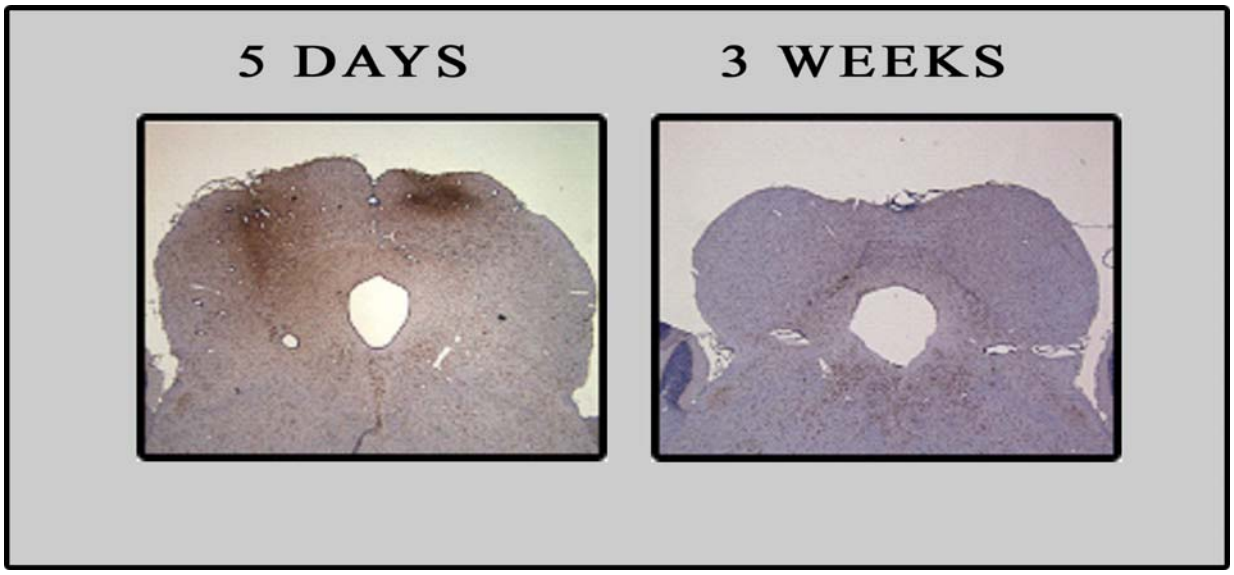

Figure 4-4. Immunohistochemical analysis of FMRP expression in the inferior colliculus of mice by the F81 vector. Expression of FMRP was observed in the inferior colliculus of KO mice injected with the F81 vector at 5 days PI, but not at 3 weeks.

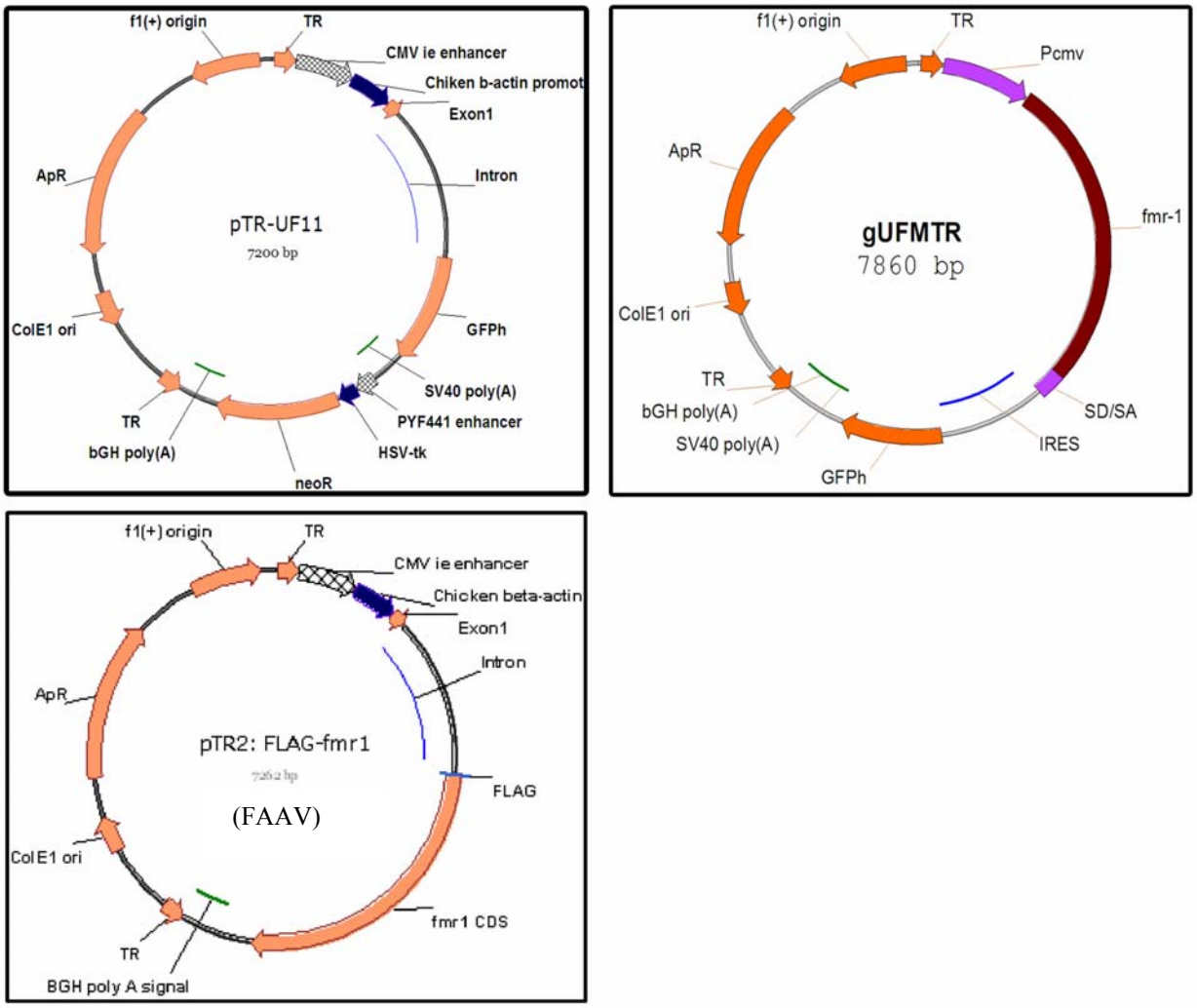

Figure 4-5. Recombinant AAV Plasmids. The UF11 control vector contains a GFP reporter gene driven by the CBA promoter. UFMTR contains a CMV promoter and the *Fmr1* gene, as well as a GFP reporter gene. The pTR2: FLAG-*Fmr1* plasmid, used to construct the FAAV vector contains the CBA promoter and a flag-tagged *Fmr1* gene.

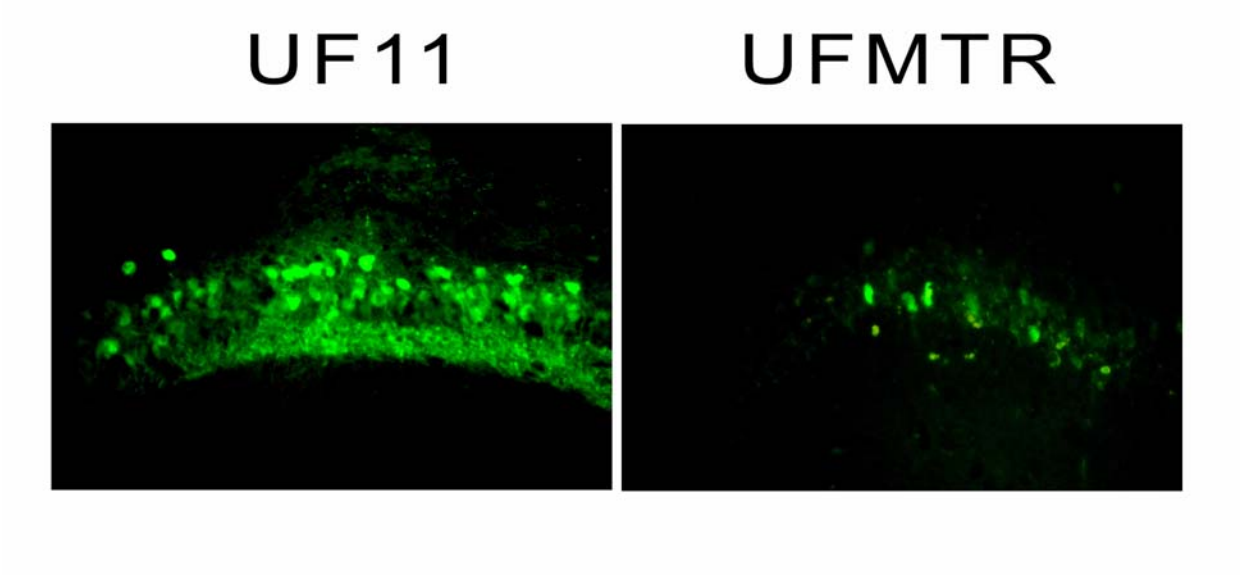

Figure 4-6. Detection of GFP expression by the AAV vectors by fluorescent microscopy. GFP reporter gene expression in the hippocampus following injection with UF11 or UFMTR demonstrates more robust expression by UF11.

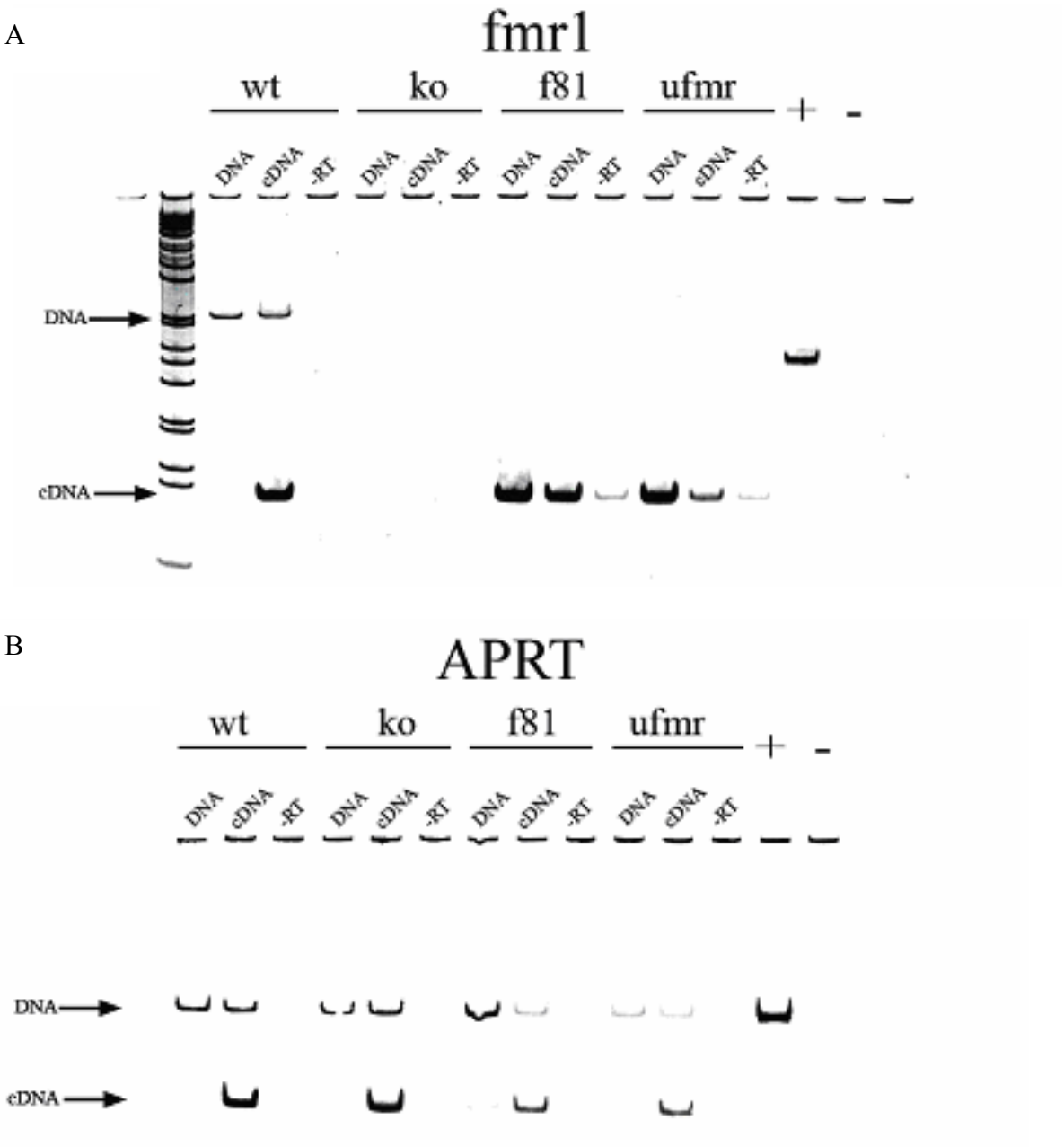

Figure 4-7. *Fmr1* RNA expression by UFMTR. A) Conventional RT-PCR demonstrates detectable expression of *Fmr1* RNA by UFMTR, but at levels lower than wild type or the F81 vector. B) Cellular APRT controls were used to normalize *Fmr1* expression between samples.

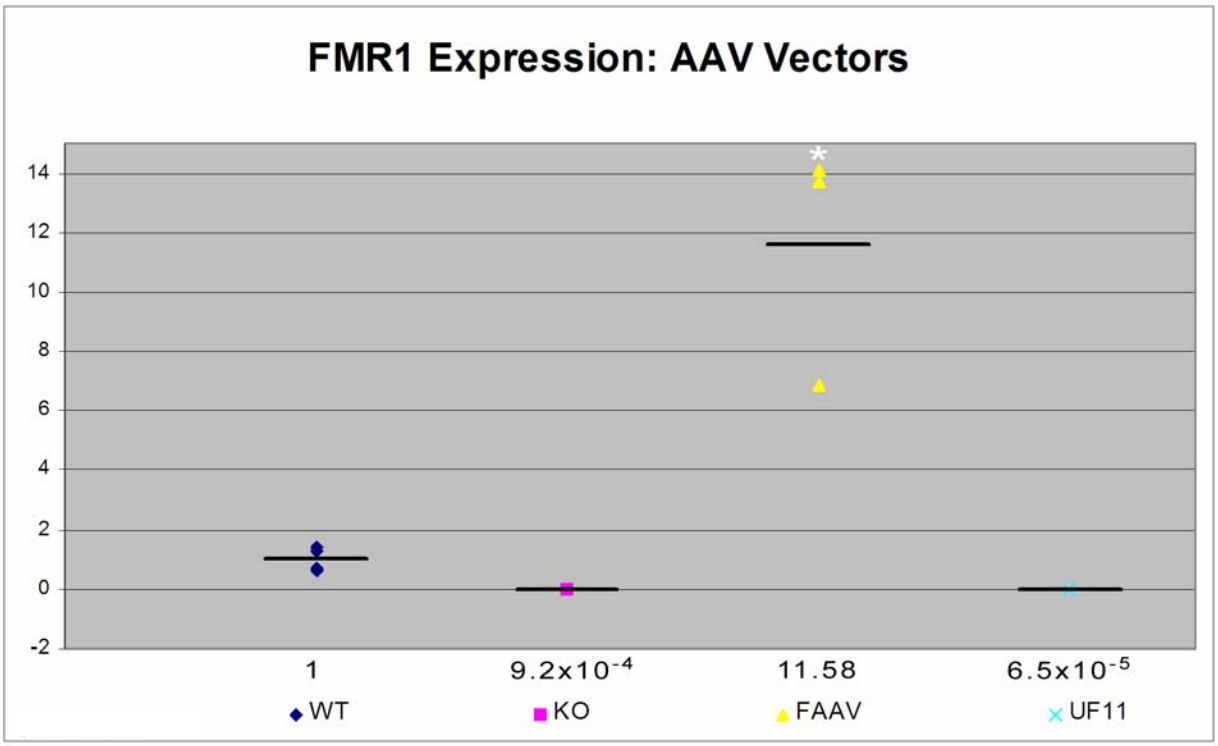

Figure 4-8. *Fmr1* RNA expression by FAAV. Levels of *Fmr1* RNA expression increased approximately 12 fold relative to WT following injection of the FAAV vector (*$p<0.05$). No significant change in expression was observed after injection of the control vector UF11, which demonstrated similar levels as observed in un-injected KO mice.

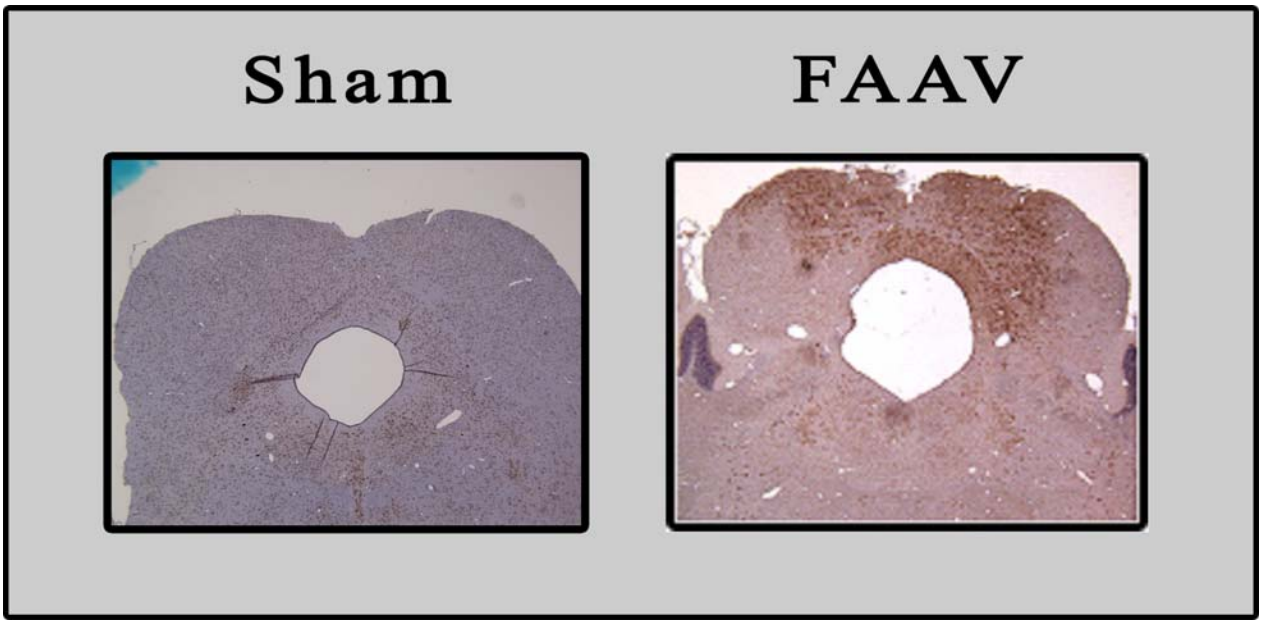

Figure 4-9. Immunohistochemical detection of FMRP expression by FAAV in the inferior colliculus. Injectors were stereotactically placed bilaterally into the IC of KO mice (sham). Some KO mice received an injection of the FAAV vector (FAAV). Animals were perfused 3 weeks later and the tissue prepared for immunohistochemical detection of FMRP using the IC3 monoclonal antibody and peroxidase/substrate visualization (brown). Sections are counterstained with Hematoxalin (blue) (see materials and methods).

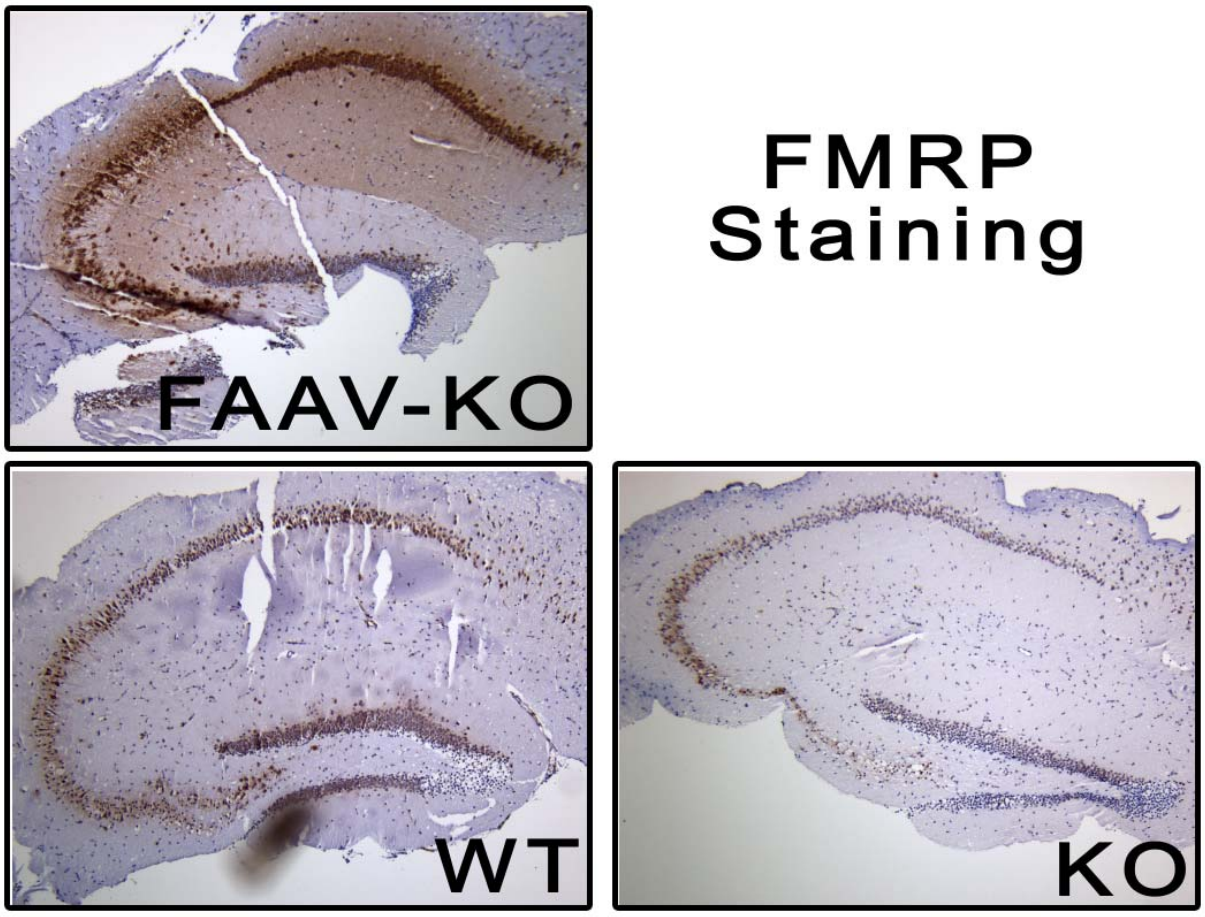

Figure 4-10. Immunohistochemical detection of FMRP expression by FAAV in the hippocampus. KO mice received 3 injections (1µL/injection) of the FAAV vector in each side of the hippocampus around the coordinates (-0.19mm AP, +/-0.15mm Lat, -0.17mm DV, from Bregma) to ensure complete transduction. Three weeks later, animals were sacrificed, and hippocampal slices were obtained for electrophysiological analysis. Subsequently, hippocampal slices were fixed, sectioned, and analyzed by immunohistochemistry for the expression of FMRP using the IC3 monoclonal antibody and peroxidase/substrate visualization (brown). Sections are counterstained with Hematoxalin (blue) (see materials and methods). Robust staining in FAAV injected KO mice is apparent, with lower levels seen in WT mice. Due to antibody cross-reactivity with FMRP homologs, some background staining is observed in KO mice.

CHAPTER 5
MICROARRAY ANALYSIS OF THE HOST RESPONSE TO REPLICATING AND NON-REPLICATING HSV-1 VECTORS IN THE MOUSE CNS

Abstract

A hallmark of the herpes simplex virus type one (HSV-1) life cycle is the establishment of a latent infection in sensory ganglia of the peripheral nervous system. Eliminating the essential viral immediate early gene ICP4 abrogates viral replication and relegates HSV-1 to latency. This ability to attenuate HSV-1, together with its high transduction efficiency in neurons, large payload capacity, and anti-tumor characteristics, make HSV-1 vectors particularly amenable to gene therapy applications within the CNS. However, HSV-1 based vectors demonstrate a limited duration of transgene expression which limist their utility. Furthermore, the degree of toxicity and immunogenicity associated with HSV-1 vectors, which could lead to transgene inactivation, is not well defined, nor is the host response to replication competent HSV-1 when delivered directly to the CNS. Therefore, we examined the host response to a non-replicating HSV-1 vector and replication competent HSV-1 using Affymetrix microarray analysis. In parallel, HSV-1 gene expression was tracked using HSV-specific oligonucleotide-based arrays in order to correlate viral gene expression with observed changes in host response. 1×10^5 pfu of either a replication-competent glycoprotein C (gC) minus recombinant of HSV-1 (HSVlacZgC) or a non-replicating ICP4 minus recombinant of HSV-1 (8117/43) were stereotactically delivered to the right hippocampal formation of 6 – 8 week old mice (N=9). At 2 and 3 days post-injection (PI), hippocampi were dissected, and RNA was isolated. For each group, three RNA samples pooled from 3 mice each were used for microarray analysis. 2,969 genes (15% of genes passing detection criteria) demonstrated a significant change in expression ($p<0.001$) in response to HSVlacZgC compared to a mock injection, whereas only 433 (2.2%) were identified in response to 8117/43. Ingenuity Pathway Analysis (IPA) revealed several major pathways induced by

replicating virus, including toll-like-receptor (TLR) signaling, death receptor signaling, NFκB induction, and antigen presentation. Both the gC-negative and ICP4-negative vectors induced robust antigen presentation but only mild interferon, chemokine and cytokine signaling responses. The ICP4-negative vector appeared to be restricted in several of the TLR-signaling pathways, indicating reduced stimulation of the innate immune response. These array analyses suggest that while the non-replicating vector induces detectable activation of immune response pathways, the number and magnitude of these induced responses are dramatically restricted compared to the replicating vector, and with the exception of antigen presentation, the non-replicating vector gene expression pattern resembles a mock infection.

Introduction

Herpes Simplex virus type 1 (HSV-1) is an enveloped icosahedral virus with a large (150 Kb) double stranded DNA genome. Normally, HSV-1 infects the oral mucosal epithelium and following primary infection, travels along sensory neurons to the trigeminal ganglion where it maintains a latent life cycle (Wagner and Bloom, 1997; Fields et al., 2001). During latency, only the non-protein encoding latency associated transcript (LAT) is produced from the otherwise inactive, nuclear, episomal viral genome. During reactivation from latency virions retrace their path to the mucosal epithelium and re-establish lytic replication. Since HSV-1 only reactivates in a sub-population of hosts it is apparent that individual host differences play a crucial role in determining its pathogenesis. In rare cases, the virus can induce lethal encephalitis; occurring more readily in immuno-compromised individuals which is an important factor for infants and in anti-tumor applications of HSV-1 vectors (Burton et al., 2002).

Elucidating the host factors that determine HSV-1 latency, reactivation, and ability to cause encephalitis is of significant clinical importance. However, HSV-1 has also been utilized for construction of recombinant viral vectors (Burton et al., 2002). The large payload capacity,

neural-transduction capability, and ease of construction make HSV-1 vectors amenable to applications within the central nervous system (CNS). Both non-replicating HSV-1 vectors and anti-tumor replication-conditional HSV-1 vectors have great potential as therapeutic agents, but concerns regarding their toxicity and efficacy exist. Therefore, it is of interest to characterize the host response to HSV-1 vectors in the CNS for prevention of disease and for improving vector technology.

In the CNS viral infections are unique because adaptive immunity is poorly induced. This is a result of the blood brain barrier (BBB), lack of classic lymph drainage, and lack of professional antigen presenting cells (Lowenstein, 2002). Also, HSV-1 has evolved several host-defense evasion mechanisms that conceal its presence from adaptive immunity. Therefore, the most critical aspect of warding off HSV-1 in the CNS is the innate immune response, and in particular, the interferon response (Mossman, 2005; Pasieka et al., 2006). Interferons (IFNs) are cell-signaling molecules that can limit viral infection by regulating gene expression and modulating the subsequent immune response to infection. *In vitro*, pre-treatment of cells with IFN precludes HSV-1 infection (Johnson et al., 1992), and although protective against typical HSV-1 infections this can be harmful in the CNS and may limit vector efficacy. Therefore, reducing IFN signaling and subsequent induction of innate immunity by attenuating HSV-1 vectors is essential to improving their efficacy.

Attenuation of HSV-1 is achieved by mutating viral immediate early (IE) genes, two of which are essential for viral replication: infected cell proteins (ICP) 4 and 27. ICP27 interferes with host mRNA splicing and transcription while activating IE genes, and may also help to prevent apoptosis (Spencer et al., 1997; Fields et al., 2001). ICP4 is a transactivator that initially upregulates IE gene expression as well as playing a critical role in activating early and late viral

gene expression. *In vitro*, ICP4-minus HSV-1 recombinants over-express the other IE genes which can be cytotoxic (DeLuca et al., 1985; Johnson et al., 1992; Johnson et al., 1994). Therefore, multiple IE gene deleted viruses have been constructed, however, these highly attenuated vectors often express transgenes less efficiently (Samaniego et al., 1998; Burton et al., 2005). In fact, maintaining ICP0 activity clearly improves transgene expression despite its cytotoxic properties (Eidson et al., 2002). When HSV-1 vectors are examined *in vivo* results are conflicting. Some suggest that significant host responses are mounted including inflammation and necrosis (Wood et al., 1994; Ho et al., 1995) yet others suggest minimal viral toxicity (Dobson et al., 1990; Bloom et al., 1994; Burton et al., 2002). In support of latter, it was shown that neurophysiology was not altered in response to an amplicon-based vector (Dumas et al., 1999; Bowers et al., 2003; Olschowka et al., 2003). These seemingly contradictory findings are difficult to reconcile due to the diversity of vectors and analysis methods employed.

Factors such as viral gene leakiness and transgene expression may contribute to vector immunogenicity, however, even the most attenuated HSV-1 vectors demonstrate limited transgene expression, indicating that innate immune induction may not necessarily be correlated with vector efficacy (Samaniego et al., 1998; Burton et al., 2002; Eidson et al., 2002; Kramer et al., 2003). The lack of understanding transgene silencing and if such silencing is exacerbated by vector immunogenicity represents a void in HSV-1 gene therapy technology. Furthermore, the toxicity of attenuated HSV-1 *in vivo* has not been well characterized, and is a point of contention.

The goal of the current study was to characterize the host response to a productive HSV-1 CNS infection *in vivo*, and to determine the degree of cytotoxicity and immunogenicity caused by an ICP4-mutant HSV-1 viral vector. Two HSV-1 viruses were utilized; a replication-competent virus (HSVlacZgC) containing a *lacZ* reporter gene inserted into the non-essential

viral glycoprotein C (gC) gene, and a non-replication-competent HSV-1 vector (8117/43) with *lacZ* inserted into the essential IE gene ICP4 (Dobson et al., 1990; Singh and Wagner, 1995). The host response to these viruses was analyzed by Affymetrix microarray technology in conjunction with IPA software which has become a powerful tool for simultaneous analysis of a broad range of cellular pathways providing a more comprehensive understanding of HSV-1 infection than previously possible (Figure 5-1). Furthermore, we employed an HSV specific oligonucleotide based spotted array to track viral gene expression allowing us to correlate viral gene expression with the corresponding Affymetrix analyzed host gene expression profile (Aguilar et al., 2005). To our knowledge this is the first *in vivo* analysis of lytic and non-productive HSV-1 infection following delivery directly to the CNS and coupled with our ability to correlate viral and host gene expression, represents the most sophisticated HSV-1 array study to date.

Following stereotaxic injection of HSVlacZgC into the CNS, we expected gene expression analysis to reveal a drastic induction of innate immunity and cell death pathways caused by productive infection despite viral host-defense evasion strategies. We surmised that *in vivo*, HSVlacZgC cannot completely block these host defense responses in light of cellular infiltration, incomplete transduction, and the unsynchronized nature of infection. Conversely, we expected only minimal induction by the ICP4 mutant 8117/43 despite the cytotoxicity and immunogenicity associated with IE gene expression. This was based on the fact that the amount of HSV-1 is not amplified in a non-productive infection, as well as evidence that ICP4 mutants limit the IFN response, perhaps due to ICP0 mediated inhibition of interferon stimulated gene (ISG) expression (Mossman et al., 2001; Eidson et al., 2002). Furthermore, non-replication competent mutants have a propensity to go latent, and compared to a productive infection,

immunogenicity is relatively weak and expected to be associated with limited infiltration of immunocytes.

Results

Viral Dissemination in the CNS

Both the HSVlacZgC and 8117/43 vectors contain *lacZ* reporter genes allowing for visualization of viral gene expression following x-gal staining. Following stereotactic inoculation into the hippocampus by the strategy outlined in Figure 5-1, 8117/43 expression was mostly limited to the immediate area around the injection site in the CA1 region of the hippocampus, with some expression occurring in cortical neurons (Figure 5-2). Given the efficiency of HSV-1 axonal transport, it is not surprising that attenuated virus was found at distal locations. However, 81117/43 showed only modest changes in the expression pattern between 2 and 3 day time points indicative of a non-replicating virus. Alternatively, replication competent HSVlacZgC demonstrated massive transduction and gene expression not limited to the injection site. Furthermore, one can clearly see viral dissemination to the contralateral hemisphere at 3 days post infection (Figure 5-2).

Viral Gene Expression

An oligonucleotide-based, HSV-specific, spotted array analysis of viral gene expression from tissue surrounding the HSVlacZgC injection site demonstrated typical viral gene expression of all classes at 3 days post infection (Stingley et al., 2000; Aguilar et al., 2005; Sandri-Goldin, 2006). Conversely, 8117/43 IE gene expression was limited to low levels of ICP47 and ICP22, and to a lesser extent ICP0 and ICP27 (Figure 5-3). While previous studies *in vitro*, suggest that ICP4 mutants overexpress other IE genes in the absence of ICP4, our *in vivo* analysis did not corroborate that finding (Johnson et al., 1992; Johnson et al., 1994). Overall, a comparison of the gene expression patterns of these two viruses in the hippocampus indicates that in contrast to the

expected abundant lytic gene expression pattern exhibited by the replication competent virus, the non-replicating vector displayed an extremely restricted pattern of expression except for the LAT. We next wished to determine the effect of these two dramatically distinct viruses on the host gene expression using a mouse microarray.

Host Gene Expression

To examine the immunogenicity and cytotoxicity of the non-replicating HSV-1 vector 8117/43, and to characterize the host response to productive HSV-1 infection in the CNS, we analyzed gene expression using a mouse-specific microarray. Gene expression alterations induced by these viruses were compared to alterations induced by a mock infection, and to one another. Biological functions and biochemical pathways mediated by the significantly altered genes were identified using BRB array tools and IPA.

Supervised Cluster Analysis

A BRB array tools class comparison analysis of mock, 8117/43, and HSVlacZgC injected arrays was performed. Significant genes ($p<0.001$) were used to perform a supervised cluster analysis in dChip (Figure 5-4). Arrays from the HSV-gC (HSVlacZgC) at 2 day and 3 day time points clustered tightly together whereas mock and HSV-4 (8117/43) clustered in a separate node indicating the two groups are more similar to one another, than either is to HSVlacZgC. Not surprisingly, these data indicate that the host response to an ICP4 minus HSV-1 vector is much more similar to mock injection than to a replication competent virus. Although the arrays did not strongly cluster based on time points, future analysis comparing the injected hemisphere to that of the contralateral hemisphere should demonstrate larger chronological effects.

Host response to mock injection

Class comparison analysis of arrays from mock-injected and uninjected samples at 2 and 3 day time points revealed few (6) significant genes and did not cluster together based on time points. Therefore, to improve statistical power, arrays from the two time points were combined. When the combine arrays from mock injected samples were compared to those from the un-injected ones, class comparison analysis revealed 405 significant genes at the $p<.001$ level and passed cross-validation in several tests. Molecular and biological gene ontology (GO) classification of the significant genes identified by BRB array tools are shown in tables 5-1 and 5-2 respectively.

Host response to 8117/43 injection

Similar to arrays from mock injected samples, few significant genes were identified when 2 and 3 day 8117/43 arrays were compared separately, therefore the time points were combined. Using BRB array tools, a class comparison analysis was performed between all 8117/43 and mock arrays revealing 268 significant genes at the $p<.001$ level. However, one array (081404A_81-2d-R) failed all cross-validation tests (Appendix Table C-1), and did not cluster well with either mock or 8117/43 arrays (Appendix Figure C-1). Furthermore, biological functions identified by IPA analysis without the outlier were consistent, therefore the array was removed (Appendix Figure C-2). Without the putative outlier, 433 significant genes were identified. Gene ontology (Table 5-3) and biological processes (Table 5-4) are shown.

Mock vs. 8117/43 analysis

To examine the host responses to mock injection and 8117/43 more thoroughly, arrays from samples in each group were compared to arrays from un-injected tissue. Significant genes identified by class comparisons were separated into three groups: significantly altered genes specific to mock injection, genes common to both mock and 8117/43, and genes specific to

8117/43 (Figure 5-5). The three pools of genes were then analyzed using IPA which is web-based bioinformatics software package that constructs networks of genes in the data set based on a peer reviewed knowledge base. A score is assigned to networks derived by the significance of gene relationships. Biochemical pathways, and biological processes associated with these networks can then be delineated (Calvano et al., 2005). 566 genes were found to be significant in the 8117/43 vs. un-injected arrays, of which 340 were specific to 8117/43 injection at $p<0.001$ with 284 of them up regulated and 56 down regulated. 160 of the up regulated genes exceeded a 3 fold change. Mock injection induced 179 specific genes most of which (174) were up regulated and 19 of those exceeded 3 fold. 226 significant genes were common to both mock and 8117/43. Almost all (225) were up regulated and 40 of them exceeded 3 fold change (Figure 5-5). In the current analysis the putative outlier was not rejected, however, if it were left out, 781 significant genes are identified instead of 566 (Appendix Table C-2).

Ingenuity pathway analysis revealed that the host response to 8117/43 was dominated by the immune response, with nearly half (81 of 161) significant genes recognized by IPA falling into that category (Figure 5-6). The most significant canonical pathway driving the immune response to 8117/43 is antigen presentation. Little induction of toll-like-receptor (TLR) signaling, interferon (IFN), and chemokine (CC) signaling was seen. Furthermore, limited infiltration of leukocytes indicates a small inflammatory response to non-replicating vector.

Only one high scoring (58) network was identified by IPA in an analysis of the mock specific genes (Figure 5-7). Its associated functions include cell growth, proliferation, and movement. Major nodes (genes with the most links to other genes in the network) include cyclinD1 (CCND1), and integrin β1 (ITGB1).

The two highest scoring networks (65) constructed by IPA from the genes significantly altered by both 8117/43 and mock injection were combined (Appendix Figure C-3). The major biological function is the immune response (82 genes), and the major pathway is antigen presentation (7 of 40). Chemokine ligand 10 (CXCL10) and chemokine ligand 2 (CCL2) were up-regulated by a 243 and a 40-fold change by 8117/43 respectively. The interferon activated gene 202B was up-regulated by a 200 fold change. Major network nodes include the transcription factor STAT3 (signal transducer and activator of transcription), TGFβ1 (transforming growth factor, beta 1), and ICAM (intracellular adhesion molecule 1).

340 significantly altered genes specific to 8117/43 injection, were analyzed by IPA. Two high scoring networks (61) were identified and merged (Figure 5-8). Major nodes include the pro-inflammatory molecule interleukin-6 (IL6), transcription factors STAT1 and STAT3, MYD88 (myeloid primary differentiation gene 88), and chemokine ligand 5 (CCL5) also known as RANTES. Other genes in the network include chemokine ligands, interferon factors (IRFs), and major histocompatability genes. The major biological function is the immune response (81 genes), and the top conical pathway is antigen presentation (12 of 40 genes). A few of the most dramatically altered genes include the interferon inducible protein 78 (MX1) which was up-regulated 80-fold. Others include complement factor β1 (CFB) up-regulated 107 fold, and IFIT1L, an interferon induced protein up-regulated 344-fold.

8117/43 vs. HSVlacZgC analysis

To compare the total number of significant genes induced by 8117/43 and HSVlacZgC, arrays from the 2 and 3 day time points were combined. All of the 8117/43 arrays were compared to all HSVlacZgC arrays, both controlled against the mock injected arrays. Many more genes were significantly altered in response to HSVlacZgC (2969) than to 8117/43 (268), with

245 genes being common to both groups (Figure 5-9). All arrays in the HSVlacZgC vs. mock comparison passed cross validation (Appendix Table C-3)

Analysis of molecular and biological functions using BRB array tools showed few categories with high observed/expected ratios. Similarly, IPA analysis of the combined time points resulted in few high scoring networks, or significant conical pathways and functions (data not shown). This is probably because the replication competent HSV-1 alters such a massive number of genes that it is difficult to identify specific pathways. Therefore, analyses were performed on samples from each time point separately.

8117/43 vs. HSVlacZgC at 2 and 3 days PI

A comparison of arrays from the non-replicating vector (8117/43) injected samples to arrays from replication competent virus (HSVlacZgC) injected samples at 2 and 3 day time points normalized against arrays from mock-injected samples was conducted (Table 5-6). The 812d outlier, when included in the 2day time point analysis, failed all cross validation, and only 26 significant genes were identified. Therefore, it was removed and 206 significant genes were subsequently identified with good cross validation (Appendix Table C-4,5). At the 3 day time point 253 genes were significantly altered by 8117/43, however one mock array failed cross validations and if removed 1246 genes would be significant and cross validation improves (Appendix Table C-6). When the putative mock outlier was removed from the analysis molecular and biological functions remained similar despite a vast increase in the number of significant genes from 253 to 1246 (Appendix Table C-7,8,9,10). Although more significant genes were identified when the mock outlier was removed from the analysis, higher observed over expected ratios were seen when the mock array was included, therefore, it was kept in the analysis. No arrays failed cross validation of HSVlacZgC Vs mock at both 2 and 3 day time points (Appendix Table C-11,12)

Roughly 5 times more genes were significantly altered in response to HSVlacZgC than in response to 8117/43. In both cases most significant genes were altered more than 3 fold, and most were up regulated. IPA recognized most significant genes (Table 5-6).

Both 8117/43 and HSVlacZgC induce alterations in genes associated with the immune response (Figure 5-10). In the case of 8117/43, 59 immune response genes were altered at 3 days whereas 239 were altered by HSVlacZgC at the same time point. Immune and lymphatic system development and function was more significantly represented in the HSVlacZgC comparison, as was cell movement and cell death. Induction of the viral infection category was similar in both 8117/43 and HSVlacZgC comparisons, with surprisingly little up regulation.

Based on the ratio of significantly altered genes in each condition to the total number of genes in a given pathway, 8117/43 and HSVlacZgC induce antigen presentation and interferon signaling similarly, whereas HSVlacZgC induces more genes in each of the other pathways. At the 3 day time point HSVlacZgC induced 37 percent (17 of 46) of toll-like receptor (TLR) signaling pathway genes (Appendix Figure C-4).

Considering that HSVlacZgC alters many more genes than 8117/43, more genes are expected to be assigned to a given pathway by chance alone. Since this can be somewhat misleading, IPA calculates the probability (significance) that a given pathway was assigned to the data set by chance rather than calculating the ratio of genes in a pathway from the data set to the total number of genes in a pathway.

Based on significance, 8117/43 strongly induced the antigen presentation pathway, and to a lesser extent interferon and chemokine signaling (Figure 5-11). Both viruses induced gene expression changes in about 20% of genes in the antigen presentation pathway, but given the smaller number of genes altered by 8117/43, it represents a more significant induction by that

virus. When the time points were combined and 8117/43 was compared to mock, 12 of 40 (30%) of genes in the antigen presentation pathway were up regulated including 3 major histocompatability class I genes (HLAC, HLAE, HLAF), 3 major histocompatability class II genes (HLADQB2, HLADQA1, HLADMB), 2 proteolytic antigen processing peptidase genes (PSMB8, PSMB9), both tap1 and tap2 transporter genes, as well as the tap binding protein (TAPBP). At the 2 day time point 8117/43 up-regulated 4 out of 19 genes in the IFN pathway (IFNb1, ISGF3G (ISG9), STAT1, and STAT2). HSVlacZgC did not significantly induce IFN signaling; however, it induced STAT1 and STAT2 similar to 8117/43. Chemokine ligands CCL2 (MCP-1), CCL5 (RANTES), and CCL7 (MCP-3) were up regulated at both 2 and 3 day time points for 811743 and HSVlacZgC analyses. Fold-change values tended to be much higher for HSVlacZgC than for 8117/43 suggesting a more robust induction as a result of viral replication. In addition, other chemokine pathway molecules were induced by HSVlacZgC including CCL4, CCL11, CCL13, as well as c-Fos and c-Jun transcription factors. HSVlacZgC strongly up regulated death receptor and apoptotic signaling, toll-like receptor signaling, leukocyte extravasation, and NFκb signaling pathways. The death receptor and apoptotic signaling pathways have many genes in common, and in our analysis the same genes were found in both pathways for HSVlacZgC including caspases 7, 8, 12 and TNF. Daxx was up-regulated by both viruses, but 8117/43 did not significantly induce either pathway at 2days or 3 days. Double-stranded RNA-dependent protein kinase (PKR) (EIF2AK2) and TLR3 were up regulated at both time points, and for both viruses, but HSVlacZgC induced additional TLR signaling genes including MYD88, TLR 2,4,6,7, and Map3k1 (MAPK).

IPA identified one high scoring network (69) at 2 days for 8117/43. Major nodes included IRF1 and STAT1. At 3 days PI, one high scoring network was identified (66), also having

STAT1 and IRF1, but also IRF7, TNFSF10 ad IFB1 as major nodes. These two networks were merged, and associated functions and pathways are indicated (Appendix Figure C-5).

Many networks were identified by IPA in the HSVlacZgC conditions at both 2 days and 3days PI, but none were high scoring. Four networks were merged; major nodes include IL6, TGFb1, and TNF (Appendix Figure C-6).

Discussion

Several aspects of neuroimmunology make HSV-1 infections of the CNS unique (Peterson and Remington, 2000; Lowenstein, 2002; Sandri-Goldin, 2006). First, the CNS lacks classical lymph drainage and professional antigen presenting cells, limiting priming of adaptive immunity. Secondly, valuable neurons are somewhat protected from cytolytic T lymphocyte (CTL) activity, and rather than eliminating them, CD8+ and CD4+ cells contribute by producing IFN-γ to aid infected neurons by setting up an anti-viral state. Third, the selective permeability of the BBB isolates the CNS to an extent (although it is easily disrupted) from molecules like cytokines and immunoglobulins, as well as limiting access to immunocytes. Infiltration of leukocytes such as Natural killer (NK) cells and macrophage/monocytes occurs but neutrophils are less efficiently attracted due to low levels of P-selectin on the BBB endothelium (Peterson and Remington, 2000). These factors, coupled with the fact that productive infections often occur too quickly for adaptive immunity to take place in naïve hosts means that innate immunity plays a critical role in warding off HSV-1 infection in the CNS. Although adaptive immunity is not efficiently induced in the CNS, long-term transgene expression from non-replicating vectors can be limited by the induction of adaptive immunity which is facilitated by the innate response. (Peden et al., 2004).

Major components of the innate response are the complement system and interferon response as well as resident cellular immunity mediated by astrocytes and microglia (the major antigen presenting cells (APCs) of the CNS) (Peterson and Remington, 2000). Induction of the

IFN response by HSV-1 is thought to result from viral dsRNA, and toll-like-receptor (TLR) recognition of HSV-1 (Morrison, 2004; Mossman and Ashkar, 2005). IFNs can induce the expression of interferon stimulated genes that limit viral transcription and protein activity, as well as attract immune cells. HSV-1 has evolved several mechanisms for circumventing the IFN response (Mossman et al., 2001; Eidson et al., 2002; Broberg and Hukkanen, 2005; Sandri-Goldin, 2006). The key viral proteins in preventing the IFN response are ICP0, ICP27, VHS, γ34.5 and US11. ICP0 limits ISG transcription perhaps by disrupting normal cellular transcription, ICP27 interferes with cellular RNA splicing, VHS non-selectively degrades cellular mRNA, and γ34.5 and US11 work in concert to prevent host protein synthesis shutoff mediated by PKR and eIF2α. Together these viral functions limit the cellular IFN defense mechanism, and prevent host shutoff and apoptosis. In the present work, we have determined the degree to which innate immunity is induced by HSV-1 *in vivo*, and to what extent non-replication competent vectors induce innate immunity, as well as establish other host immune responses mechanisms that are induced by these vectors.

Microarray technology has been employed by other groups to examine the host response during latency and in response to reactivation stimuli (Hill et al., 2001; Tsavachidou et al., 2001; Higaki et al., 2002; Kramer et al., 2003), while others have examined the cellular response during lytic infections *in vitro* (Khodarev et al., 1999; Eidson et al., 2002; Taddeo et al., 2002; Brukman and Enquist, 2006; Pasieka et al., 2006). In one such study it was determined that while WT HSV-1 circumvented the IFN response, a γ34.5 mutant did not, presumably due to PKR mediated host shutoff activity which occurs in the absence of γ34.5 (Pasieka et al., 2006). However, in this study only 101 of the 1,906 significantly altered genes in a WT infection were recognized by the IPA, representing a limitation of the analysis. Another study using multiple IE

mutants suggests that ICP0 instead of γ 34.5 plays a dominant role in circumventing the IFN response by inhibiting ISG transcription (Eidson et al., 2002).

Despite the advantages of microarray analysis, obstacles exist. First, microarray analysis cannot reveal the rate of mRNA synthesis or degradation, only the steady state level of a given transcript, thus it represents only a snapshot of a dynamic process. In fact, several viral genes can induce a generalized reduction in mRNA not specific to any biological process. For example, VHS non-selectively degrades mRNA and ICPO can alter transcription by modulating RNApolII and disrupting ND10 structures. Despite the expected reduction in mRNA levels following HSV-1 infection, we and others have observed a global increase in expression (Taddeo et al., 2002; Kramer et al., 2003; Pasieka et al., 2006; Paulus et al., 2006), although others have observed a decrease (Khodarev et al., 1999). Another obstacle is that HSV-1 is notorious for redirecting cellular protein functions and is capable of altering cell biology at the level of proteins, a process that cannot be directly traced by array analysis. The role of γ34.5 and US11 in circumventing host translational shutoff is a good example. Also, microarray analysis is not likely to discriminate between pre-mRNA and spliced mRNA, an important aspect when one considers ICP27's ability to inhibit splicing. Another confounding factor is that *in vivo* studies examine a population of cell types, including infiltrating cells, which can add variability to the microarray analysis. Finally, *in vitro* studies have the benefit of synchronizing infections whereas our study must consider that the stage of viral infection is varied across the tissue sample. Despite these limitations, we have characterized the host response to both replication competent and non-replicating HSV-1 when delivered directly to the CNS *in vivo* and have identified specific aspects of the innate response that seem to be the dominant in HSV-1 infections. Aspects of

innate immunity and other biological mechanisms relevant to HSV-1 biology are discussed below.

The Interferon Response

In our analysis very little IFN induction was seen in response to a mock injection or 8117/43 when the two were compared to arrays from un-injected samples. Neither group met the significant threshold of IFN induction in IPA analysis. However, when 8117/43 and HSVlacZgC were compared to mock arrays at separate time points, 8117/43 did reach threshold significance in IPA. HSVlacZgC did not meet threshold in the same analysis. Others have suggested that ICP4 mutants do not strongly induce an IFN response *in vitro*, perhaps do to ICP0 activity (Eidson et al., 2002; Lin et al., 2004; Mossman, 2005). Others claim that γ 34.5 is critical (Pasieka et al., 2006). Our analysis demonstrates that HSVlacZgC, having both ICP0 and γ 34.5 at its disposal did not induce a strong IFN response, although it is possible that the lack of IFN induction by HSVlacZgC is partially due to the gC mutation. In contrast, 8117/43 did seem to induce changes in expression of some (4 of 19) IFN pathway molecules, including STAT1 and STAT2, as well as IFNb1 and ISG9 in one analysis. We conclude that 8117/43 induces a mild IFN response that is only partially blocked by low its low level of ICP0 expression.

Toll-Like Receptor Signaling

Toll-like-receptors (TLRs) are an innate immune host defense mechanism that detects common microbial peptide and nucleotide patterns. TLRs 2 and 9 likely recognize HSV-1 glycoprotein D, and TLR 3 detects dsRNA common to viral transcriptomes. TLRs signal through NFκB to induce type I IFNs, as well as chemokine and cytokine induction which leads to inflammation and recruitment of lymphocytes(Morrison, 2004). One study demonstrated that TLR2 -/- mice had less inflammation and less mortality with no increase in titers suggesting that

the TLR response is not beneficial to the host defense to an HSV-1 infection(Kurt-Jones et al., 2004).

Our results demonstrate a strong induction of TLR signaling pathways for HSVlacZgC but not 8117/43, although both viruses induced PKR and TLR3. This indicates that ICP4 minus vectors do not induce a strong innate immune response mediated by TLRs.

Antigen Presentation

The most striking finding of our study is the robust induction of antigen presentation in response to both 8117/43 and HSVlacZgC. Both viruses induce genes involved with multiple stages of antigen processing including proteolytic degradation, transport, and MHC I and MHC II presentation to CD8+ and CD4+ lymphocytes respectively.

In our analysis it is impossible to determine exactly what cells are presenting antigen, however it is likely that neurons which normally do not have MHCI or MHCII presentation up regulate MHC I presentation when transduced by either virus. Microglia, the resident APC of the CNS, are likely the source of MHC II antigen presentation (Peterson and Remington, 2000; Lowenstein, 2002).

In any case, the lack of professional APC's, and lack of lymph drainage in the CNS means that poor adaptive immune priming takes place regardless of antigen presentation (Lowenstein, 2002). If care is taken not to disrupt the tissue, then virus may be delivered without causing significant production of neutralizing antibody, has been shown with AAV vectors (Peden et al., 2004). With respect to viral vectors this is encouraging as it allows for vector re-administration strategies to be employed.

Another consideration of our analysis is that HSV-1 UL47 is capable of inhibiting the TAP transporter at the level of protein. Therefore, although HSVlacZgC induces gene expression changes in antigen presentation pathways, actual presentation may not take place.

NFκB

Inhibition of NFκB reduces titers suggesting that its induction benefits HSV-1 infection (Amici et al., 2001). Furthermore, many genes associated with the NFκB pathway are induced by HSV-1, likely due to PKR activation (Taddeo et al., 2002; Taddeo et al., 2003), and may inhibit apoptosis mediated by TNF (Goodkin et al., 2003; Goodkin et al., 2004; Sandri-Goldin, 2006). However, this is a point of contention as others suggest that NFκB induction does not prevent apoptosis, because infection of NFκb defective mice is not associated with increased apoptosis (Taddeo et al., 2004).

Our analysis shows a mild induction of NFκb by HSVlacZgC at 2 days, and a strong induction of NFκb at 3 days PI, but not by 8117/43 at either time point. This induction of NFκB by HSVlacZgC did not correlate with a reduction of apoptotic signaling over the same two time points suggesting that NFκb does not preclude apoptosis.

Apoptosis

Several HSV-1 β and γ genes (ICP6, γ34.5, and gD) are able to block apoptosis which is mediated by caspases and induced by TNF and Fas signaling (Sandri-Goldin, 2006). Our data show significant upregulation of the related pathways of apoptotic and death receptor signaling in response to HSVlacZgC, but not to 8117/43. Only HSVlacZgC infection was associated with induction of apoptotic pathways despite its expression of anti-apoptotic viral genes. We conclude that induction of apoptotic and death receptor pathways is much more robust in response to HSVlacZgC than to 8117/43 due to the replication competence of HSVlacZgC rather than anti-apoptotic viral functions.

Chemokines

Pro-inflammatory chemokine signaling can be particularly harmful in a confined organ such as the CNS, and may not effectively limit HSV-1 infections (Marques et al., 2004; Marques

et al., 2006). However, HSV-1 does not induce an immunopathogenic effect in mice as robustly as other alphaherpesviruses such as HSV-2 or pseudorabies virus (PRV) (Paulus et al., 2006).

In our analysis we found more robust induction of chemokine receptor ligands, MCP-1, MCP-3, and Rantes in HSVlacZgC than in 8117/43 analysis. Several other chemokine ligands were also found in HSVlacZgC analysis, as well as transcription factors c-Fos and c-Jun. Taken together these data indicate a stronger chemokine mediated inflammatory response to HSVlacZgC than to 8117/43 which only mildly induced chemokine signaling at 3 days when compared to mock injection.

Cytokines

IL-6 and IL-10 signaling were both significantly up regulated in the HSVlacZgC analysis, but not for 8117/43 at the 2 and 3 day time points. However, when 8117/43 time points were combined IL-6 was a major node of the highest scoring networks. Therefore, 8117/43 induces IL-6 mediated inflammation, but not as drastically as HSVlacZgC. TNF and TGF were both significantly up regulated in the HSVlacZgC and 8117/43 analysis. Although somewhat contradictory, it is obvious that the inflammatory response was much larger in HSVlacZgC than 8117/43, which closely resembled mock infection.

Materials and Methods

Viruses

The non-replication competent ICP4 defective 8117/43 virus (Dobson et al., 1990) was amplified on complementing E5 cells (DeLuca et al., 1985) in Eagle minimum essential medium (MEM) with 10% fetal bovine serum, penicillin (100U/mL), and streptomycin (100 µg/ml). Cells were maintained at 37°C under 5% carbon dioxide. The replication competent virus HSVlacZgC (Singh and Wagner, 1995) contains a *lacZ* reporter gene inserted into the non-essential viral glycoprotein C (gC) gene which is driven by the HSVlacZgC promoter (early gene kinetics).

HSVlacZgC was amplified on rabbit skin (RS) cells in MEM with 5% calf serum, penicillin (100U/mL), and streptomycin (100 μg/ml). Amplification was performed by infecting ten 90% confluent T-150 flasks at a multiplicity of infection (moi) of 0.01. After 3-4 days the contents were centrifuged at 16,000 x g for 40 minutes at 4° C. The supernatant was removed and pellets were resuspended in 2 mL of supplemented MEM. The re-suspensions were freeze/thawed, vortexed, and clarified by centrifugation at 5,000 x g for 2 minutes. 8117/43 stock was titrated on 24 well plates of E5 cells; the final concentration was $6x10^8$ particle forming units (pfu)/mL. HSVlacZgC was titrated on RS cells in similar fashion with a final concentration of $2.5x10^8$ pfu/mL. Viral stocks were aliquoted and stored at -80°C until use.

Stereotaxic Injection

Female ND4 Swiss mice aged 6-8 week were obtained from Harlan Sprague Dawley and maintained in standard housing on a 12 hr light dark cycle in accordance with approved animal husbandry procedures. On the day of surgery animals were anesthetized with ketamine (70-80mg/kg)/ xylazine (14-15mg/kg), and an incision was made along the midline of the skull. A burr hole was made in the skull and a single 1 μL injection of 8117/43, HSVlacZgC, or vehicle (MEM with 10% FBS) was delivered via cannula into the right CA1 region of the hippocampal formation (AP=-0.19cm, L=-0.15cm, V=-0.17cm) at a rate of 0.35 μL/min. Following injections, bone wax was used to repair the burr hole, and a surgical staple was used to close the wound.

Tissue Collection

After 2 or 3 days, animals were anesthetized with halothane and euthenized by cervical dislocation. A 1 mm^3 tissue sample was immediately collected from the CA1 region of the hippocampus surrounding the injection site, and from the same region of the contralateral, un-injected hippocampi. Both tissue samples were immediately placed in 5 volumes of RNA later. (Figure 5-1)

X-gal Staining

Utilizing the *lacZ* reporter genes in 8117/43 and HSVlacZgC to visualize viral dissemination, two animals from each experimental group were prepared for X-gal staining. Animals were deeply anesthetized with xylene (8mg/kg) ketamine (24mg/kg) acepromazine (80mg/kg) and perfused with 4% paraformaldehyde. Brains were blocked and placed in x-gal fixation solution (0.1% Sodium deoxycholate (NaDOC), 0.02% NP-40, 2% formaldehyde, 0.2% glutaraldehyde, 0.1 M HEPES (pH 7.4), 0.875% NaCl) for 1 hr at 4° C. Tissue samples were then washed 2x in PBS and 1x in PBS/DMSO (3%) and transferred to x-gal staining solution (0.15 M NaCl, 100mM HEPES (pH 7.4), 2mM $MgCl_2$, 0.01% NaDOC, 0.02% NP-40, 5mM potassium ferricyanide, 5mM potassium ferrocyanide, 1mg/mL x-gal (from a 20mg x-gal/mL dimethylformamide stock) overnight at 31°C. Samples were washed with PBS and images were captured using a dissection microscope fitted with a digital camera.

RNA Preparation

Total RNA from brain slices were carried out using the RNesy® midi procedure (Qiagen) with some modification in the homogenization of the sample. Tissue samples (ca 60 mg) buffer were homogenized in 0.5 ml of RTL in a rotor homogenizer designed for Ependorf tubes (Fisher). To the resulting homogenate, 1 ml of H_2O and proteinase K (to 100 μg/ml) were added. The homogenate was digested at 55 °C for 20 min, centrifuged for 10 min at 4000xg and the supernatant was collected. Then, 1.5 ml of RTL, 3 ml of H_20 and 3 ml of ethanol were added sequentially to the supernatant, and mixed well by pipetting. The mixture was applied to an Rneasy midi column and the procedure of purication was carried out following the manufacture's protocol. Typically, ca 30 μg of total RNA were obtained.

Data Analysis

Affymetrix

Normalization of hybridization intensities and creation of a gene expression matrix was performed using the perfect-match-only method by inputting data (.cel files) into dChip (Li and Hung Wong, 2001). No outlying arrays were identified. Probesets with signal intensities below background levels in all replicates as calculated by an Affymetrix detection algorithm were removed from the analysis. BRB array tools (version 3.5.0-_beta 1, developed by Richard Simon, Amy Peng Lam, Supriya Menezes, EMMES Corp.) was used to identify genes that significantly differed ($p< 0.001$) between treatment classes. Also using BRB array tools, leave-one-out-cross-validation by the nearest neighbor-model was used to predict the treatment class of a data set based on differentially expressed genes. Hierarchical, unsupervised cluster analysis was performed in dChip using genes that differed by a coefficient of variation greater than 0.5. Supervised cluster analysis was performed using lists of differentially expressed genes. The chief molecular functions and biological processes mediated by those genes were categorized by gene ontology and ranked according to the observed/expected ratio with a cut off value of 3. In addition, the differentially expressed genes were analyzed by Ingenuity pathway analysis (Ingenuity systems®, http://www.ingenuity.com). Ingenuity pathway analysis (IPA) is a web-based bioinformatics software package that constructs networks of genes in the data set based on a peer reviewed knowledge base. A more detailed description of the analysis, modified from IPA guidelines follows.

To generate networks, a data set containing gene identifiers and corresponding expression values were uploaded into in the IPA application. Each gene identifier was mapped to its corresponding gene object in the IPA knowledge base. The genes, whose expression was significantly differentially regulated, called focus genes, were overlaid onto a global molecular

network developed from information contained in the IPA knowledge base. Networks of these focus genes were then algorithmically generated based on their connectivity.

The functional analysis identified the biological functions and/or diseases that were most significant to the data set. Genes from the dataset that were associated with biological functions and/or diseases in the IPA knowledge base were considered for the analysis. Fischer's exact test was used to calculate a p-value determining the probability that each biological function and/or disease assigned to that data set is due to chance alone.

Canonical pathways analysis identified the pathways from the IPA library of canonical pathways that were most significant to the genes from the data set. Genes from the data set that were associated with canonical pathways in the IPA knowledge base were considered for the analysis. The significance of the association between the data set and the canonical pathway was measured by Fischer's exact test to calculate a p-value determining the probability that the association between the genes in the dataset and the canonical pathway is explained by chance alone.

A network is a graphical representation of the molecular relationships between genes/gene products. Genes or gene products are represented as nodes, and the biological relationship between two nodes is represented as an edge (line). All edges are supported by at least 1 reference from the literature, from a textbook, or from canonical information stored in the IPA knowledge base. The intensity of the node color indicates the degree of up- (red) or down- (blue) regulation. Nodes are displayed using various shapes that represent the functional class of the gene product. Edges are displayed with various labels that describe the nature of the relationship between the nodes.

Spotted array

HSV-1 RNA was analyzed by the resonance light scattering (RSL) method as in previous publications (Sun et al., 2004; Aguilar et al., 2006). For each microarray, 10 µg of total were used to synthesize and labelling cDNA using the HiLight dual-color kit (Invitrogen). HSV-1 oligonucleotide arrays were constructed as previously described (Wagner et al., 2002; Yang et al., 2002). Hybridizations were carried out at 52°C in a MAUI hybrid mixer assembly for 18h. After hybidization the slices were processed as described in the instructions with the labeling kit. Microarrays were scanned with a GSD-501 HiLight reader (Invitrogen). Analysis of the signals was carried out as described previously (Sun et al., 2004).

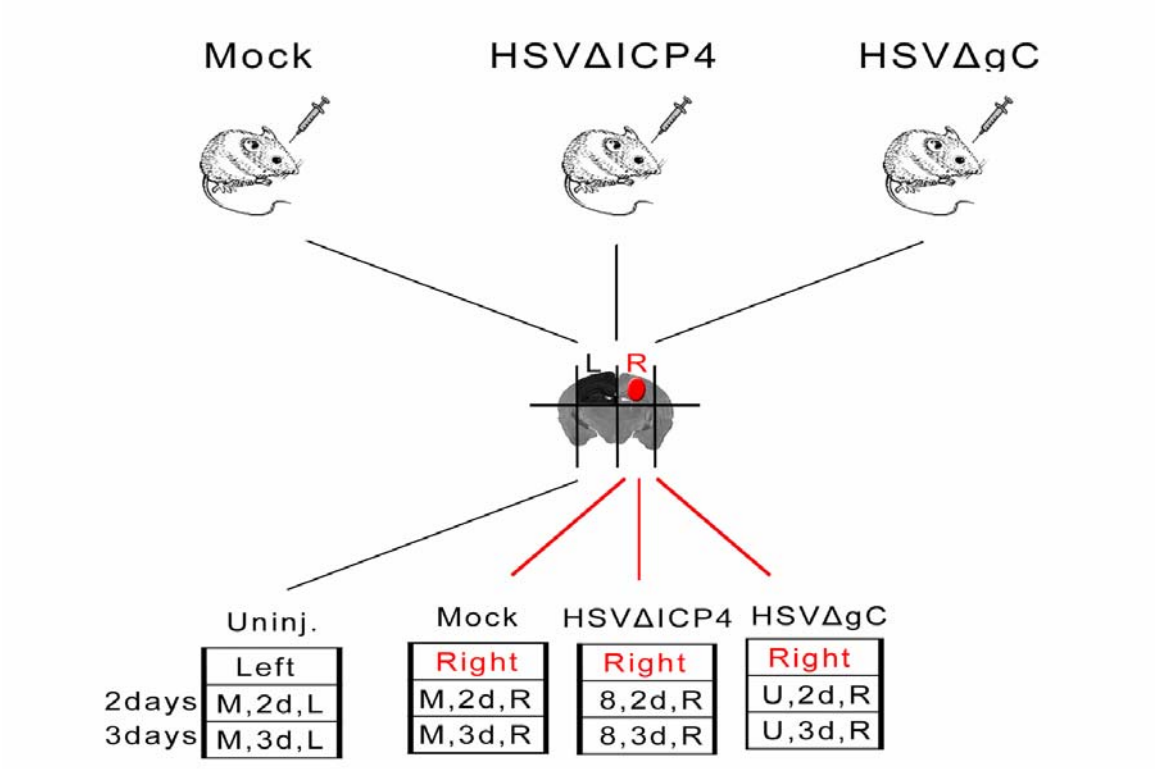

Figure 5-1. Experimental design of vector injections into the mouse CNS for microarray analysis. Vehicle (mock), 8117/43 (HSVΔICP4), or HSVlacZgC (HSVΔgC) was injected into the right hippocampus of mice (N=9). Tissue was then collected from the injection site and from the contralateral side of mock injected mice (un-injected) at two and three days. For each experimental group triplicate RNA samples, each pooled from three animals were analyzed by Affymetrix and HSV-specific microarrays.

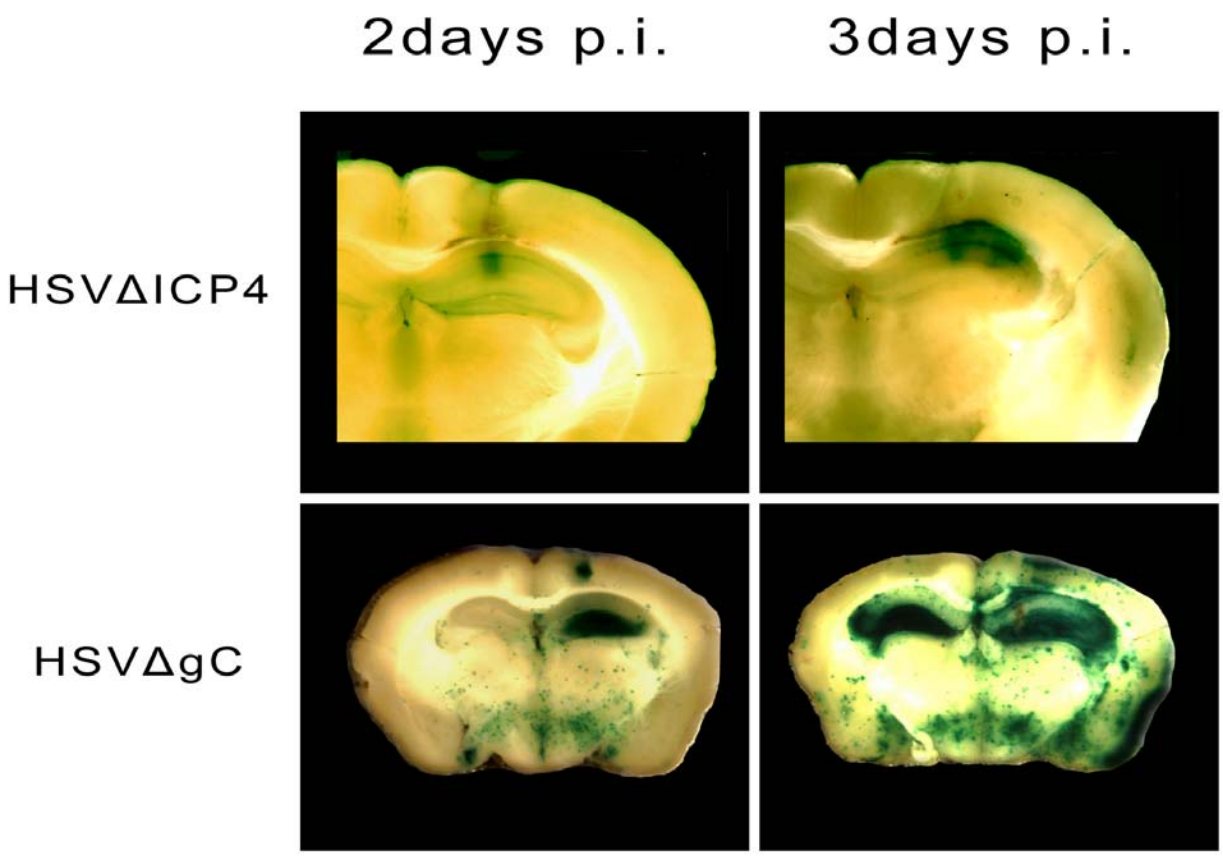

Figure 5-2. Coronal sections of mouse brains fixed and x-gal stained 2 or 3 days following injection of either HSVlacZgC (HSVΔgC) or 8117/43 (HSVΔICP4) HSV-1 viruses into the right CA1 region of the hippocampus.

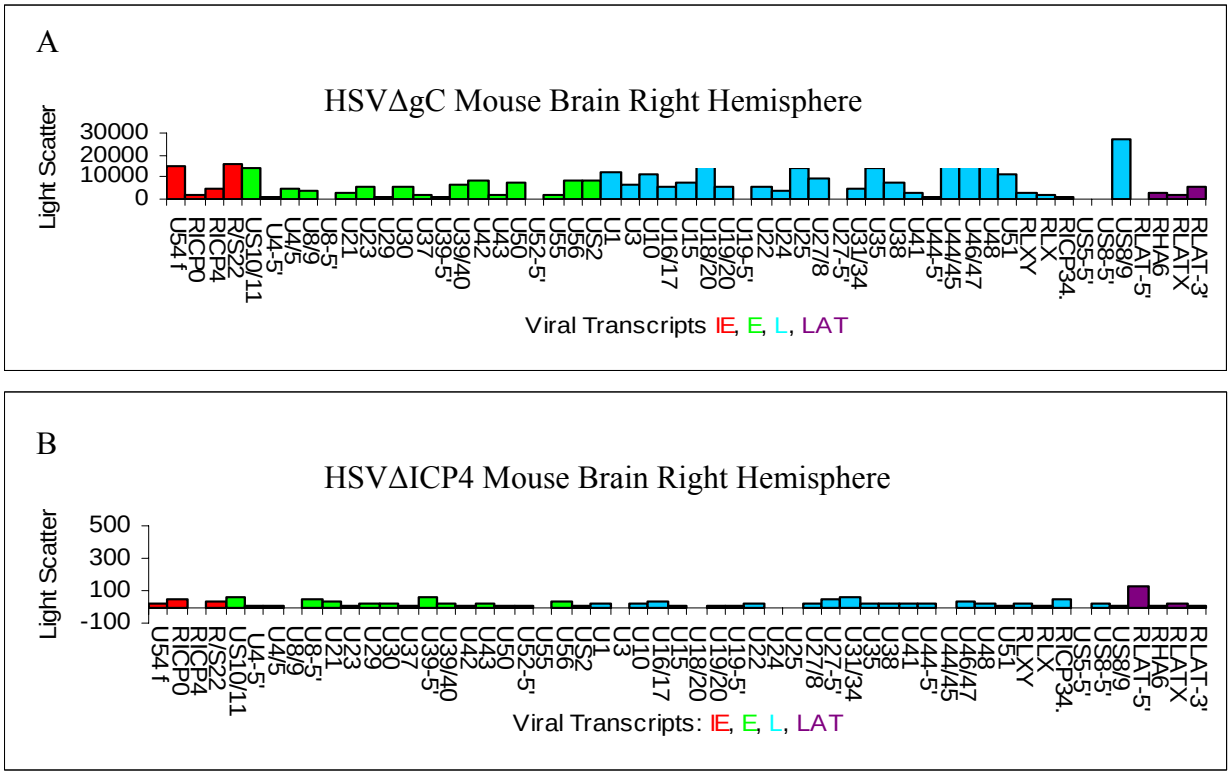

Figure 5-3. Herpes simplex virus type 1 viral gene expression. A) Median resonance light scatter signal from triplicates of HSV specific spotted arrays representing viral gene expression 3 days PI in CNS tissue injected with replication competent HSVlacZgC (HSVΔgC) or B) non-replicating virus 8117/43 (HSVΔICP4) 3 days PI.

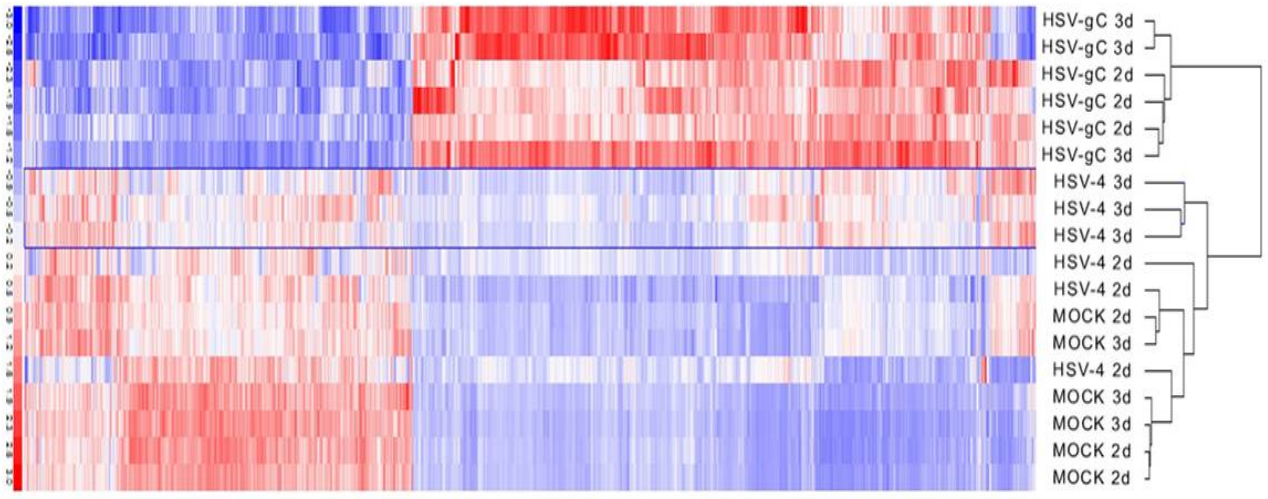

Figure 5-4. Supervised cluster analysis. HSVlacZgC (HSV-gC), 8117/43 (HSV-4), and mock injected arrays at 2 days (2d) or 3 days (3d) post injection. Red indicates up-regulation, and blue indicates down-regulation of gene expression represented by fold change.

Table 5-1. Molecular functions of 405 genes altered by mock injection vs. un-injected samples

GO id	GO classification	Observed	Expected	Observed/Expected
30106	MHC class I receptor activity	8	0.67	11.89
42379	Chemokine receptor binding	5	0.61	8.20
8009	Chemokine activity	5	0.61	8.20
16538	Cyclin-dependent protein kinase regulator activity	5	0.67	7.43
1664	G-protein-coupled receptor binding	5	0.78	6.43
4866	Endopeptidase inhibitor activity	9	1.83	4.92
30414	Protease inhibitor activity	9	1.85	4.86
19887	Protein kinase regulator activity	5	1.09	4.57
19207	Kinase regulator activity	5	1.20	4.17
5506	Iron ion binding	5	1.22	4.10
4857	Enzyme inhibitor activity	10	2.63	3.81
5516	Calmodulin binding	5	1.43	3.50
5125	Cytokine activity	9	2.82	3.19
30246	Carbohydrate binding	10	3.30	3.03
5529	Sugar binding	7	2.31	3.03

Table 5-2. Biological processes of 405 genes altered by mock injection vs. un-injected samples.

GO id	GO classification	Observed	Expected	Observed/Expected
45103	Intermediate filament-based process	5	0.25	19.78
6979	Response to oxidative stress	7	0.65	10.72
51049	Regulation of transport	6	0.63	9.49
6800	Oxygen and reactive oxygen species metabolism	8	1.01	7.91
6954	Inflammatory response	9	1.26	7.12
50778	Positive regulation of immune response	6	0.86	6.95
7626	Locomotory behavior	8	1.16	6.90
51240	Positive regulation of organismal physiological process	6	0.95	6.33
16042	Lipid catabolism	6	0.97	6.19
42330	Taxis	5	0.82	6.09
6935	Chemotaxis	5	0.82	6.09
7610	Behavior	8	1.41	5.67
50776	Regulation of immune response	6	1.07	5.58
9611	Response to wounding	15	2.82	5.31
8285	Negative regulation of cell proliferation	5	0.95	5.27
45321	Immune cell activation	7	1.41	4.96
1775	Cell activation	7	1.41	4.96
16477	Cell migration	6	1.24	4.83
1525	Angiogenesis	5	1.05	4.75
48514	Blood vessel morphogenesis	5	1.07	4.65
51707	Response to other organism	7	1.52	4.62

GO id	GO classification	Observed	Expected	Observed/Expected
1944	Vasculature development	5	1.16	4.32
1568	Blood vessel development	5	1.16	4.32
9607	Response to biotic stimulus	32	7.52	4.25
9613	Response to pest\, pathogen or parasite	13	3.16	4.11
6955	Immune response	22	5.41	4.06
6952	Defense response	24	6.59	3.64
51239	Regulation of organismal physiological process	6	1.69	3.56
1501	Skeletal development	5	1.43	3.49
6928	Cell motility	6	1.73	3.47
45595	Regulation of cell differentiation	5	1.45	3.44
51649	Establishment of cellular localization	5	1.47	3.39
40011	Locomotion	6	1.77	3.39
46483	Heterocycle metabolism	5	1.50	3.34
30036	Actin cytoskeleton organization and biogenesis	7	2.13	3.29
51641	Cellular localization	5	1.56	3.21
9605	Response to external stimulus	20	6.26	3.20
30029	Actin filament-based process	7	2.21	3.16
6950	Response to stress	26	8.22	3.16

Table 5-3. Molecular functions of 433 genes altered by 8117/43 vs. mock samples.

GO id	GO classification	Observed	Expected	Observed/Expected
30106	MHC class I receptor activity	18	0.71	25.28
42379	Chemokine receptor binding	9	0.65	13.95
8009	Chemokine activity	9	0.65	13.95
1664	G-protein-coupled receptor binding	9	0.82	10.93
3924	GTPase activity	10	1.56	6.42
5125	Cytokine activity	16	2.98	5.37
4866	Endopeptidase inhibitor activity	9	1.94	4.65
30414	Protease inhibitor activity	9	1.96	4.60
4888	Transmembrane receptor activity	22	4.90	4.49
17111	Nucleoside-triphosphatase activity	13	3.29	3.95
16462	Pyrophosphatase activity	13	3.38	3.84
16818	Hydrolase activity\, acting on acid anhydrides\, in phosphorus-containing anhydrides	13	3.47	3.74
16817	Hydrolase activity\, acting on acid Anhydrides	13	3.49	3.72
16829	Lyase activity	5	1.51	3.3
5529	Sugar binding	8	2.45	3.27
4857	Enzyme inhibitor activity	9	2.78	3.24

Table 5-4. Biological functions of 433 genes altered by 8117/43 vs mock samples.

GO id	GO classification	Observed	Expected	Observed/Expected
19882	Antigen presentation	7	0.47	15.03
6471	Protein amino acid ADP-ribosylation	5	0.51	9.84
6955	Immune response	50	5.44	9.19
6952	Defense response	57	6.63	8.60
9607	Response to biotic stimulus	58	7.56	7.67
51093	Negative regulation of development	5	0.66	7.62
45596	Negative regulation of cell Differentiation	5	0.66	7.62
42330	Taxis	6	0.83	7.27
6935	Chemotaxis	6	0.83	7.27
45637	Regulation of myeloid cell differentiation	5	0.7	7.16
1816	Cytokine production	5	0.72	6.95
50778	Positive regulation of immune response	6	0.87	6.91
30099	Myeloid cell differentiation	6	0.93	6.44
51240	Positive regulation of organismal physiological process	6	0.95	6.30
6954	Inflammatory response	8	1.27	6.30
50776	Regulation of immune response	6	1.08	5.56
51707	Response to other organism	8	1.52	5.25
8285	Negative regulation of cell proliferation	5	0.95	5.25
45595	Regulation of cell differentiation	7	1.46	4.79
50874	Organismal physiological process	55	12.09	4.55
48534	Hemopoietic or lymphoid organ development	9	2.03	4.43
50896	Response to stimulus	61	15.16	4.02
50793	Regulation of development	9	2.35	3.83
9613	Response to pest\, pathogen or parasite	12	3.18	3.78
30097	Hemopoiesis	7	1.91	3.67
51239	Regulation of organismal physiological process	6	1.69	3.54
45321	Immune cell activation	5	1.42	3.52
9611	Response to wounding	10	2.84	3.52
1775	Cell activation	5	1.42	3.52

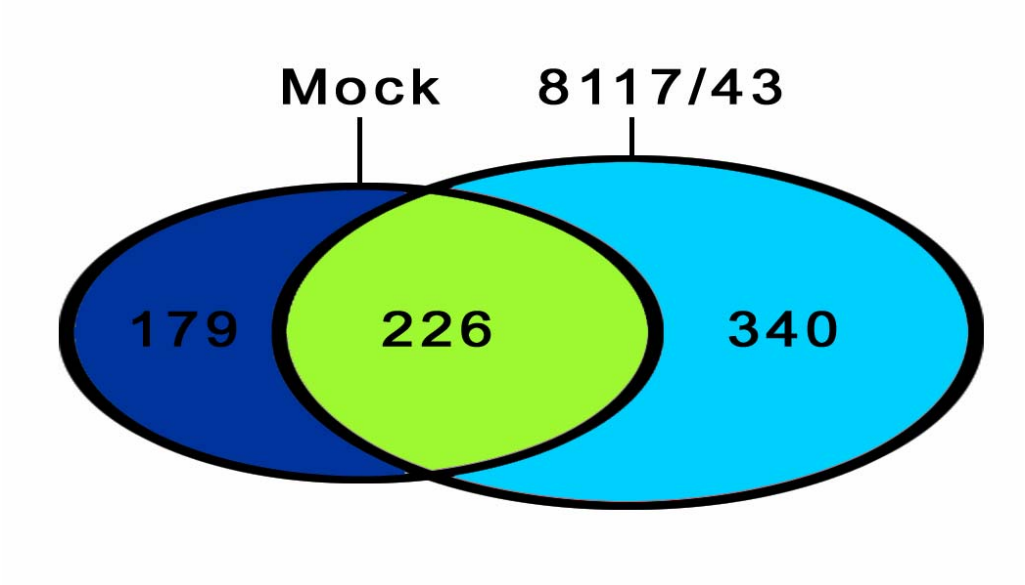

Figure 5-5. Comparison of mock vs. un-injected arrays and 8117/43 vs. un-injected arrays demonstrating significant genes specific to mock (dark blue) or (8117/43 light blue), as well as genes common to both (green).

Table 5-5. Three pools of genes significantly altered by mock, 8117/43 or both were analyzed separately using IPA.

	Mock vs un-injected	Common	8117/43 vs. un-injected
Significant genes	179	226	340
Up regulated	174	225	284
Down regulated	5	1	56
>3Fold Change	19	40	160
IPA recognized	104	140	161

A

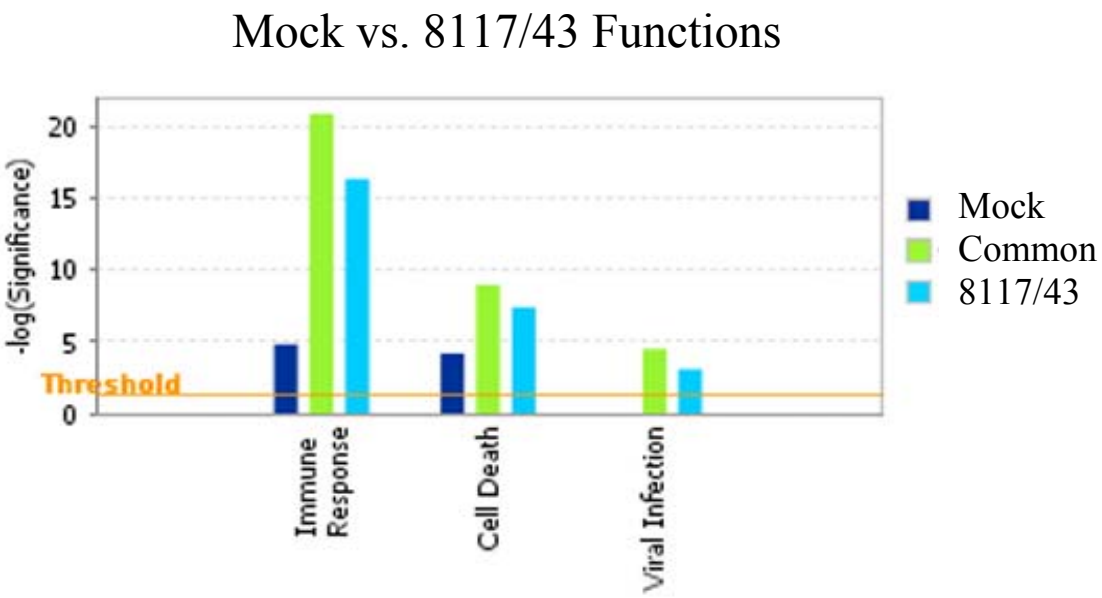

B

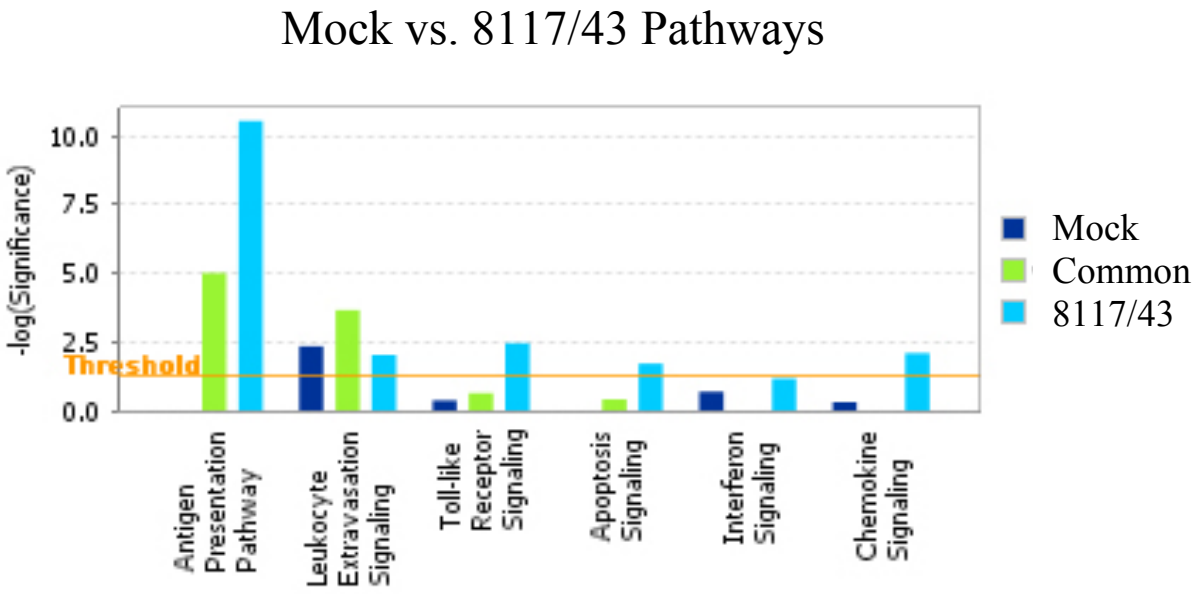

Figure 5-6. IPA of genes altered by mock (dark blue), 8117/43 (light blue), or genes altered by both mock and 8117/43 (green) vs. un-injected samples. A) Selected biological functions and B) canonical pathways. The Y axis (-log of the p-value) is the probability that each biological function was assigned to the gene set by chance alone. Threshold is indicated by an orange line and corresponds to $p<0.05$. Analysis and figure generation were performed using Ingenuity Pathway Analysis with permission (Ingenuity® Systems, www.ingenuity.com).

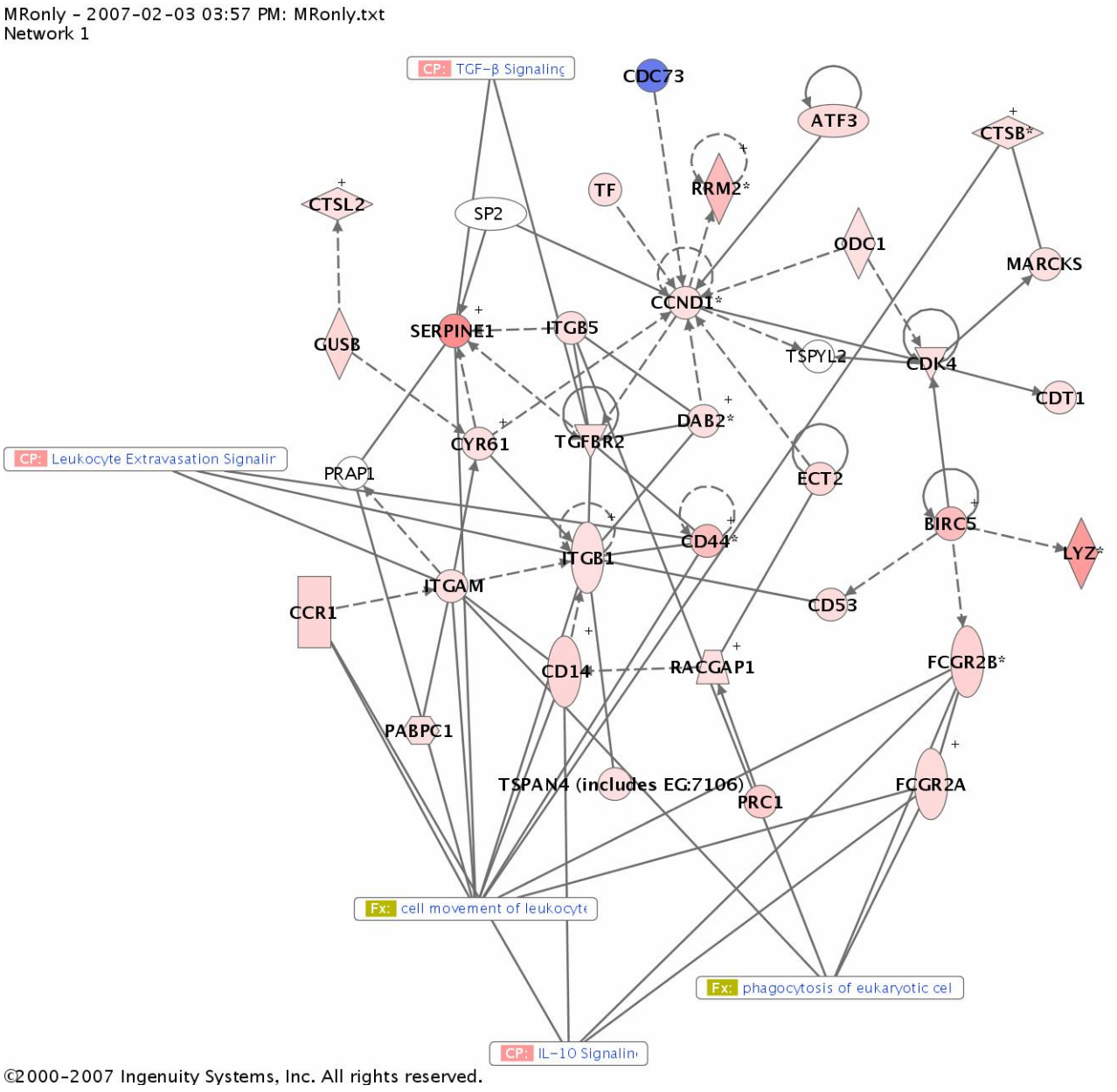

Figure 5-7. Ingenuity pathway analysis network of significant genes specific to mock injection. Increasingly dark shades of red indicate increasing up-regulation of gene expression as measured by fold change. Similarly, increasingly dark shades of blue represent increasing down-regulation. Analysis and figure generation were performed using Ingenuity Pathway Analysis with permission (Ingenuity® Systems, www.ingenuity.com).

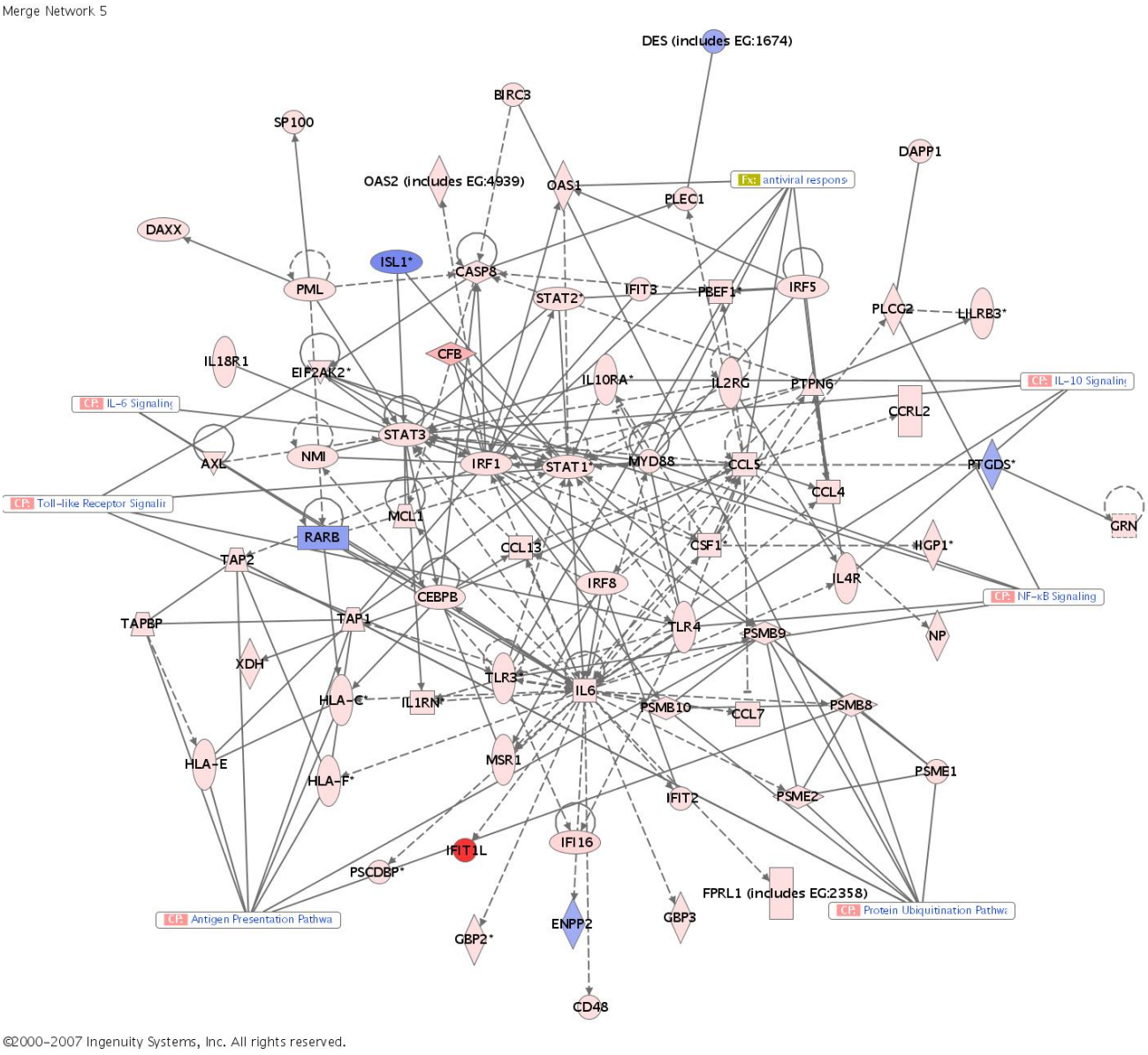

Figure 5-8. Ingenuity pathway analysis network of significantly altered genes specific to 8117/43. Analysis and figure generation were performed using Ingenuity Pathway Analysis with permission (Ingenuity® Systems, www.ingenuity.com).

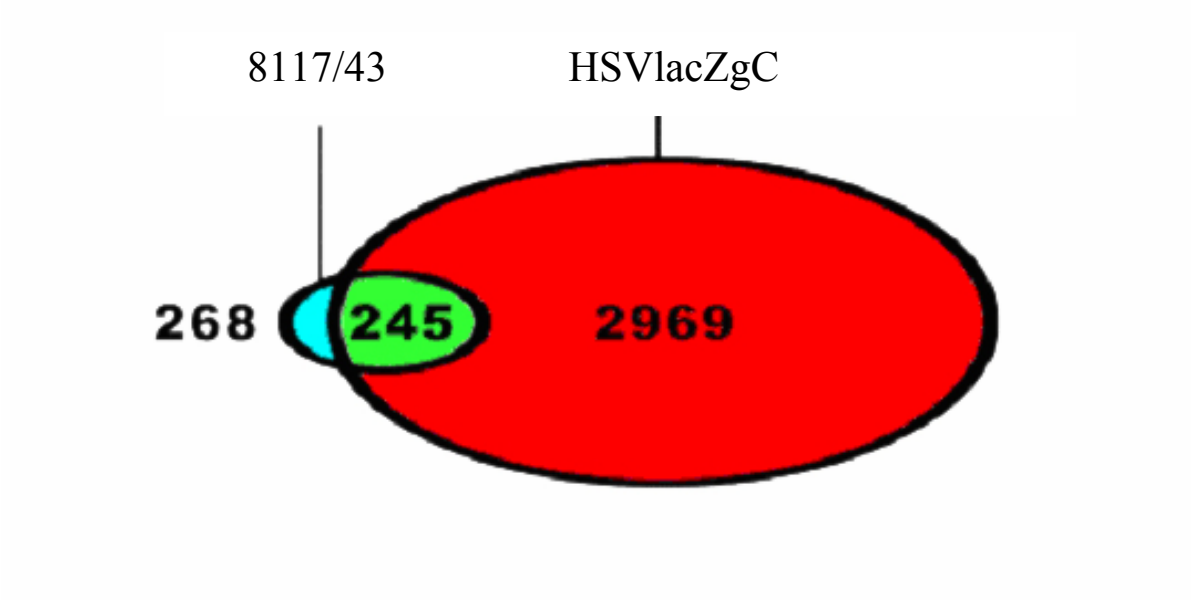

Figure 5-9. The total number of significantly altered genes (from combine time points) specific to the 8117/43 vs. mock comparison (HSVΔICP4) (light blue) and those specific to the HSVlacZgC vs. mock (HSVΔgC) (red) comparison are shown. The number of genes significantly altered by both viruses is shown in green.

Table 5-6. Significantly altered genes in 8117/43 vs. mock and HSVlacZgC vs. mock.

	8117/43 vs. mock		HSVlacZgC vs. mock	
Time post injection	2days*	3days	2days	3days
Total genes	206	253	930	1204
>3 fold change	180	184	479	716
Up regulated	197	229	681	1014
Down regulated	9	24	249	190
IPA recognized	103	117	399	545

Comparisons were analyzed using IPA after the 812d outlier was removed.

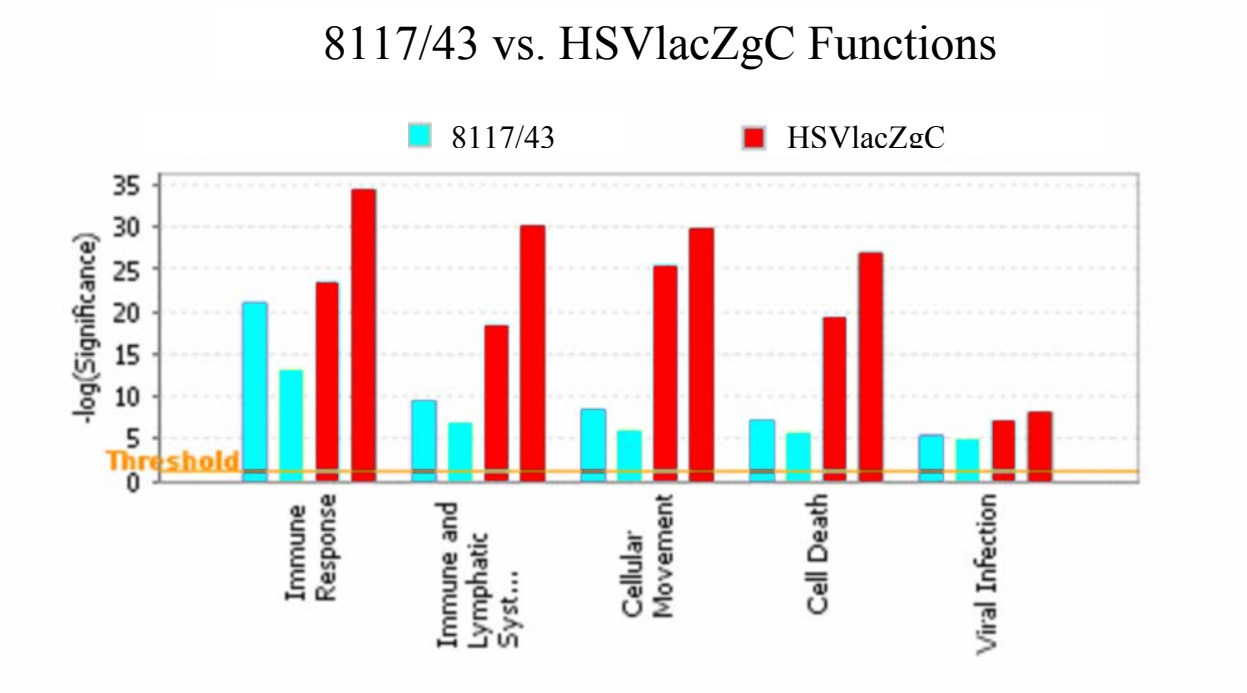

Figure 5-10. Biological functions induced by 8117/43 (ΔICP4) and HSVlacZgC (ΔgC). Selected functions identified by IPA at 2 days (first and third bars in each functional category) and 3 days (second and fourth bars) are shown. Analysis and figure generation were performed using Ingenuity Pathway Analysis with permission (Ingenuity® Systems, www.ingenuity.com).

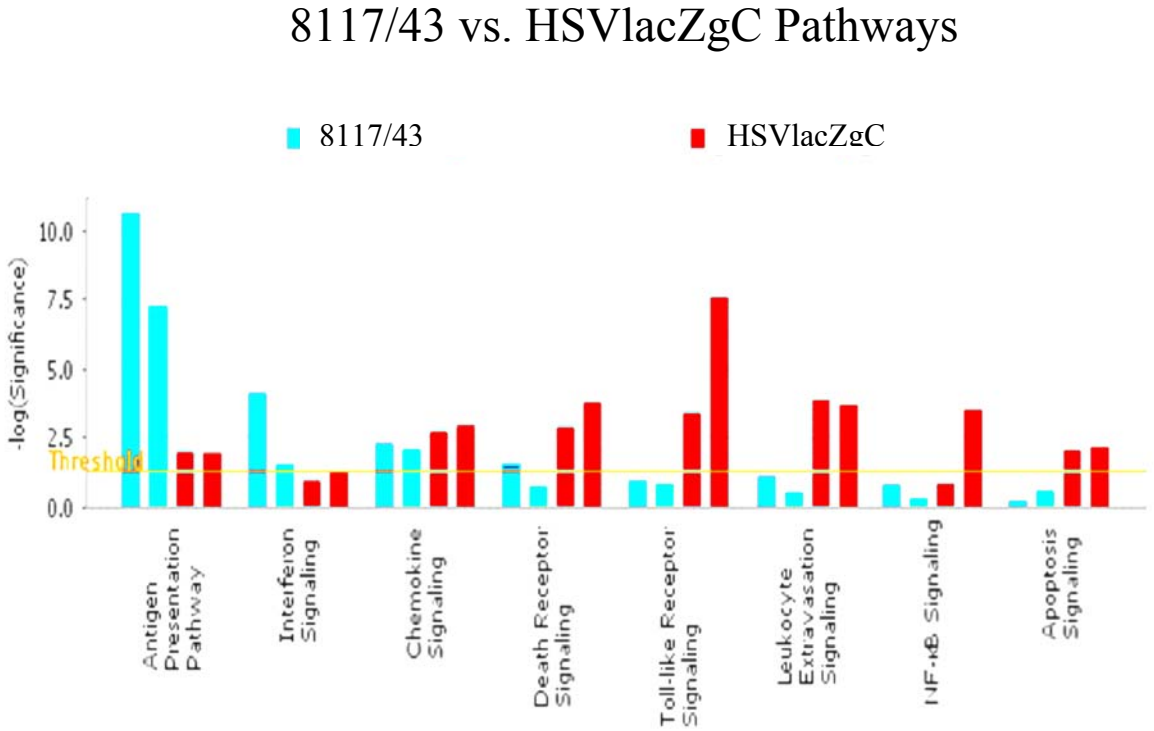

Figure 5-11. Canonical pathways induced by 8117/43 (ΔICP4) and HSVlacZgC (ΔgC). Selected pathways identified by IPA at 2 days (first and third bars in each pathway) and 3 days (second and fourth bars) are shown. Analysis and figure generation were performed using Ingenuity Pathway Analysis with permission (Ingenuity® Systems, www.ingenuity.com).

CHAPTER 6
PHENOTYPIC RESCUE IN A MOUSE MODEL OF FRAGILE X SYNDROME

Introduction

Fragile X syndrome (FXS) is the most common inherited form of mental retardation. It is caused by a mutation that silences the *FMR1* gene that encodes the Fragile X mental retardation protein (FMRP) (O'Donnell and Warren, 2002). To determine if FMRP replacement can rescue phenotypic deficits in an *Fmr1* knockout (KO) mouse model of FXS, we constructed herpes simplex virus type 1 (HSV-1) and adeno-associated virus (AAV)-based viral vectors, both of which express the major murine isoform of FMRP (Chapter 4). Analyses of the expression characteristics of these two vectors revealed that while the AAV vector continued to express FMRP over the course of the study, expression of FMRP by the HSV-1 vector was negligible by three weeks. Based on these analyses, we chose to use the AAV vector to determine if FMRP replacement can rescue phenotypes associated with the *Fmr1* KO. The most robust and relevant phenotypes of the KO mouse are susceptibility to audiogenic seizures (AGS) (Musumeci et al., 2000), enhanced long term depression (LTD) (Huber et al., 2002; Nosyreva and Huber, 2006), and abnormal dendritic spine morphology (Comery et al., 1997; Irwin et al., 2002). In addition, several reports have documented changes in steady state levels of certain mRNA transcripts putatively regulated by FMRP (Brown et al., 2001; Darnell et al., 2001; Miyashiro et al., 2003; Darnell et al., 2005). LTD is a form of synaptic plasticity that weakens the connectivity between neurons and may be linked to cognitive impairments associated with FXS. Analyses of hippocampal function in *Fmr1* KO mice that received hippocampal injections of vector showed that the paired pulse low frequency stimulated LTD (PP-LTD) in the CA1 region of the hippocampus was restored to wild-type levels, suggesting that expression of the major isoform of FMRP alone is sufficient for rescue. In parallel, we measured the levels of several mRNA

transcripts reported to be mis-regulated in the KO, but did not observe significant differences in their total brain mRNA levels using real-time RT-PCR. In addition, we have established the age dependency and pervasiveness of AGSs in two different strains of *Fmr1* KO mice and conducted a power analysis that suggests vector rescue of the AGS phenotype is not feasible using current induction and analysis methods. Our ability to reverse the PP-LTD phenotype suggests that post-developmental protein replacement may improve cognitive function in FXS and raises the possibility that other neurological deficits associated with FXS may be treatable by a gene therapy approach.

mRNA Regulation in the *Fmr1* KO

Introduction

FMRP is an RNA binding protein that shuttles between the nucleus and cytoplasm (Ashley et al., 1993), associates into RNA-Protein (mRNP) particles in an RNA dependent manner (Feng et al., 1997b; Tamanini et al., 1999), preferentially binds G-quartet structures of mRNA (Darnell et al., 2001; Schaeffer et al., 2001), and negatively modulates translation of its RNA ligands including its own message (Schaeffer et al., 2001). Furthermore, synaptic regulatory pathways initiated at mGluR receptors require FMRP for normal synaptic plasticity (Huber et al., 2002). However, identification of the FMRP RNA ligands subject to abnormal regulation in FXS has been more difficult to achieve. Several lines of research employing a variety of methods have failed to identify consensus RNA ligands that are misregulated in FXS and can be directly linked to pathology (Brown et al., 2001; Darnell et al., 2001; Miyashiro et al., 2003; Darnell et al., 2005).

Until more clarity is achieved on the issue, we have chosen three RNA transcripts involved with synaptic function that have been confirmed as mis-regulated transcripts in FXS. We wished to confirm this mRNA mis-regulation in the CNS of adult *Fmr1* KO mice in order to establish a

molecular KO phenotype that could potentially be rescued by reintroduction of FMRP using viral vectors. Transcripts whose mis-regulation had been confirmed by two different assays were preferentially selected and quantitated by real-time RT-PCR. Furthermore, we have analyzed total-brain RNA samples since the observed misregulation has not been independently examined in specific brain regions.

We chose Map1b, because it contains a G-quartet motif, and appears to be linked to *Fmr1* in the Drosophila model of FXS. In this model, mutation of the *Fmr1* homologue delays neurodegeneration in Map1b homologue mutants (Zhang et al., 2001). Map2, another important microtubule associated protein acts in concert with Map1b to form properly structured synaptic architecture, and was found to be decreased 1.6 fold in *Fmr1* KO mice (D'Agata et al., 2002). Map1b and Map2 double mutants do not survive into adulthood, and have abnormal dendritic spine morphology (Teng et al., 2001). The observation that these transcripts are mis-regulated in the KO, and that dendritic spines are abnormal in the KO mouse, makes them potential downstream mediators of FXS. Another transcript GRK-4 was found to be decreased 3-4 fold in the CNS of KO mice by an antibody positioned RNA amplification assay (APRA), and was confirmed by RT-PCR. Furthermore, protein levels were altered in synaptoneurosome preparations, although not significantly (Miyashiro et al., 2003). G protein-coupled receptors (GPRCs) are a large class of signal transduction mediators that respond to a variety of signaling molecules, including neurotransmitters (Premont and Gainetdinov, 2007). Because GPRCs play a critical part in biological processes, their natural regulation and pharmacological manipulation is of key interest. Normally, GPRCs are regulated by phosphorylation by GPRC kinases (GRKs) and subsequent binding by Arrestin which abrogates G protein signaling and initiates Arrestin

signaling. In the CNS, GRK4 is expressed mainly in Purkinje cells, and may regulate GABA receptors. GRK4 KO mice display no distinct phenotypes.

Results

To establish the *Fmr1* KO mouse phenotype of mRNA mis-regulation, total brain mRNA was isolated from adult WT and KO mice by guanidine isothiocyanate (GTC) extraction and analyzed by real-time RT-PCR. Three putatively mis-regulated transcripts associated with synaptic function did not significantly differ in expression levels (Figure 6-1).

Discussion

To feasibly treat FXS by gene replacement, reintroduction must occur post-natally. Therefore, we wished to establish adult phenotypes that may be reversible using viral vectors. To this end we have analyzed total brain RNA from WT and *Fmr1* KO mice for expression of three mis-regulated transcripts that had been previously identified, and confirmed by real-time RT-PCR. No significant difference was seen in the expression of these transcripts (Map1b, Map2, GRK4) in our analysis.

Since Map1b may only be transiently mis-regulated (Lu et al., 2004), we were not surprised to see similar expression between the WT and KO mice. However, its importance in the Drosophila model makes Map1b of critical interest and was therefore selected. Another mis-regulated transcript that was selected, Map2, is a key mediator of synaptic architecture, known to be altered in FXS (D'Agata et al., 2002). No difference was observed in our study, and only a small difference (1.6 fold decrease) had been observed previously suggesting that the mis-regulation is subtle at best. The third transcript we selected, GRK4, belongs to a class of GPRC regulation molecules that are critical for proper neuronal function. Previously it had been shown to be decreased in the CNS of KO mice by 3-4 fold, but this was not observed in our experiment.

Perhaps if the cerebellum (where GRK4 is primarily expressed) were analyzed independently, a difference would have been observed.

Taken together, we failed to confirm the mis-regulation of three mRNA transcripts thought to be altered in the absence of FMRP. However, transient or cell specific mis-regulation, as well as altered localization or regulation of these transcripts could not be observed by our methods. Therefore, we can not rule out that these transcripts are indeed mis-regulated, and might play a role in the pathogenesis of FXS. We can confirm however that mis-regulation of total adult CNS mRNA of these three transcripts does not represent a testable *Fmr1* KO phenotype.

Materials and Methods

Total RNA was isolated from the CNS of C57 *Fmr1* KO or WT mice by the guanidine isothiocyanate (GTC) extraction method and reverse transcribed. cDNA was amplified by real-time PCR using TaqMan Universal PCR Master Mix, No AmpErase UNG (Applied Biosystems) and FAM-labeled TaqMan target-specific primer/probes (Table 6-1). PCR reactions were run in triplicate and analyzed using Applied Biosystems 7900HT Sequence Detection Systems. Cycle conditions used were as follows: 50°C for 2 min. (1 cycle), 95°C for 10 min. (1 cycle), 95°C for 15 sec., and 60°C for 1 min. (40 cycles). Threshold values used for PCR analysis were set within the linear range of PCR target amplification. Relative values of *Fmr1* cDNA in each sample was determined by normalization with the cellular cDNA for adenosine phosphoribosyltransferase (APRT). For conventional RT-PCR, *Fmr1* cDNA was amplified using the primers S1: (GTG GTT AGC TAA AGT GAG GAT GAT) and S2: (CAG GTT TGT TGG GAT TAA CAG ATC) (D-B-C, 1994). The cellular control APRT cDNA was amplified using the DB510: (GGC ATT AGT CCC GAA GAC C) and DB511: (GGC GAA ATC ATC ACA CAC C). HotStar Taq was used to amplify cDNA for 15 min. 95°C (1 cycle); 94°C 3 min., 65°C 3 min. 72°C 3 min. (1 cycle); 94°C 1min., 65°C 1min., 72°C 1min., (30 cycles).

Audiogenic Seizures (AGS) in the *Fmr1* KO

Introduction

Of those who suffer from FXS, 20% suffer from seizures, and all are hypersensitive to sensory stimulation (Musumeci et al., 1999). This corresponds well with AGS susceptibility in the KO mouse which provides a model to test potential therapeutics. AGS susceptibility in the *Fmr1* KO mouse has been mapped to the mutated *Fmr1* allele itself, although the background strain can contribute to the phenotype. This has been demonstrated by comparing *Fmr1* KO mice of several background strains including hybrids of FVB and C57 *Fmr1* KO mice (Yan et al., 2004; Yan et al., 2005). However, there is little consensus as to the age dependency and pervasiveness of this phenotype in both C57 and FVB *Fmr1* KO mice (Musumeci et al., 2000; Chen and Toth, 2001; Yan et al., 2004; Yan et al., 2005; Musumeci et al., 2007). These discrepancies may be due to differences in acoustic stimulation used to induce AGSs, or the early auditory environment in which animals are reared (Yan et al., 2005).

AGSs in rodents have been extensively studied due to their commonality among inbred strains and because the phenotype provides a test bed for anticonvulsant pharmaceuticals. AGSs can result from a genetic predisposition or be induced by an acoustic insult during a critical phase of development (termed priming) or by an ethanol withdrawal paradigm (Ross and Coleman, 2000; Faingold, 2002; Garcia-Cairasco, 2002).

Much has been done to investigate the pathological neural circuitry responsible for AGS susceptibility, and what has emerged is that the IC, and in particular the central cortex of the IC, plays a dominant role in triggering seizures (Faingold, 2002). The IC is located in the midbrain, represents the major integrative center for auditory information, and is interconnected to motor systems. Indeed, projections to the reticular formation, superior colliculus, and periaqueductal gray propagate AGS. In rodents, AGSs manifest in response to high decibel acoustic stimulation,

initiating behaviors such as wild running followed by clonicity, tonicity, and in the most severe cases (including in the *Fmr1* KO mouse) culminates in death due to respiratory arrest. The wealth of evidence implicating the IC has come from studies based on c-Fos (immediate early gene) expression, lesion, focal microinjection, 2-deoxyglucose metabolic changes, electrical stimulation, and *in vivo* neurophysiological studies (Faingold, 2002).

The exact molecular underpinnings of this behavioral phenotype are not fully understood, but ultimately result from enhanced glutamatergic (excitatory) activity and/or a decrease in GABAergic (inhibitory) signaling in the IC (El Idrissi et al., 2005). As expected, n-methyl-d-aspartate (NMDA) and agonists of NMDA receptors (NMDAR) applied to the IC can induce an AGS. Conversely, antagonists of NMDARs delivered to the IC block the phenotype. In a recent study, injection of MPEP (2-methyl-6-phenylethynyl pyridine hydrochloride), a metabotropic glutamate receptor (mGluR) group I antagonist, was found to block AGS in the *Fmr1* KO (Yan et al., 2005). Together, these experiments clearly demonstrate the importance of glutamatergic neurotransmission in facilitating AGS. γ-Aminobutyric acid (GABA) neurotransmission in the IC is also purported to underlie or at least contribute to AGS susceptibility. Specifically, the IC of AGS susceptible animals demonstrates reduced GABA inhibition occurring locally, as well as inhibitory projections originating from other loci. Furthermore, it requires a greater amount of GABA receptor agonist to achieve inhibition in the IC of AGS animals. One caveat is that levels of GABA receptors and GAD (glutamic acid decarboxylase), the GABA synthesizing enzyme, are elevated in the IC of AGS susceptible animals (Faingold et al., 1994). This seemingly paradoxical scenario is not fully understood. Finally it should be noted that increased susceptibility to AGS in the KO is not due to a general increase in brain excitability, as chemical convulsants elicit similar effects in KO and WT mice (Chen and Toth, 2001).

In the current study, we assessed the AGS phenotype in both C57 and FVB *Fmr1* KO strains to determine the age dependency and pervasiveness. Furthermore, we investigated the feasibility of FMRP expressed post-natal via viral vectors to reduce this phenotype. A viral vector approach has advantages over conventional transgenic "rescue" experiments because expression can be restored post developmentally, only in a particular brain region, and can translate into a viable treatment for FXS if therapeutic effects are observed. Also, a viral vector approach has advantages over a pharmaceutical one because they are targeted to a particular brain structure without affecting other regions, allowing for systematic rescue of the AGS pathway. Secondly, unlike pharmaceutical agents that globally alter neural excitability, we are able to reintroduce only the missing protein responsible for the phenotype, potentially giving us a much more relevant rescue than previously achieved.

Results

Given the discrepancy in recent literature as to the age dependency and severity of AGSs in *Fmr1* KO mice it was necessary to examine the phenotype first hand. C57 KO mice demonstrated a mild phenotype with only 22.73% of males displayed any type of seizure behavior (Table 6-2). Furthermore, young C57 KO mice seemed more susceptible, although more animals would need to be tested to accurately establish age dependency. Data is represented as the total number of animals displaying any seizure behavior (wild running, clonic seizures, tonic seizures, or respiratory arrest) over the total number of animals tested.

A more robust AGS phenotype has been observed in FVB *Fmr1* KO mice, and although strain effects likely contribute to the increase, the contribution of the KO allele has been established (Yan et al., 2005). In male FVB KO mice, seizure frequency increased with age. At 9 weeks, 6 out of 8 males displayed seizure behavior. This time frame is conducive to vector rescue because it allows accurate injections to be made, and for AAV vectors to begin expressing

transgenes. 37.93% of all male FVB KO mice displayed seizure behaviors, in contrast to only 4.17% of WT males. Adult animals (6 weeks of age and older) demonstrated an AGS frequency of 57.9% compared to only 4.76% of WT males at the same ages (Table 6-3).

For both C57 and FVB strains of *Fmr1* KO mice, females have fewer seizures than males (Table 6-2, Table 6-3). In addition, the age dependency was not as robust in female mice as males, although few C57 females were tested. The variability of the female KO is similar to what is observed in FXS, and has been documented in previous studies. The gender differences are likely the result of females possessing two X chromosomes where the *Fmr1* gene is located.

Comparing our results (Zeier) to those of previous reports (Yan et al., 2005; Musumeci et al., 2007) we found that seizure frequency was similar among studies (Table 6-4, Figure 6-2). Although (Yan et al., 2005) reported a higher frequency, the animals tested were younger than in the other two studies. In age matched animals, seizure frequency was similar to our results and those of (Musumeci et al., 2007).

Another way to measure the AGS phenotype is to assign a seizure severity score (SSS) calculated from the progression of seizure behaviors from wild running (1), to clonic seizures (2), tonic seizures (3), and respiratory arrest (4) (Musumeci et al., 2007). Using this ordinal rating system we compared our results with previous reports (Yan et al., 2005; Musumeci et al., 2007) and found that our animals displayed less severe seizures (Table 6-4, Figure 6-3).

Next, we wished to determine the sample size that would be required to show rescue of the AGS phenotype. To do this, we used the SSS to calculate the effect size of genotype (KO vs. WT) representing complete rescue (Table 6-4). We found large effect sizes (*d*) in each study with our data having a value of 1.052. Using these estimates of effect size we plotted the required sample size for significance in a t-test at varying effect sizes (Figure 6-4). In three studies,

complete rescue (KO vs. WT) was found to be 1.052, 3.060, and 1.670 corresponding to required total sample sizes of 32, 6, and 13 respectively.

Using our current methods of seizure induction, viral vector rescue would have to equal that of genotype (WT) corresponding to an effect size of 1.052 in order to show significance of $p<0.05$ in a t-test with a sample size of 16 animals per group (32 total animals). For an effect size of 0.5 (a rough estimate of partial rescue) 64 animals per group would be required.

No indication of rescue was observed in animals that were injected wit FAAV vectors (Table 6-2, Table 6-3) although, only a few animals (N=5) were tested, and vector delivery was not confirmed. The results do however demonstrate that injection alone does not appear to eliminate the AGS phenotype, as FVB KOs injected with FAAV or UF11 had seizures (Table 6-3).

Discussion

The *Fmr1* KO mouse provides a valuable animal model for testing potential therapeutic treatments. Arguably the most robust behavioral phenotype of the KO is susceptibility to audiogenic seizures which has been demonstrated in a number of studies (Yan et al., 2005; Musumeci et al., 2007). However, the age dependency and severity of this phenotype varies among reports, perhaps due to the disparity in seizure induction methods. Therefore, we wished to establish this phenotype ourselves, and to determine the feasibility of conducting a study using it as a measure of viral vector rescue.

We have confirmed that the C57 KO phenotype is less robust than the FVB KO, and that females are less susceptible than males. Furthermore, we have found that AGSs in C57 KO mice are less severe than in FVB KO mice with fewer mice succumbing to seizures (data not shown). Our results also indicate that in the FVB KO mouse, AGS susceptibility increases with age similar to what has been reported elsewhere (Musumeci et al., 2007) but in contrast to another

report (Yan et al., 2005). In C57 KO mice the age dependency was not restricted in young mice, although few animals were tested. For accurate injection of the inferior colliculus and to allow time for AAV vector expression to take place, rescue in young animals would be difficult. Therefore, our results are encouraging since older mice display a robust phenotype providing a logistically possible experiment to be conducted. However, if expression at a very young age is compulsory, animals as young as 3 weeks can be injected, and HSV-1 vectors could be employed which are capable of more rapid expression.

In some reports a doorbell is used to induce AGSs which is a difficult stimulus to recreate due to differences among doorbells in tone, frequency and loudness. Furthermore, the stimulus is not adjustable and therefore difficult to optimize. Therefore, we employed TonGen to create specific acoustic stimuli so that an optimal induction protocol could be established. We tested 3 tones (12kHz, 5-20kHz, and 8-63kHz) and found that the 12kHz tone worked the best (personal observation). However, our data indicate that although the frequency of AGS was similar in our study and others, the severity was not as robust. Indicating that further optimization of AGS induction is needed.

Our data indicate that given current methodology, a vector rescue study that measures SSS would require a large number of animals to be tested animals (64 animals for 2 groups). Therefore, improvements in induction are needed, as well as alternative analysis measurements. We propose that non-parametric data such as seizure frequency measured by Fisher's exact test (FET) provides a viable analysis strategy. Also, a biologically relevant rescue marker such as survival could be measured, and significance determined by FET. Alternatively parametric data could be collected such as latency to onset of seizure so that more sensitive distribution based statistical analyses could be employed. This type of measure may allow for subtle vector rescue

effects to be observed. This is an important point because complete rescue is not a likely outcome. Possible reasons for this are that vector transduction is not complete, inappropriate expression levels may not completely restore function, expression is required throughout development, or expression in multiple brain regions is required. Furthermore, it is possible that rescue is only possible when the phenotype is directly dependent on neuronal plasticity. One leading hypothesis is that enhanced long-term depression (LTD) in FXS leads to the cognitive deficits associated with the disease. Therefore, AGSs propagated in the IC, where plasticity is modest may not lend itself to rescue, whereas more plasticity dependent behaviors such as spatial learning and memory would be.

Materials and Methods

Mice

C57 and FVB *Fmr1* KO mice used in this study (D-B-C, 1994) were obtained from Dr. Bill Greenough at the University of Illinois and Dr. Bauchewitz at Columbia University respectively. Both colonies are being maintained as a breeding colony at the University of Florida.

Stereotactic injections

5-week-old *Fmr1* KO mice were anesthetized, an incision made along the midline of the scalp, and holes burred in the skull, allowing for an injector to be inserted into the CNS. Using a stereotactic frame, 2 μL injections were delivered bilaterally into the IC (AP –5.02, L+/- 1.25, V 2mm) via a glass micropipette fitted to a 10 μL Hamilton syringe at an infusion rate of 0.5μL/min. UF11 or FAAV vectors (see chapter 4) were allowed to absorb for 2 minutes before the injector was withdrawn. AGS susceptibility of vector injected animals was performed at 8 weeks of age.

Seizure induction

Mice were placed in a box 10”x10”x10” fitted with a speaker on the lid and exposed to three one minute acoustic stimuli of 12KHz, 5-20KHz, or 18-63KHz. To produce these frequencies Tone Generator software (NCH Swift Sound) was employed. The sound intensity level of approximately 120dB was confirmed using a decibel meter (purchased from Radio Shack) prior to testing. Animals were observed for seizure behaviors which include: wild running, clonicity (rhythmic muscle spasms), tonicity (rigidity), or *status epilepticus* (respiratory arrest).

Statistical analysis

Seizure susceptibility was measured by the percentage of animal that displayed any seizure behavior. Seizure severity was measured by assigning a score to seizure behaviors: wild running (1), clonic seizures (2), tonic seizures (3), or respiratory arrest (4). Power analysis was performed using G Power Version 3.0.3: a t-test between independent groups was conducted to determine the sample size required to meet significance at $p<0.05$, and a power level of 0.8 at various effect sizes. Expected effect sizes were estimated by comparing KO and WT AGS phenotypes as measured by SSS in two published reports.

Long Term Depression (LTD) in the *Fmr1* KO

Introduction

In almost all cases FXS is caused by an inherited triplet repeat expansion mutation that induces DNA methylation-dependent silencing of the Fragile X Mental Retardation gene (*FMR1*) resulting in an absence of the Fragile X mental retardation protein (FMRP) (O'Donnell and Warren, 2002). Recent evidence suggests that the lack of FMRP leads to aberrant synaptic plasticity which may be a seminal mechanism underlying mental retardation and other FXS phenotypes (Huber et al., 2002; Nosyreva and Huber, 2006). This disruption of mature synaptic

plasticity suggests that post-developmental restoration of FMRP may be therapeutic, an exciting prospect for those who suffer from FXS.

Altering the strength of neuronal interconnectivity is essential to learning and memory. This malleability or plasticity which either potentiates or depresses synaptic signaling has been extensively studied in the hippocampus, a brain structure intimately involved in learning and memory. Long term maintenance of either potentiation (LTP) or depression (LTD) relies on protein synthesis, partially occurring at the site of synaptic plasticity, particularly in dendritic spines (Sutton and Schuman, 2005; Pfeiffer and Huber, 2006). Such local protein synthesis allows for a rapid and specific response following synaptic activity. Depression of synaptic strength is mediated by at least two different pathways involving either N-methyl-D-aspartate (NMDA) or metabotropic glutamate receptor (mGluR) signaling (Pfeiffer and Huber, 2006).

FMRP binds RNA and associates with the protein synthesis machinery in dendritic spines (Ashley et al., 1993; Feng et al., 1997b; Kooy et al., 2000). Moreover, levels of the protein increase following mGluR activation, and mGluR-LTD is enhanced in the *FMR1* knock-out mouse (KO), an animal model of FXS (D-B-C, 1994; Weiler et al., 1997; Huber et al., 2002). One hallmark of FXS and the KO mouse are immature-appearing dendritic spines, and it has been suggested that enhanced mGluR-LTD may partially be responsible for the aberrant spine morphology (Irwin et al., 2000; Irwin et al., 2002; Nosyreva and Huber, 2006). These observations are an indication that FMRP is critical for normal mGluR-LTD and possibly spine maturation.

In the present study we sought to determine if FMRP replacement in an adult hippocampus could rescue the KO phenotype of enhanced mGluR-LTD. To achieve FMRP replacement we employed an adeno-associated virus (AAV) based vector that has demonstrated an ability to

robustly express transgenes within the central nervous system (CNS) (Burger et al., 2005a). Expression of transgenes from AAV vectors is long-lasting and provides a valuable tool for studying and potentially treating various neurological diseases (Mandel et al., 2006) and may also have potential to treat FXS.

KO mice (P21-30) have enhanced mGluR-LTD, induced by a mGluR type 1 agonist RS 3,5 dihydroxyphenylglycine (DHPG) or by paired-pulse low frequency stimulation (PP-LFS) (Huber et al., 2002). In older mice (P 30-60) it was subsequently shown that while wild type (WT) mGluR-LTD is protein synthesis dependent, KO mGluR-LTD is not (Nosyreva and Huber, 2006). A remarkable difference between WT and KO mGluR-LTD was observed in the presence of protein synthesis inhibitors (anisomycin or cycloheximide) using either DHPG (WT=10%, KO=30%) or PP-LFS (WT=-5%, KO=18%) induction. In the absence of these inhibitors a smaller difference was seen in DHPG induced mGluR-LTD (WT=24%, KO=32%), similar to what was seen in the earlier experiment using younger mice (WT=12%, KO=23%). However, PP-LFS induced mGluR-LTD appears to be no different between older WT and KO mice (WT=20%, KO=20%), contrary to the same analysis of younger mice (WT=7% KO=18%). These data indicate that the mGluR-LTD phenotype is most obvious in older mice when protein synthesis is inhibited. Therefore, we employed anisomycin in order to separate adult WT and KO mGluR-LTD so that the ability of vectored FMRP to rescue this phenotype could be determined.

Results

Expression of FMRP in the hippocampus

FMRP protein expression by the vector was demonstrated by immunohistochemical detection of FMRP in hippocampal slices used for the subsequent electrophysiology studies. Staining was robust, particularly in the pyramidal cell layer of CA1, the location of mGluR-LTD analysis. High levels of vectored protein corroborate mRNA expression data (Refer to chapter 4),

demonstrating more robust FMRP staining than in WT hippocampi. Additionally, the staining indicates that protein replacement has been achieved in the same neurons of the hippocampus that are known to exhibit enhanced LTD (Figure 6-5).

Rescue of enhanced PP-LTD in *Fmr1* KO mice by the FAAV vector

Analysis of adult WT and KO (P56-70) PP-LFS induced mGluR-LTD revealed a significant difference ($p<0.05$) in the presence of anisomycin (20μM) (WT=1.74%, KO=22.12%) confirming what had been shown previously (Nosyreva and Huber, 2006) (Figure 6-6, Figure 6-7).

mGluR-LTD following injection of a control vector that expresses the inert reporter gene GFP (20.38%) resembled the KO mouse group (22.12%). In contrast, KO mice that received hippocampal injections of FMRP expressing vector (6.15%) had less mGluR-LTD than un-injected KO (22.12%), or control vector injected KO mice (20.38%), and was similar to WT mGluR-LTD (1.74%). These data indicate that in the absence of protein synthesis the FMRP expressing vector reversed the KO mouse phenotype of enhanced mGluR-LTD (Figure 6-6, Figure 6-7).

No significant difference was observed between WT and KO mouse DHPG-LTD (Figure 6-8). Nor was there a difference observed between FAAV and UF11 injected KO animals, although a slight trend for FAAV injected animals to have less DHPG-LTD was observed (Figure 6-9, Figure 6-10).

Discussion

The mGluR theory of FXS postulates that protein synthesis dependent processes downstream of mGluR-signaling pathways in the CNS are enhanced in FXS resulting in cognitive deficits (Bear et al., 2004). Building upon this idea, recent findings suggest that synaptically-localized FMRP reduces steady-state levels of LTD inducing proteins (Nosyreva

and Huber, 2006). Thus, in the absence of FMRP (KO) an excess of these proteins leads to enhanced mGluR-LTD without the need for *de novo* protein synthesis. Furthermore, this group has shown that KO mGluR-LTD resembles the mature form, as it is associated with AMPA receptor internalization (Nosyreva and Huber, 2005, 2006).

Here, we show that the FAAV vector restores FMRP expression in the hippocampus of KO mice, and rescues the phenotype of enhanced mGluR-LTD when induced by PP-LFS. In accord with the mGluR theory of FXS, we hypothesize that vectored FMRP reduces the steady state levels of LTD inducing proteins, likely by sequestering their respective mRNA transcripts. Therefore, like WT mice, FAAV injected KO mice require *de novo* protein synthesis in order to maintain mGluR-LTD.

Despite encouraging results for PP-LFS, we were not able to establish the phenotype of enhanced LTD by DHPG induction, nor did we observe a difference in LTD between FAAV and UF11 injected KO animals following DHPG treatment. Previously a dramatic difference had been observed under similar conditions (Nosyreva and Huber, 2006). Since hippocampal slices were taken from the same animals for both PP-LTD and DHPG-LTD there is no difference in the age of the tissue used between the two assays, although it is possible that the induction methods could differ in their age dependency. Previously it had been shown that WT and KO animals have 24% and 32% DHPG-LTD in the absence of anisomycin respectively. For PP-LTD, WT and KO groups demonstrated equivalent LTD (20%) in the absence of anisoymycin. Therefore, a lack of anisomycin activity in our experiment could account for similar levels among WT and KO groups, but it does not account for the lack of DHPG-LTD altogether. Our sample size was similar to the previous report, making it unlikely that testing more animals would reveal an effect (Nosyreva and Huber, 2006). Transection of CA3 was performed in DHPG-LTD slices, similar

to the previous work, although we cannot rule out that the exact same removal was performed. mGluR-LTD represents only a small fraction of total LTD, especially in the presence of protein synthesis inhibitors, and is a technically difficult phenomenon to measure.

In summary, two critical questions about FXS have been addressed in this study. First, it appears that post-developmental restoration of FMRP expression can restore neuronal function as measured here. Second, our results suggest that expression of the major isoform of FMRP is sufficient to restore function making a gene therapy approach, and analysis of FMRP function more straightforward. Furthermore, our data suggests that although global transduction of the CNS may not be feasible with current vectors, a targeted delivery strategy to specific brain structures can be therapeutic, and may present substantial benefits to individuals with FXS.

Materials and Methods

Immunohistochemistry

Hippocampal slices were post-fixed in 4% paraformaldehyde following electrophysiological analysis. The following day they were paraffin embedded and 5 micron sections were cut using a microtome. Sections were stained for FMRP as described (Chapter 4).

Mice

Male C57Bl/6 *Fmr1* KO mice (D-B-C, 1994) were obtained form Dr. Greenough and maintained in standard housing on a 12 hr light/dark cycle. Wild type C57Bl/6 mice were purchased from Harlan Sprague Dawley and maintained exactly as KO mice. All procedures for animal care and use were in accordance with AAALAC guidelines.

Stereotaxic injection

At 5 weeks of age animals were anesthetized with ketamine (70-80mg/kg) and xylazine (14-15mg/kg). An incision was made on top of the skull along the midline and burr holes were placed in the skull. Injections of FAAV or UF11 vectors (approximately 1 x 10^{13} genomes/mL)

were conducted using a Kopf stereotaxic frame with a 10μL Hamilton syringe fitted with a glass micropipette. Three 1μL injections made around the coordinates AP 2.3mm, L +/-1.6mm, DV 1.5mm (from Bregma) were administered bilaterally to maximize the area of transduction in the hippocampus (CA1 *st.rad*.). A syringe pump was used to ensure accurate delivery of vector at a rate of 0.35 μL/min. One minute was allowed to elapse before the injector was removed. To alleviate pain Flunixin meglumine, (1.1mg/kg, IM) was administered twice a day as needed following surgery.

Electrophysiology

Electrophysiology was conducted using methods previously described as a guide (Huber et al., 2000; Huber et al., 2002; Nosyreva and Huber, 2006). Briefly, 400 micron hippocampal slices were collected in ice cold artificial cerebral spinal fluid (ACSF), transferred to an interface chamber (PP-LTD) or a submersion recording chamber (DHPG-LTD) (ACSF replaced at 2mL/min), and allowed to recover at 30°C for approximately 1.5 hours. Field potentials (FP) were recorded extracellularly from the CA1 for 60 minutes in response to Schaffer collateral axon stimulation (200 μsec current pulses). Baseline responses (50-60% of maximal response) were measured with simulation (10-30μA) at 30 second intervals. PP-LTD was induced with pairs of stimuli (50 ms interstimulation interval) at 1Hz for 20minutes (2,400 pulses). DHPG-LTD was induced with application of 100 μM RS 3,5 dihydroxyphenylglycine (DHPG) for 5 minutes. DHPG was purchased from Tocris 0342. 100X stocks in H_20 were prepared and stored at -20°C then diluted in ACSF prior to use. For both PP-LTD and DHPG-LTD, NMDA-LTD was eliminated by application of 100μM D,L-APV (Sigma A5282). 10X stocks were prepared in ACSF and stored at 4°C. Also, in both cases anisomycin (20μM) was used to prevent protein synthesis (Sigma A9789, prepared in ACSF prior to use). Analysis was performed blind to genotype or treatment. Average response values for a 5 minute period 60 minutes post induction

were used to calculate the % LTD. Mean response values form the same time period were used to determine significance between groups.

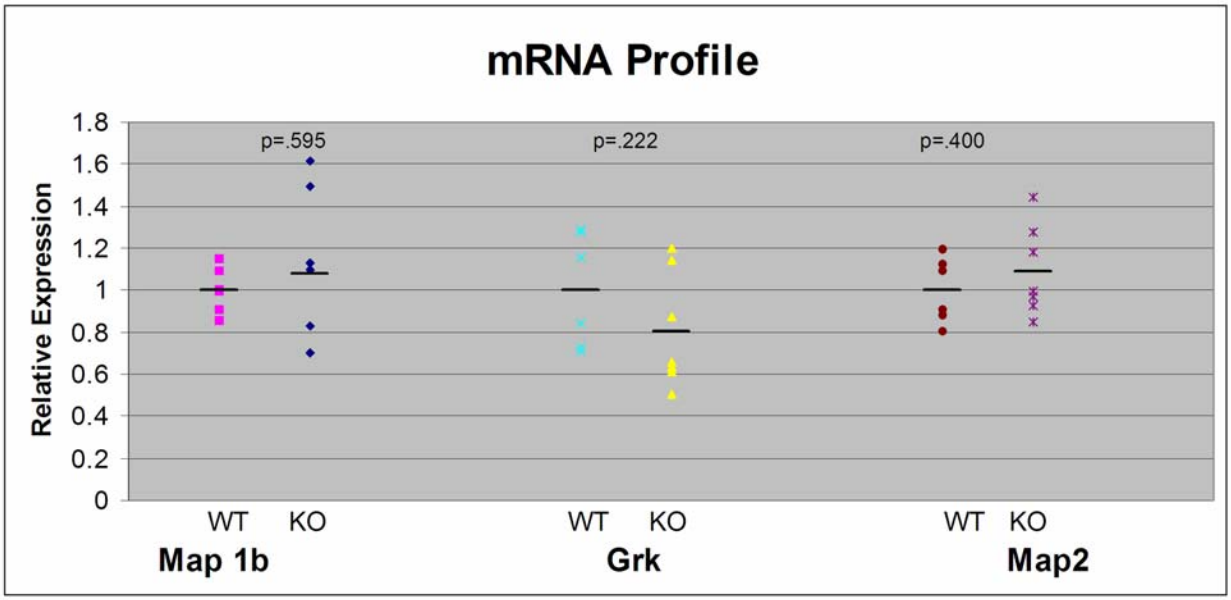

Figure 6-1. Expression of mRNA in the *Fmr1* KO mouse. Real-time RT-PCR of total brain mRNA revealed no significant difference in levels of three transcripts (Mtap1b [Map 1b] , GPRK21 [Grk], and Mtap2 [Map2]) associated with synaptic function in the *Fmr1* KO mouse.

Table 6-1. Primers used for real-time RT-PCR analysis of putative mis-regulated genes in the CNS of *Fmr1* KO mice.

Primer/Probe	Forward Primer	Reverse Primer	Probe
GPRK21	GCAGGCTGGAAGC AAATATGTTAGA	GCCCAATATCCAAGATG TTCCTACA	ACCTTTCATTCC TGATCCTC
MTAP2	GCTTTAGCCTTTGA GAACCTGTTT	GACCCAGAGTGTGTGAG TTTATTGA	CAGAGCTCGGA AGAGTT
MTAP1B	GCGAGACCGTAAC CGAAGAG	AATCAGGTTTGTGTCCC ACGAT	CCAGCTCGATG TTGCC

Table 6-2. Audiogenic seizures in C57 *Fmr1* KO mice.

Weeks of age	3	4	5	6	7	8	9	10	>10	Total	Total(%)
Male KO		1/3		1/1			3/7	0/3	0/8	5/22	22.73%
Female KO	0/1	2/4		0/3				0/3	0/6	2/17	11.76%
Male WT								0/8	0/6	0/14	0.00%
Female WT											
UF11							0/2			0/2	0.00%
FAAV							0/2			0/2	0.00%

Table 6-3. Audiogenic seizures in FVB *Fmr1* KO mice.

Weeks of age	3	4	5	6	7	8	9	10	>10	Total at all ages	Total at >6
Male KO	0/2	0/5	0/3		1/3	0/1	6/8	0/1	4/6	11/29 (37.93%)	11/19 (57.90%)
Female KO	3/7		1/5	0/4	4/13	0/1	1/6		2/13	11/49 (22.45%)	7/33 (21.21%)
Male WT	0/1		0/2	0/4	0/3	0/3	0/2	0/3	1/6	1/24 (4.17%)	1/21 (4.76%)
Female WT	0/4			0/3					0/2	0/9 (0.00%)	0/2 (0.00%)
UF11							1/2	1/3		2/5 (40.00%)	
FAAV							0/2	3/4		3/6 (50.00%)	

Table 6-4. FVB/NJ KO audiogenic seizure susceptibility across studies.

Study	Genotype	AGS (%)	N	AVG(SSS)	SD	EFFECT(d)
Zeier (PND >42)	KO	57.89%	19	1.211	1.548	1.052
	WT	4.76%	21	0.048	0.218	
Yan (PND 21-30)	KO	93.33%	15	3.330	1.397	3.060
	WT	18.18%	11	0.182	0.405	
Musumeci (PND 45)	KO	63.60%	33	2.600	1.660	1.670
	WT	0.00%	43	0.280	1.050	

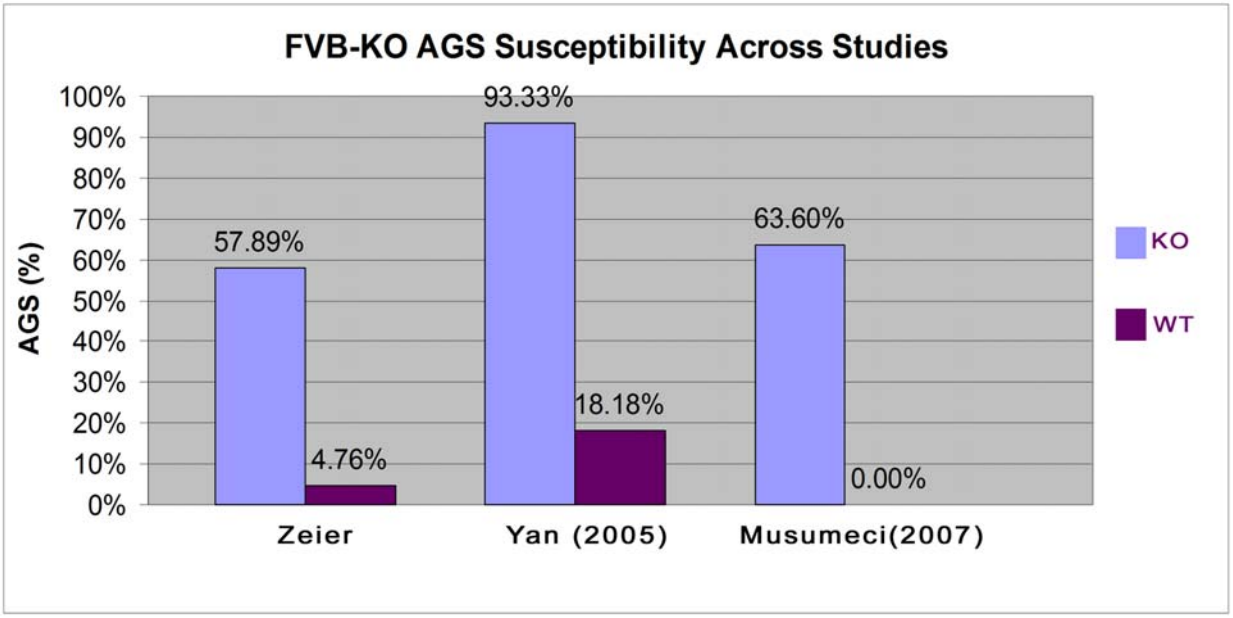

Figure 6-2. FVB/NJ-KO AGS susceptibility across studies. The frequency of seizures (number of animals displaying any seizure behavior divided by the total number of animals tested) was calculated and compared across reports of the phenotype (see Table 6-4 for N values).

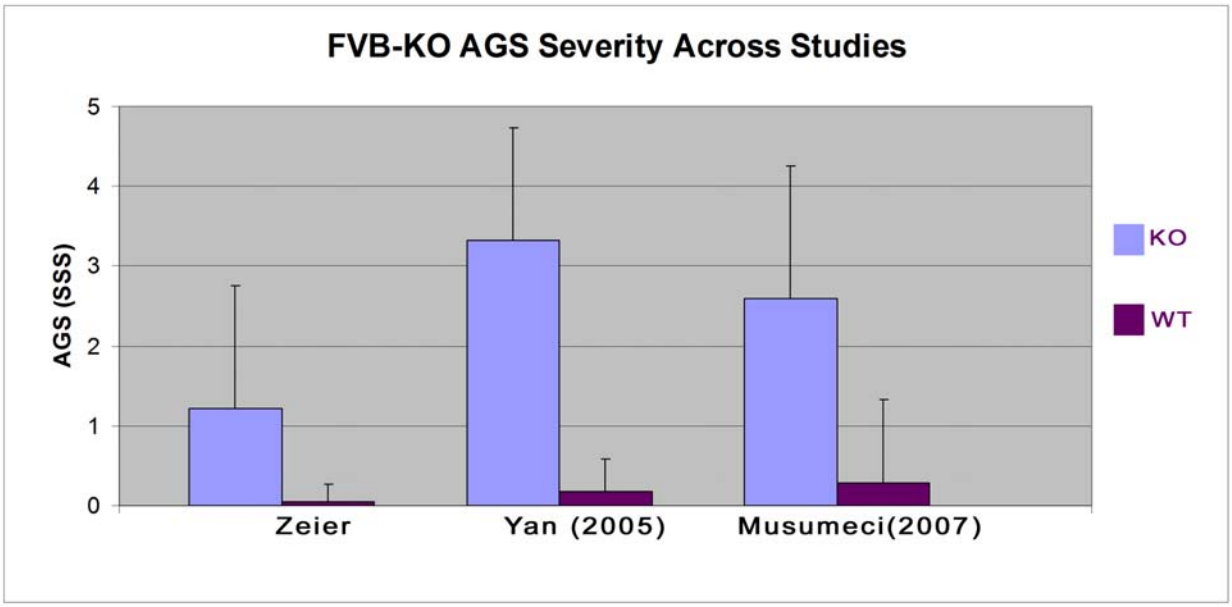

Figure 6-3. FVB/NJ-KO AGS severity across studies. To measure the seizure severity, a score of 1 for wild running, 2 for clonic seizures, 3 for tonic seizures, and 4 for respiratory arrest was assigned (see Table 6-4 for N values).

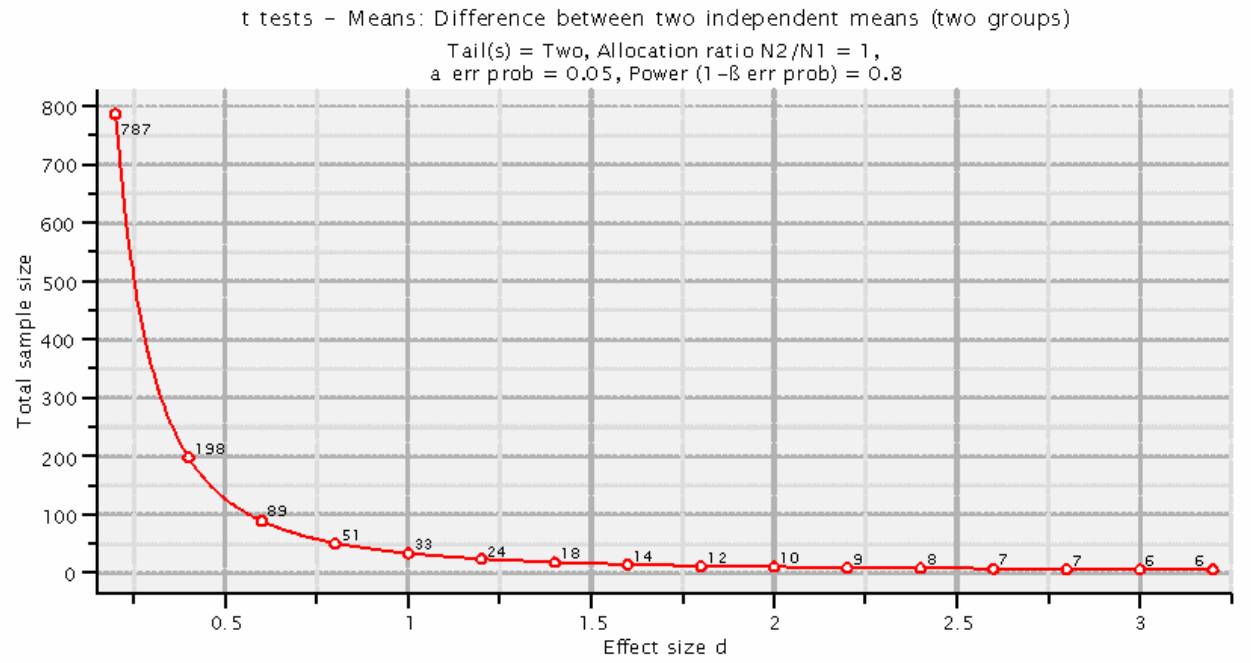

Figure 6-4. Power analysis of AGS rescue. The required sample size (Y axis) needed to show significance ($p<0.05$) in a t-test is plotted against the effect size (X axis) Power analysis was performed using G Power Version 3.0.3.

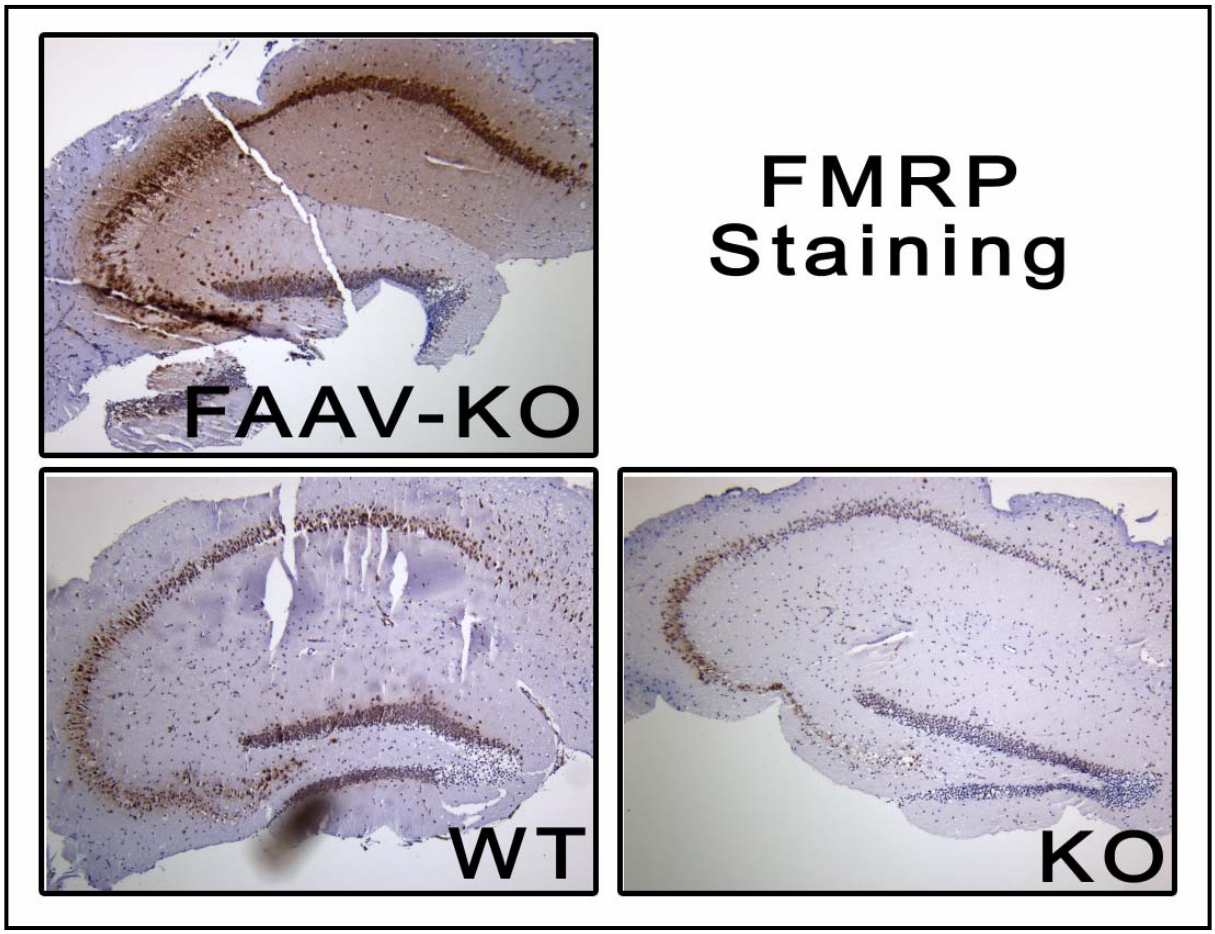

Figure 6-5. Immunohistochemical detection of FMRP expression by FAAV in the hippocampus. KO mice received 3 injections (1µL/injection) of the FAAV vector in each side of the Hippocampus around the coordinates (-0.19mm AP, +/-0.15mm Lat, -0.17mm DV, from Bregma) to ensure complete transduction. Animals were perfused 3 weeks later and the tissue prepared for electrophysiological analysis. Subsequently, hippocampal sections were prepared for immunohistochemical detection of FMRP using the IC3 monoclonal antibody and peroxidase/substrate visualization (brown). Sections are counterstained with Hematoxalin (blue) (see materials and methods).

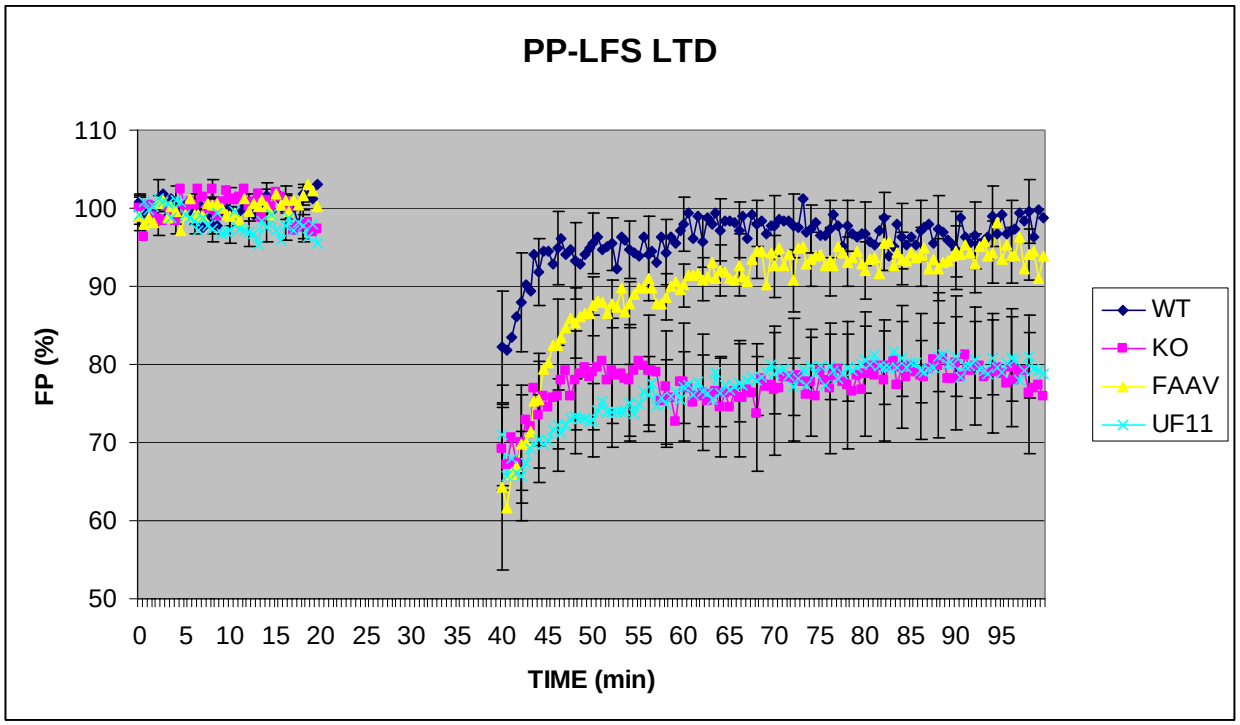

Figure 6-6. Enhanced PP-LFS induced mGluR-LTD in the hippocampus of *Fmr1* KO mice is rescued following hippocampal injection of the FAAV vector. PP-LTD is measured as the slope of field potentials (+/-SE), normalized to baseline, and plotted against time. In the presence of a protein synthesis inhibitor (anicomycin), and an NMDA receptor antagonist (AP5), KO mice (purple squares [N=8]) demonstrate enhanced PP-LTD compared to WT mice (blue diamonds [N=8]). 3 weeks post injection of the control, GFP expressing vector UF11, KO mice shows no change in PP-LTD (light blue hatches [N=10]). In contrast, KO mice receiving injections of the *Fmr1* expressing vector FAAV, demonstrate WT levels of PP-LTD (yellow triangles [N=7]).

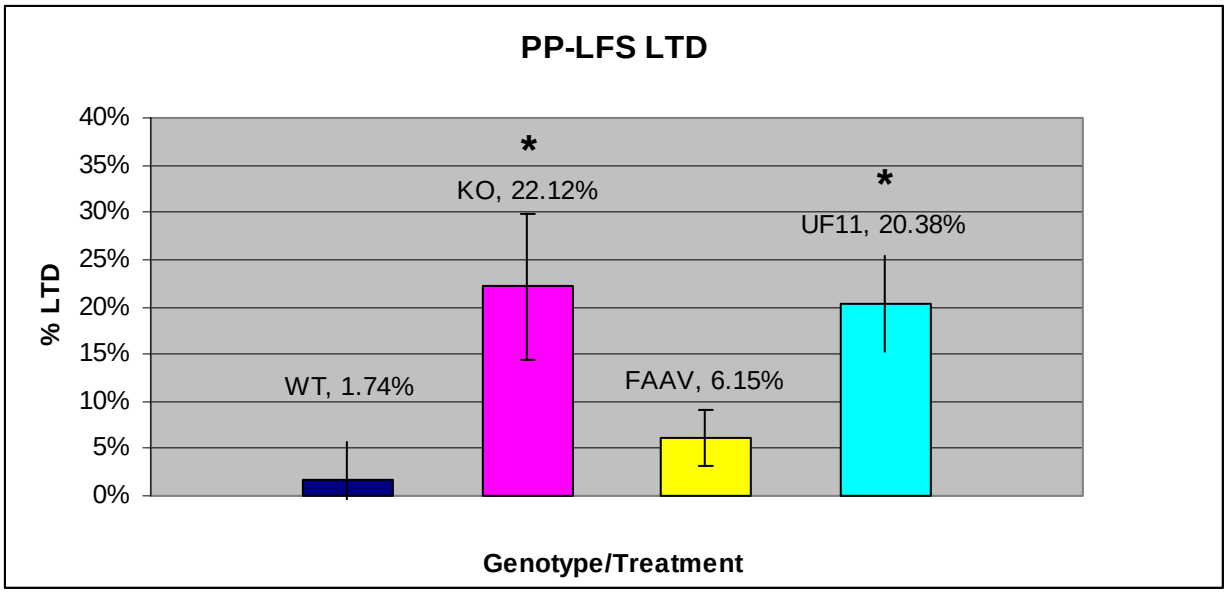

Figure 6-7. Percent reduction of PP-LTD from baseline in field potential recordings (+/-SE). KO mice and UF11 injected KO mice demonstrate significantly more depression (*) than WT mice whereas FAAV injected mice do not.

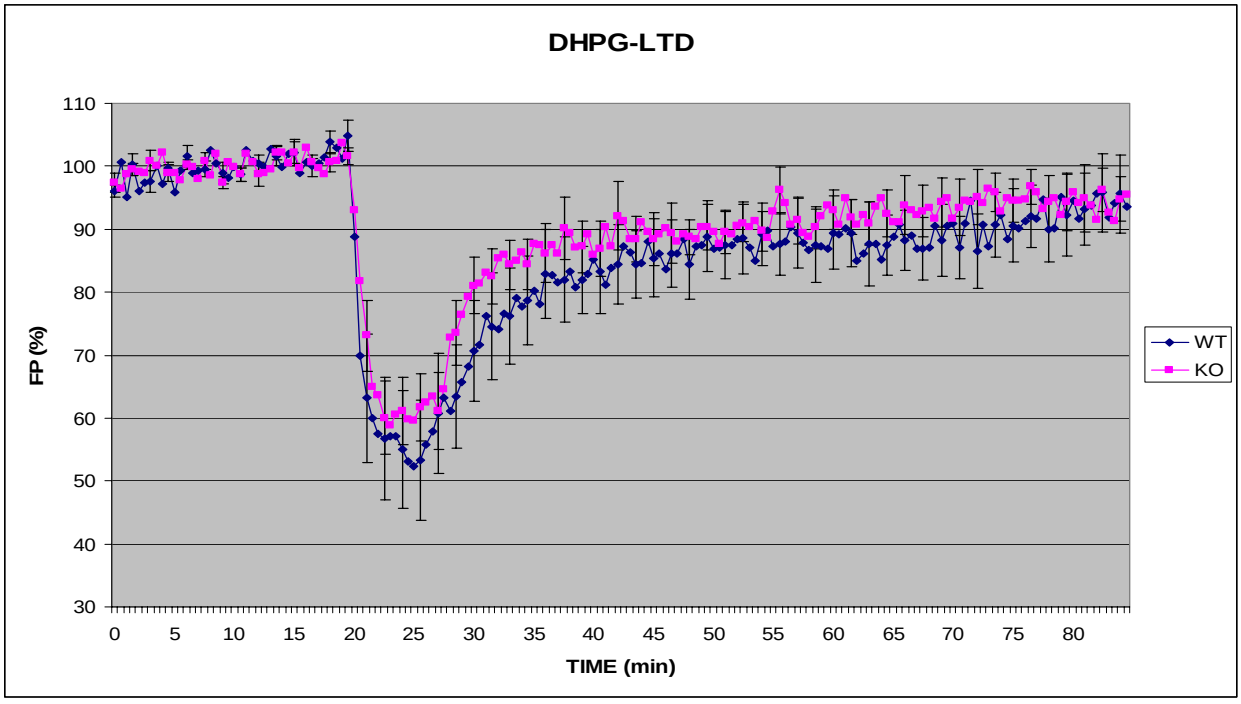

Figure 6-8. Analysis of DHPG-LTD in the hippocampus of WT and KO mice. In the presence of anisomycin and AP5, the group 1 mGluR agonist DHPG-induced LTD was not found to be different between WT (N=7) and KO (N=8) mice in our analysis.

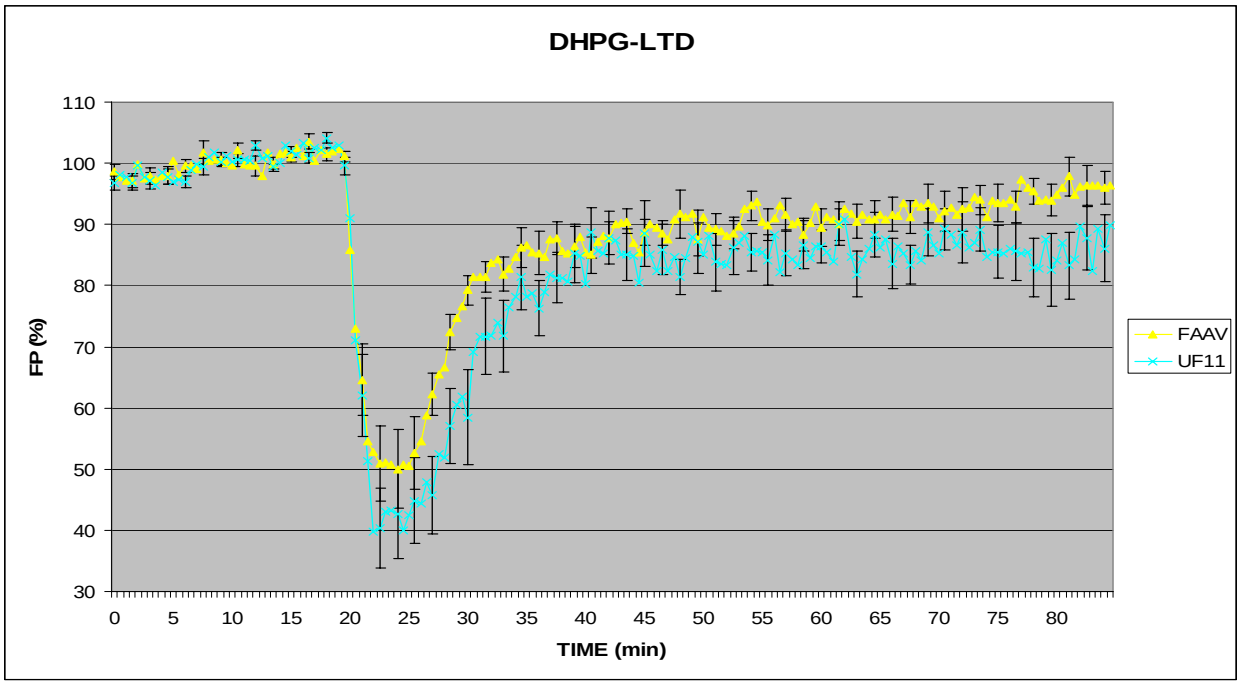

Figure 6-9. Analysis of DHPG-LTD in the hippocampus of UF11 and FAAV injected KO animals. 3 weeks post-injection, KO mice injected with UF11 (N=8) or FAAV (N=12) did not differ in the level of drug induced mGluR-LTD.

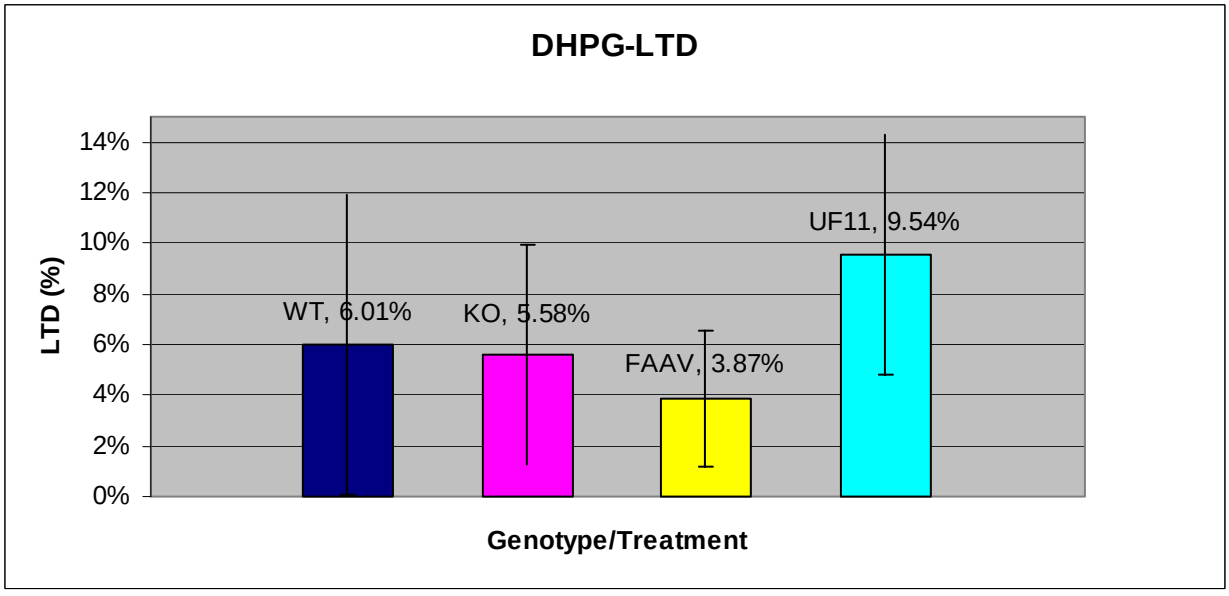

Figure 6-10. Analysis of DHPG-LTD shown as percent reduction from baseline recordings of field potentials revealed no significant difference between WT and KO mice. Nor was a significant difference observed between FAAV and UF11 injected mice 3 weeks post injection.

CHAPTER 7
DISCUSSION

Our overriding hypothesis of this dissertation was that facets of FXS are treatable by a gene therapy approach. The syndrome results from a single gene loss of function mutation and has a well characterized animal model in which to test potential therapies. Furthermore, adult synaptic plasticity is abnormal in FXS indicating that post-developmental restoration of protein function may translate into therapeutic behavioral alterations. Therefore, we constructed viral vectors capable of restoring gene expression. To validate our hypothesis, we tested these vectors for their ability to rescue several phenotypes associated with FXS and have demonstrated that some can be rescued. However, for such therapy to ultimately be successful, several challenges must be addressed.

First, it must be established that the major isoform of FMRP in the CNS, accounting for approximately 40% of total FRMP, is sufficient to restore normal function. This is especially critical if AAV vectors are employed, as the virion is not capable of accommodating multiple genes encoding the various isoforms, or the natural *Fmr1* locus which is approximately 38 Kb. However, if the critical isoforms were to be identified, then co-infection of multiple AAV vectors, each expressing a different isoform, could potentially overcome this problem. An alternative approach is the use of HSV-1 based vectors capable of accommodating large portions of genetic material which are currently being developed and may prove useful for expression of the entire *Fmr1* locus. Nonetheless, recent findings have shown that audiogenic seizures are reversed by expression of the major isoform of FMRP in a transgenic mouse indicating that it alone is therapeutic (Musumeci et al., 2007). Similarly, our results suggest that the major isoform is sufficient to restore function with respect to mGluR-LTD. These studies provide strong evidence that restoration of the major isoform of FMRP has therapeutic value for FXS and

makes a gene therapy approach to the disease using either AAV or HSV-1 vectors a feasible one. Furthermore, expression of only one isoform at a time using viral vectors may be advantageous for elucidating the mechanistic properties of FMRP because it allows for each isoform to be investigated independently.

Another important consideration is that limiting expression to only the coding sequence of *Fmr1* may not be ideal since the 3'UTR may be important for localization and regulation of the transcript, possibly by FMRP itself (Brown et al., 1998). Furthermore, the mouse and human 3'UTRs share 80% homology suggesting that there are conserved functions. However, FMRP likely binds its own transcript at a location within the coding sequence (Schaeffer et al., 2001). Therefore, it is interesting to speculate that FMRP negatively modulates the translation of its own mRNA providing a feedback inhibition mechanism. Such regulation would not be abrogated in our approach since the binding site now appears to be located in the coding sequence and not in the 3'UTR as previously thought (Brown et al., 1998).

While the ability to perform phenotypic rescue in animal models is encouraging, a practical limitation for human gene therapy is that global transduction of the CNS is not feasible using current vectors. Therefore, a targeted approach like the one we have taken must prove efficacious if clinical application is to be attempted. Indeed, systematically treating behavioral symptoms of FXS by restoring FMRP expression in locations of the brain responsible for them is a practical treatment strategy. Furthermore, multiple injections, or utilization of agents that increase vector dissemination could be used to enhance vector delivery (Burger et al., 2005b).

Another practical consideration related to the controlled expression of transgenes is that current vectors are not capable of utilizing endogenous promoters due to shutdown, a mechanism that is not fully understood, although in some cases DNA methylation is thought to be

responsible (Lo et al., 1999). Instead, to achieve long-term expression, we are relegated to artificial promoters engineered to overcome transgene silencing. The implications of this are expression of FMRP in neuronal as well as non-neuronal cells, and artificial gene regulation. Nonetheless, using artificial promoters, long-term transgene expression has been achieved (Burger et al., 2005a; Mandel et al., 2006). A vector re-administration strategy can increase expression duration but is inherently hazardous and can induce a vector neutralizing immune response (Peden et al., 2004). It has been suggested that expression of *FMR1* using artificial promoters would not be useful in treating FXS since normal (synaptic activity dependent) gene expression would be abrogated (Rattazzi et al., 2004). However, in a recent study, a reversal of the AGS phenotype was seen when an artificial (CMV) promoter driven *FMR1* gene was introduced into a KO strain by transgenic methods (Musumeci et al., 2007); although other phenotypes were not (Gantois et al., 2001). Furthermore, it is likely that regulation of FMRP in the context of synaptic function does not occur at the level of transcription. Indeed, mGluR-LTD itself is not dependent upon *de novo* transcription (Huber et al., 2001). Rather, FMRP regulation at the level of translation and proteolysis may be critical for proper mGluR-LTD (Hou et al., 2006).

Another possible obstacle to our approach is the finding that over-expression of *FMR1* and FMRP by transgenic methods leads to abnormal phenotypes in mice, suggesting that over-expression may be pathological (Peier et al., 2000; Rattazzi et al., 2004). However, this conclusion may have been premature. First, the transgenic over-expression occurs throughout development which may cause the harmful effects that were seen. Our gene therapy approach only restores expression in the adult, perhaps circumventing this problem. Second, the conclusions regarding over-expression in the transgenic mouse were based on the finding that

while KO mice demonstrate hyperactivity and reduced anxiety, transgenics that over-express *FMR1*, demonstrate hypoactivity and elevated anxiety. To conclude that over-expression is pathological based on these findings is not warranted in our opinion especially since the KO phenotypes do not entirely correspond to FXS. A more relevant finding is that both WT and KO mouse mGluR-LTD is abolished when *FMR1* is over-expressed in the transgenic mouse. Therefore, over-expression may not restore normal mGluR-LTD but rather over compensate (Hou et al., 2006). Whether this over-compensation is pathological or therapeutic remains to be determined. Third, the transgenic mouse used in these experiments express the human *FMR1* gene in a mouse. Although the mouse and human FMRP share 97% homology, they are known to differ in mRNA binding properties (Denman and Sung, 2002). Fourthly, over-expression of every isoform in the transgenic mouse may have deleterious effects in the CNS whereas expression of only the major CNS isoform may not. Finally, it is known that premutation carriers that over-express mutant *FMR1* mRNA develop Fragile X tremor/ataxia syndrome (FXTAS) later in life despite having normal levels of FMRP (Hagerman and Hagerman, 2002). Since the mutant *FMR1* mRNA (as exists in permutation carriers) is etiological rather than over-expression itself, our approach is not likely to induce pathology associated with FXTAS. In summary, we do not believe that over-expression of FMRP is deleterious, and our success in phenotypic rescue supports this conclusion. Nonetheless, vectors have been generated that express low levels of *FMR1* and could be employed if over-expression is found to be harmful.

Safety is a major consideration for any potential therapy, especially for viral vector based gene therapy. Both HSV-1 and AAV viral vectors are highly efficacious in the CNS and both can be attenuated to ensure a high degree of safety. However, minimally attenuated HSV-1 vectors, which are the most efficacious, are also the most toxic *in vitro*. *In vivo*, there have been

conflicting reports as to the toxicity of ICP4 mutant HSV-1 vectors. Therefore, we examined the host response to an ICP4 mutant HSV-1 vector using microarray technology. We determined that the ICP4 mutant induced antigen presentation pathways but did not induce innate immune pathways such as toll-like-receptor signaling, death receptor signaling, and NFκB induction, and only mildly induced interferon, chemokine, and cytokine signaling pathways. These findings indicate that ICP4 mutants offer a high degree of safety, and that transgene silencing is not likely induced by a strong innate immune induction.

In summary, our gene therapy approach represents a viable approach to restoring *FMR1* gene expression in FXS, yet several challenges must be overcome before it can translate into an actual therapeutic method for treatment. Nevertheless, two critical questions about FXS have been addressed in this study. First, it appears that post-developmental restoration of FMRP expression can restore some normal neuronal function as measured here, and that this restoration is therapeutic. Second, our results suggest that expression of the major isoform of FMRP is sufficient to restore function making a gene therapy approach, and analysis of FMRP function, more straightforward.

Future experiments using the FAAV vector are aimed at answering other critical questions about FXS. First, we wish to determine if the vector can rescue abnormal dendritic spines found in the KO mouse (Irwin et al., 2002; Grossman et al., 2006). Dendritic spine dysmorphism occurs in other diseases associated with mental retardation and may represent a shared feature of such cognitive disorders. Therefore, phenotypic rescue of spine dysmorphism in FXS would indicate that the phenotype may be rescued in other forms of mental retardation. Furthermore, it would suggest that dendritic spine dysmorphism in FXS is more likely due to aberrant neuronal plasticity rather than an irreversible developmental malformity.

A second question is whether audiogenic seizures in *Fmr1* KO mice can be prevented using viral vectors. The phenotype in KO mice corresponds to FXS since an estimated 20% of individuals with FXS suffer from seizures and are hypersensitive to sensory stimulation (Musumeci et al., 1999). Reversal of this KO phenotype would provide evidence that gene therapy may be used to treat seizures in FXS. Recently it has been shown that low levels of expression of the major FMRP isoform can rescue the AGS phenotype using transgenic methods (Musumeci et al., 2007). This is encouraging news, but from a treatment standpoint we wish to determine if post-developmental delivery of FMRP in a targeted brain structure can produce the same results. To this end we have confirmed the age dependency of the AGS phenotype. We found that older mice are susceptible to AGSs, providing the opportunity to assess viral vector rescue. However, a power analysis has demonstrated that current induction methods are not sufficient to induce AGSs in a testable manner. Future studies may refine the induction methods and employ alternative measures of seizure behaviors allowing for vector rescue of the phenotype to be assessed.

APPENDIX A
RECOMBINANT HSV-1 PREPARATION PROTOCOLS

Preparation of HSV-1 Transfection DNA

1) Trypsinize 5 confluent T75 flasks of rabbit skin cells and resuspend each flask in a total of 15 mLs of MEM. Seed 10-150mm dishes (or 10 T-150 flasks) with 7 mLs of this cell suspension by adding the cells to 20 mLs of supplemented media in each dish. Incubate overnight at 37˚C. Note: This prep typically yields 300-1000µg of HSV-1 DNA. This can be scaled down if desired. Note that this procedure can be adapted to perform to isolate virus from a single 15 mm well (see "Virus Mini-prep Protocol").

2) The following day (the dishes should be approximately 90% confluent at this point) the media is removed and cells infected with 5 ml of media containing 2 x 106 pfu (moi = 0.01) of HSV-1. The virus is allowed to adsorb to the cells for 60 min at 37˚C. The dishes are rocked gently 1/2 way through the incubation.

3) After 1 hour, 25 ml media is added to the cells, and the dishes incubated until all of the cells have rounded, and detach easily when the dish is swirled. This usually takes 2-3 days.

4) Harvest the cells from the frisbees by pipeting and "blasting" the cells off the bottom of the dish. Transfer to Sorvall bottles, and centrifuge at 16,000 x g (~10,000 rpm in a GSA rotor) at 4˚C for 40 min. (This pellets the cells and free virus).

5) Pour off the supernatant and resuspend the pellet in hypotonic lysis buffer (10ml) and transfer to a conical 15 ml Falcon™ tube. Vortex hard, and incubate 5 min on ice. After the incubation on ice, vortex again briefly.

6) Centrifuge at 3000 xg (~ 2500 rpm in an IEC centrifuge) for 10 min at 4˚C (this pellets the nuclei).

7) Transfer the supernatant to a new conical tube and add: 1 ml 10% SDS and 0.5 ml 20 mg/ml Pronase (this gives a final concentration of 1% SDS and 1 mg/ml Pronase).

8) Incubate for 1 hour at 50˚C.

9) After 1 hour, add another 0.5 ml of 20 mg/ml Pronase and incubate an additional 2 hours at 50˚C (or overnight at 37˚C).

10) Phenol extract 2 x.

11) Phenol/SEVAG (1:1) extract 2 x.

12) SEVAG extract 1x.

13) Dialyze vs. 1 x TE overnight at 4˚C (with 2 changes of buffer). (Alternatively the DNA can be "spooled" following the addition of 1/10 vol of NaAc (3M) and 2.5 vol of cold EtOH. This approach is quicker and often yields slightly cleaner DNA).

14) Determine the concentration of DNA spectrophotometrically by reading at A260.

15) Digest 1µg of DNA with HindIII and electrophorese on an agarose gel along with uncut to determine the purity of the DNA. There will be some cellular contamination, but the viral DNA should be the predominant form, and there should be little evidence of smearing.

16) For long-term storage of the DNA, it is advisable to aliquot the DNA into small fractions and freeze.

Notes

1) If you are preparing DNA for transfections, probably the biggest single parameter in determining how efficient transfections are is the quality of the transfecting viral DNA. In order to work, the transfection DNA needs to be unit length--that is not sheared or degraded. Care should be taken at all steps after the SDS/Pronase digestion not to vortex or vigorously pipette the DNA.

2) In order to avoid contamination of the viral DNA with cellular DNA, do not freeze the virus prior to pelleting out the nuclei. Also, do not allow the infection to incubate after 100% CPE has been achieved.

Solutions

Hypotonic lysis buffer

10 mM Tris, pH 8

10 mM EDTA

0.5% NP-40

0.25% NaDOC

Transfection of HSV-1 DNA

Transfections are performed in 60 mm dishes on subconfluent monolayers of rabbit skin (RS) cells. The RS cells are propagated in Modified eagle's medium (MEM) supplemented with 5% calf serum and glutamine, Penn/Strep. Unit length HSV-1 DNA is co-transfected with the desired plasmid at various ratios using a modified calcium phosphate precipitation procedure. The transfections are generally allowed to proceed until 100 % CPE is evident (usually 3-4 days), though the dishes may be harvested earlier if one wishes to prevent amplification of siblings.

1) 60 mm dishes are seeded from a flask of actively growing RS cells at a ratio that will produce a cell density of approximately 50% confluence the following day (typically 1/30th of a T75 flask/60mm dish). The dishes are incubated O/N at 37˚C, 5% CO2.

2) The following day, the media is removed from the dishes (which should be at 50% confluence) and replaced with MEM supplemented with 1.5% fetal bovine serum. The dishes are then incubated O/N at 31.5˚ C, 5% CO2. This is to serum-starve the cells.

3) The transfection mix is prepared by diluting the desired amount DNA (typically 1 - 10 µg of HSV-1 per dish; and a 10-fold molar excess of the linearized plasmid DNA) in a final volume of 225 µl of TNE buffer. After the dilutions have been made, 25µl of a 2.5 M CaCl2 is added to each tube.

4) The DNA is precipitated by adding 250 µl of 2x HEPES buffer to the above sample while mouth bubbling the solution with a Pasteur pipette.

5) The solution is then incubated for 20 min at room temp.

6) Aspirate the 1.5% FBS MEM from the 60 mm dishes, and pour on the transfection mix. Incubate the dishes at room temp for 20-30 min.

7) Add 5 ml of 1.5% FBS MEM and incubate for 4 hrs at 37˚C. Do not remove the DNA solution.

8) After 4 hrs, aspirate the media and wash the monolayer with media 2 x, and then hypertonic shock the cells briefly (less than 1 min) by adding 1-2 ml of Shock buffer (1x HEPES, 20% dextrose solution).

9) Aspirate the shock buffer and wash 2x with media. After the last wash, add 5 ml of MEM 5% calf serum to the dishes, and incubate 3-4 days at 37˚C, 5% CO2.

10) The transfections are harvested by scrapping into the media. Recombinants are screened by plaqing the cells on RS cells, and picking the plaques into 96 well dishes to which media has been added to the wells. These dishes are frozen, and 50 µl of each well used to infect 96 wells dishes of confluent RS cells. These dishes are then dot blotted, and probed with the desired insert. Typical transfections yield 2-20 positives per 96 well dish.

Critical parameters

--The DNA should be clean, and the HSV-1 DNA obviously needs to be handled gently to insure that it is full-length.

--The exact amount of HSV-1 DNA used per transfection is generally in the range of 1-10μg. The optimal amount for a given DNA prep should be determined empirically by transfecting a dilution series and scoring for transfection efficiency.

Solutions

TNE: 10mM Tris (pH 7.4), 1 mM EDTA, 0.1 M NaCl

2 x HEPES: (for 100 mls): 1.6 g NaCl; 74 mg KCl; 37 mg Na2HPO4:7H2O; 0.2 g Dextrose; 1 g HEPES (free acid). pH to 7.05, aliquot and store at -20˚C.

40% Dextrose: w/v in distilled water. Store at 4˚C.

All solutions are filter-sterilized.

Plaquing of Transfections for Recombinants

Transfection mixes are plated onto confluent monolayers of rabbit skin cells in 60 mm or 100 mm dishes. Generally, from a transfection that was performed in a 60 mm dish that was allowed to go to 100% CPE, dilutions of 10-5 or 10-6 yield well-isolated plaques that are suitable for picking.

1) seed 60 mm dishes with 12-16 drops of a standard cut of RS cells. Seed enough dishes to yield at least 2 dishes per dilution (so you will have enough well-isolated plaques to pick. Generally, from a transfection that was performed in a 60 mm dish that was allowed to go to 100% CPE, dilutions of 10-5 or 10-6 yield well-isolated plaques that are suitable for picking.

2) the following day, the dishes should be confluent. Dilute the transfection stock (10-2 to 10-6) and infect the monolayers with 0.5 ml of the appropriate dilution.

3) Allow the virus to adsorb for 1 hour (in the CO2 incubator). Be sure to rock the dishes and rotate 180˚ at the half way point (30 min).

During this incubation, prepare the agarose overlay:

a) microwave 1.5% agarose (sterile) at setting 3 for 8 min. until melted, and place in 45˚C water bath.

b) place 2xMEM (complete) in 37˚C water bath

4) After 1 hour, the infected monolayers are overlayed with 0.75% (final) Agarose in 1 x supplemented media, and incubated for 2 days. Don't mix the components until right before you are ready to pour!

5) Let the agarose overlay harden at room temperature for 20 min, and return dishes to incubator.

6) On the morning of the third day, the dishes are counterstained with neutral red to aid in the visualization of the plaques. A 1:30 dilution of the Neutral red stock solution is made in unsupplemented media. An equal volume of the neutral red overlay is then added to the dishes on top of the agar overlay (for 60 mm dishes, 5 ml of diluted neutral red is added to each dish), and the dishes are incubated at 37˚C (in the CO2 incubator) until the monolayers are stained red. For rabbit skin cells this is approximately 6 hours.

3) After the monolayers are stained, the liquid overlay is aspirated and the plaques are picked using a sterile Pasteur pipette. The plaques are picked by applying slight pressure to the bulb of the pipette, then coring the plaque straight down, and twisting the pipette. The bulb is then released, and the plaque aspirated partially into the pipette. The plaque is then expelled into a well of a 96 well dish that has been filled with 2-3 drops of media.

4) After all of the plaques are picked, the dish is frozen at -70˚C, and then thawed in the incubator.

5) The plaques are then amplified by plating onto a 96 well dish of confluent rabbit skin cells. The media is "flicked" off the dish, and using a multi-channel pipetter, 50 µl of the wells with the

plaques are transferred to the 96 well plate with the rabbit skins cells. The virus is then allowed to adsorb for 1 hr at 37˚C. At the end of the adsorption period two drops of supplemented media is added to each well, and the dishes incubated until the wells show 100% CPE (usually 3 days).

Dot Blotting of 96 Well Dishes to Screen for Recombinants

1) After cells in the wells of the 96 well dishes have reached full CPE (usually 3-4 days), they are ready to be dot-blotted.

2) Set up the millipore dot-blot apparatus with 1 piece of blotting paper underneath a piece of nylon membrane (Hybond-N™ or Nytrans™). Wet the blotting paper and membrane completely before clamping the apparatus together.

3) After clamping the apparatus together apply vacuum. Using a multi-channel pipetter, transfer 50 ml of the infected cells from each well of the 96 well dish to the apparatus (Pipette the wells up and down several times to mix before transferring).

4) After the media has filtered through the apparatus, add 200 ml of Solution A to each well of the apparatus.

5) Likewise, after Solution A has filtered through all of the wells, add 200 ml of Solution B.

6) Finally, after all of Solution B has filtered through the apparatus, add 200 ml of Solution C.

7) Remove filter from apparatus, label the filter (remember to mark orientation), and bake at 80˚ C for 1 hr. The blot is now ready for hybridization.

8) Freeze the 96 well dish at -70˚ C for later use.

Amplifying Stocks of Viral Recombinants From 96-well Dishes

1) Split RS cells into a T75 flask (4 mls of trypsinized cells per flask).

2) The following day, the flask should be 80-100% confluent. Remove the medium and infect the cells by adding 5 ml of media + 50µl of virus-infected cells from the 96 well dish from the last round of plaque-purification screening.

3) Allow the virus to adsorb for 1 hr, rocking the flask after 30 min.

4) Add 15 ml of supplemented medium, and incubate 3 days (or until 100% CPE is observed).

5) The day before harvesting, split RS cells into a 24 well dish (4 drops trypsinized RS cells per well, in 2 ml medium).

6) Harvest the cells, freeze-thaw 2x, aliquot the virus into 1 ml fractions and freeze.

7) Remove 1 vial to titrate the virus.

Titration of Virus Stocks

1) Set up serial dilutions of the virus stock into MEM from 10-2 to 10-9 in 5 ml snap cap tubes as follows:

10-2 = 20µl + 1.980 ml of MEM

10-3 = 200µl (10-2 dilution) + 1.8 ml MEM

10-4 = 200µl (10-3 dilution) + 1.8 ml MEM

etc.

--Be sure to vortex the virus stock and each dilution tube prior to addition it to the next tube.

--Be sure to use a new pipette tip for each dilution to prevent carry-over!

2) Dump the media off a confluent 24-well plate and label as follows:

3) Add 200µl of each viral dilution in triplicate starting at 10-9 . (or you make different dilutions and can plate out from 10-1 to 10-8 if you prefer).

4) Place the dish in the CO2 incubator for 1 hour to allow the virus to adsorb.

5) Prepare the overlay media by adding 0.15ml of human γ globulin per 50 ml of complete MEM. Warm to 37˚C in a water bath.

6) After the 1 hour incubation period, flick the infecting inoculum into the bleach bucket and add 2 ml of the overlay medium per well.

7) Incubate 2-4 days (until plaques are clearly visible). Generally 2 days for 17+ and 3 days for KOS is a good guideline.

8) Dump off the overlay medium into the bleach bucket, and add several drops of crystal violet (enough to cover the bottoms of the wells) to each well of the dish. Rock the dish for a few seconds and dump off the crystal violet into the bleach bucket. Rinse off the crystal violet with a gentle stream of tap water (2 - 3 times) until no more crystal violet comes off. Blot the dish dry on a paper towel, and let dry.

Large Scale Growth of HSV-1

1) Ten (10) 150 cm dishes or T-150 flasks are seeded with RS (rabbit skin) cells and maintained in supplemented MEM (5% CS) until just sub-confluent.

--Seed the 10 flasks or dishes with trypsinized cells from 5- T-75 flasks (90% confluent). At this density, the flasks should be ready to infect the following day. If not, it is important to feed the cells the day before you intend to infect.

--Never infect flasks that are fully confluent or the virus yields will be greatly reduced! They should be 90% confluent.

2) The media is removed, and the dishes or flasks are infected at a m.o.i. of 0.01 in an infecting inoculum of 7 ml.

3) The virus is allowed to adsorb for 1 hour at 37˚ C (with rocking at the half-way point).

4) Supplemented media is added (25 ml per dish or flask).

5) The flasks are incubated for 3-4 days or until it is obvious that the infection is complete. (CPE and/or the cells detach).

6) Harvest the infected cells by shaking the cells off the flask (or scraping with a rubber policeman), and transferring to 250 ml Sorvall™ bottles.

7) Pellet the virus and cell debris by spinning the bottles at 10,000 rpm (16,000 x g) for 40 min. at 4˚ C in a Sorvall or Beckman JA-21 centrifuge.

8) Decant the supernatant, and resuspend the pellets in a total volume of 2 ml of MEM + 10% FBS. Freeze-thaw the stock 1 x and vortex vigorously. Aliquot into 200 µl fractions. Store the virus at -70˚ C.

9) When ready to titrate the stock, thaw 1 vial and dilute 10-2 to 10-9. Titrate dilutions in triplicate on 24-well dishes of confluent RS cells.

Harvesting HSV-1 Virus Stocks

1) Harvest virus once infection has gone to 100% CPE (all cells are rounded and are starting to come off the dish).

2) Detach the cells from the bottom of the flask by shaking.

3) Pour the cell suspension into a 250 ml Sorvall bottle.

4) Pellet the virus by spinning at 10,000K in the GSA rotor at 4˚C for 40 min. (This pellets the cells and free virus).

5) Decant the supernatant into a bleach bucket, and resuspend the viral pellets in a total of 1 ml of media (for 10 T75 flasks).

6) Freeze thaw the stock 2x, vortexing in between.

7) Aliquot the virus into 1.5 ml screw cap tubes (~300µl each) (do 1 extra with 50µl for titration).

8) Freeze and store at -50˚C or below.

9) Thaw out the 50µl aliquot and titrate

APPENDIX B
RECOMBINANT AAV PREPARATION PROTOCOLS

Large Scale Transfection

Seeding Cell Factory with 293 Cells (T225s)

Warm media to 37°, wipe with ETOH

Dilute 5 mL of trypsin-EDTA in 45 mL 1XPBS in a 50 mL conical

Take 8 T225s, discard media, and wash with 10 mL PBS

Add 4 mL diluted trypsin-EDTA and rock until cells start to peel

Shake flask to lift cells

Add 16 mL of DMEM-10 FBS to neutralize the Trypsin-EDTA (20 mL TV)

Collect cells in 250 mL conical

Add ~1090 mL of media to aspirator bottle

Add cells to aspirator bottle

Load cell factory, equalize, and incubate 37°C until transfection

Splitting 293 Cells in T225s

Take 2 T225s, discard media and wash with 10 mL PBS

Add 4 mL diluted trypsin-EDTA and rock until cells start to peel

Shake flask to lift cells

Add 16 mL of DMEM-10 FBS to neutralize the Trypsin-EDTA (20 mL TV)

Collect cells in 250 mL conical

Bring vol up to 250 mL with DMEM-10

Add 20 mL of DMEM-10 FBS to each flask

Add 25 mL of cells to 10 T225s (do not re-use more than 3 times)

Incubate 37°C

Splitting Out of Factories

From a confluent factory do a 1:4 split

Make up media and trypsin

25 mL of trypsin n a 250 mL conical, top off with 250 mL PBS

Pour off old media from factory #1

Rinse factory #1 with ~250 mL PBS

Add trypsin/EDTA-PBS to peel cells

Add 900 mL of media to aspirator bottle (1.1 liters TV)

Dilute trypsinized cells in factory #1 with media (rinse factory/cells with media)

Pour cells/media into an empty media bottle

Add 250 mL of cells and 1 liter of media to factory #1 (re-seed) which will be transfected

Add 300 mL of cells and 1 liter of media to each remaining factory

Equalize and incubate at 37°C

Transfect #1, #3, #4 in 24 hrs, carry #2 for 3 days

You can pass cells five times in one factory if you are careful.

Transfections (for one cell factory0

Thaw 2X HBS and keep at 37°C until ready to use

Pre-warm media and FBS (1 L of DMEM, 90 mL FBS)

Calculate DNA and water to add:

Want 1867.5 ug of pDG, and 622.5 ug of rAAV per factory

(60ug/plate; 45 ug pDG: 15 ug rAAV)

Calculate vol (W/H) of total input DNA in mL

Subtract total input DNA from 46.8 to calculate amount of dH20

dH20/prep = ([1.125 ml/plate X plates/prep] – total input DNA)

Prepare media, Add 2-50 mL conicals of FBS to 1 liter of DMEM

Add H20 to 250 mL conical

Add input DNA to 250 mL conical

Add 5.2 mL CaCl to 250 mL conical (CaCl/prep = (0.125 mL/plate X pates/prep)

Check cell factory for confluency, 75% is ideal

Discard media from cell factory

Add 52 mL of 2X HBS to 250 mL conical and mix well

HBS/prep = (1.25 mL/plate X plates/prep

Swirl Tx mix for 1 minute

Add transfection mix to media

Pour media into aspirator bottle and load cell factory

Equalize, and incubate at 37°C for 48-60 hrs

Harvesting Transfected Cell Factory

In AAV hood

Rock to dislodge non-adherent cells and discard media

Add 500 ml of PBS to aspirator bottle and wash the cell factory

Add 5 mL of 500mM EDTA to 500 mL PBS (1:100 dilution = 5mM final concentration)

Add 500 mL of PBS=EDTA to cell factory with aspirator bottle

Spread and shake to lift cells off plastic

Pour cells into 2-250 mL conicals

Add 500 mL of PBS to cell factory to rinse remaining cells

Pour cells into 2-250 mL conicals

Centrifuge at 1K, 4°C for 10-15 minutes to pellet cells

Discard supernatant

Store cells in -20°C

Small Scale Transfection

Seeding Plates with 293 Cells (150mm plates : 20 plate prep)

Warm media to 37°C, thaw FBS and wipe with ETOH

Prepare 1 L of DMEM-10 FBS

Dilute 5 mL of trypsin-EDTA in 45 mL of 1 X PBS in a 50 mL conical

Discard media from flask, and wash with 10 mL PBS (4-T225s or 6-7 T150s)

Seeding ratio: 5:1 150mm plates : T225

3:1 150 mm plates : T150

Add 4 mL diluted trypsin-EDTA and rock flaks until cells start to peel

Shake flask to lift cells off bottom

Add 21 mL of DMEM-10 FBS to neutralize the Trypsin-EDTA (25 mL TV/flask)

Collect cells in 250 mL conical and top with DMEM-10

Add 12.5 mL DMEM-10 to each plate (20 plate prep)

Add 12.5 mL cells to each plate (20 plate prep) [total vol/plate=25mL]

Incubate 37°C O/N, Tx next day

Splitting 293 Cells (15 cm plates : 20 plate prep)

Take 3 T225s, discard media and wash with 10 mL PBS (same for 150s)

Add 4 mL diluted trypsin-EDTA and rock until cells start to peel

Shake flask to lift cells off bottom

Add 21 mL of DMEM-10 FBS to neutralize the Trypsin-EDTA (25mL TV)

Collect cells in 250 mL conical

Bring vol up to 250 mL with DMEM-10

Add 20 mL of DMEM-10 FBS to each flask (13 mL for T150s)

Add 25 mL of cells to 10 T225s (12 mL for T150s, TV=25 ml in T150)

Incubate 37°C

Transfections (15cm plates : 20 plate prep)

Thaw 2X HBS and keep at 37°C until ready to use

Pre-warm media and FBS (11 of DMEM, 90 mL FBS)

Calculate DNA and water to add:

60ug/plate: 45ug pDG : 15ug rAAV

(20 plate prep: 1200 ug/prep: 900ug pDG : 300ug rAAV

calculate vol (W/H) of total input DNA in mL

calculate amount of dH20 to add (20 plate prep: 22.5 mL –input DNA)

dH20/prep=([1.25 ml/plate X plates/prep]-total input DNA)

Prepare media, Add 2-50 conicals of FBS to liter of DMEM

Add H20 to 250 mL conical

Add input DNA to 250 mL conical

Add 5.2 mL CaCl to 250mL conical (20 plate perop: 2.5mL)

(CaCl/prop=(0.125 mL/plate X plates/prep)

Check plates for confluency, 75% is ideal

Discard media from plates

Add new media to plates (12.5 mL DMEM-10 for 20 plate prep)

Add 2X HBS to 250 mL conical and mix well (20 plate prep : 25 mL)

HBS/prep=(1.25 mL/plate X plates/prep

Swirl Tx mix for 1 minute (cloudy is OK, but precipitants are bad)

Add media to transfection mix (top to 250 mL for 20 plate prep

Pipette cells into each plate (12.5 mL/20 plate prep : yields 25 mL TV per plate)

Swirl plates to mix well

Incubate at 37°C for 3 days in 140

Harvesting Transfected plates (15cm)

In AAV hood

Scrape plates with cell scraper to dislodge all cells

Collect cells and medium in 250 mL conicals

Centrifuge at 1K, 4°C for 10-15 minutes to pellet cells

Discard supernatant

Store pellet in -20°C

Vector Purification

Freeze/Thaws

Thaw cell pellet from harvest, resuspend in 60 mL Lysis buffer

Aliquot (4 x 15 mls) into 50 ml conicals and vortex

Freeze for 10 minutes in a dry ice and ETOH bath

Thaw for 15 minutes at 37°C and vortex

Do three total freeze thaws

Save small aliquot for quality control

Benzonase (to digest cellular DNA)

To each 15 mL aliquot add 3 uL of 5M MgCl2 and vortex

Add 1uL of Benzonase (250U/mL) (5000 U Sigma E1014)

Incubate at 37°C for 30 minutes

Centrifuge for 20 minutes at 5000 x g

Pipette lysate (supernatant) into 2-50 mL conicals and store at -80°C

OR pipette into quick seal tubes for Iodixanol step

Iodixanol

Using a Pasteur pipette add the lysate (4 x 15 mL) to 4 Beckman 39mL tubes (342414)

Carefully underlay each aliquot of lysate with:

9 mL of 15% Iodixanol

6 mL of 25% Iodixanol

5 mL of 40% Iodixanol

5 mL of 60% Iodixanol

Using a 60 ti rotor, centrifuge at 59k at 18°C for 2 hrs

Place centrifuge tube in a clamp, wipe with ETOH, vent top with needle, and remove AAV band with another needle. Pull ~7 mL of the full AAV virions (yellowish) from the interface of 40 and 60 % iodixanol layers. *avoid taking the interface between the 40% and 25% iodixanol bands.

Save small aliquot for quality control

Q-Sephaose Purification of AAV(5)

Column: Q-Sepharose Fast Flow Amersham 17-0510-01

Column pack: 1.5 x 10 cm empty column = ~10 mL volume

Buffer A (binding buffer):

20mM Tris-HCl, pH 8.5/15mM NaCl (20mLs 1M Tris + 980 mL H20 + 3 mLs 4M NaCl)

Elution buffer (Buffer A/.5M NaCl):

200 mL BufferA/15mM NaCl + 5.844 g NaCl = Buffer A /0.5M NaCl

In cold room set up column and equilibrate with buffer A

UV=2.0, flow rate = 1mL/min, chart speed = 0.5 mm/min, collect 3mL/tube

Dilute virus 1:2 with Buffer A

Collect flow through, save small aliquot for quality control

Wash, save small aliquot for quality control

Elution buffer

Pool fractions from with spike in spec reading

Save small aliquot for quality control

Place at -80 °C

Concentration of Virus

Amicon Ultra (Millipore) 100K MWCO (cat.UFC910008)

Pre-wet 100K MW cut off concentrator with 2-3 mL 1 x PBS

Apply pooled elutent from Q-sepharose column

Top concentrator to ~15 mL with 1x PBS (added dropwise)

Centrifuge at ~ 3K for 20 min. to bring volume down to 1 mL

Top with 9 mL of PBS and wash virus (1:10 wash)

Centrifuge at ~ 3K for 20 min. to bring volume down to 1 mL

Do 2 total 1:10 washes (20:1)

Bring volume down to 500 uL in final wash

Transfer virus to 1.5 mL microfuge tube and aliquot

Save small aliquot for quality control (including ~10 uL for quantification)

Vector Quantification (Dot Blot)

DNAseI

(Boehringer Mannheim 776785, to digest extra-capsid DNA)

To 4 uL of concentrated virus add:

20 uL of 10 buffer

2uL DNAseI

174 uL of dH20

Total volume = 200 uL

Incubate 37°C

Proteinase K (Roche 1373196)

(to digest capsid and inactivate DNAseI)

To the 200 uL DNAse sample add:

5 uL EDTA (0.5M) = 10mM

25 uL SDS (10% = 1 %)

12.5 uL Protinase K (20mg/mL) = 1mg/mL

Incubate 55°C 1 hr.

Ethanol Precipitation

To the proteinase K sample add an equal volume of phenol/chloroform

Vortex for 5 min.

Microfuge for 5 min at 14 K

Save aqueios layer in new 1.5 mL tube

Repeat (2 total phenol/chloroform extractions)

Chloroformextract 1x 1:1

Vortex 5 min

Centrifuge for 5 min at 14 K

Save aqueous layer in new tube

Add 1/10 volume 3M NaAcetate, vortex

Add 1 uL of glycogen (20 ug/uL)(Boehringer Mannheim 901393)

Add 2-3 x Volume 100% EtOH, vortex

Percipitate O/N at -20°C

Centrifuge for 20 min at 14K at 4°C

Wash pellet in ice cold 75% EtoH

Centrifuge for 5 min at 14 K at RT

Discard supernatant and air dry 5 min

Resuspend DNA in 40 uL of dH20, and quantitate by A260

*The initial sample was 4uL and the resuspension is 40uL therefore it's a 1:10 dilution

Dot Blot Assay

Prepare 24 tubes for standard curve, mark them from 1 to 12 and 1' to 12'. First set is for 2x dilution series and second is for standard curve itself.

Tubes 1' to 12' and tubes 1:1 and 1:10 (for samples) put 200uL of Alkaline buffer.

2x-dilution series: in tubes 2 through 12 put 50 uL of dH2O in tube 1 put dH2O according to calculation and add 1 or 2 uL of DNA.

Calculations for diluting plasmid DNA:

Needed concentration of plasmid DNA is 5 ng/uL = .005 ug/uL divide given concentration by.005ug/uL (for exp: 1.3ug/uL/.005ug/uL=260-dil fac)

To have .005 ug/uL concentration: Add 1 uL of DNA to dilution factor minus 1 (1uL add to 259 uL of H2O) or add 2 uL of DNA to 2x (dil fac minus 1)(2uL add to 518uL of H2O)

From tube 1 take 50uL and add to tube 2 and son on to tube 12, change tips and vortex tubes every time

Transfer 10 uL of solution from 2x series tubes to tubes for standard curve. Transfer, starting from tube 12 (12 to 12', 11 to 11' etc) don't have to change tips

Add virus to sample tubes:

DNAse/protinase samples (with 4uL/40uL=1uL/10uL concentration)

1:1 tubes: add 10uL of sample

1:10 tubes: add 1 uL of sample

Column or crude virus sample:

1:1 tubes: add 1uL of virus

1:10 tubes: add 10uL from diluted sample (99uL of H2O and 1uL of virus)

Wet 2 pieces of whatman paper and put on dotblotter. Wet membrane (Hybond-N+, Amersham) and put on top of whatman

Press top of dotblotter to check circles

Put 400uL of H2O into wells, vacuum fast

Transfer all solution (apprx 215uL) from standard curve tubes to the wells, do it from tube 12' to tube 1', don't have to change tips

Transfer all solution (aprx 215uL) from sample tubes to the wells, change tips!

Bang for bubbles. Connect light vacuum for 10 minutes

Add 400uL of alkaline buffer into each well with standard curve and samples. Let stand for 5 minutes, vacuum dry

Write date and probe on membrane, and place on filter paper (DNA side up)

Dry in oven at 80°C under vacuum, or in microwave to crosslink.

If virus concentration is too low, extend standard curve or use more sample

Probes for dot blot

Amersham RPN1633 RediPrimerII Random Primer Labeling System. Remove unincorporated nucleotides by G-50 spin column (Amersham 27-5335-01)

Prehybridization

Incubate membrane in Hybridization solution for 2 hr. at 65°C

Denature probe at 100C for 5 min and on ice for 5 min, quick spin

Hybridization

Add 14 uL/5mL hybridization solution. Incubate O/N at 65C

Wash membrane

Wash three times with wash solution (15 min at 65C) collect in radiation waste.

Image on phosphor image scanner.

Solutions

CaCl2 (2.5M) (147.02g/mol)

Make 6 mL aliquots and store at -20C

2X HBS

NaCl (58.44 g/mol) 16g

KCl (74.56 g/mol) 0.74g

Na2HPO4-H20 (137.99 g/mol) 0.27g

Dextrose (Sigma 9434) (180.16 g/mol) 2g

HEPES (238.3 g/mol) 10g

Q.S to 1L

pH to 7.05 with 0.5 M NaOH

place in 55mL aliquots and store at -20C

CsCl

Cesium Cl (1.377) (168.36 g/mol) 509.5g

PBS (1X) to 1 Litter

Filter sterilize

Lysis Buffer (150mM NaCl, 50mM Tris pH 8.5)

NaCl (58.44 g/mol) 8.766g

Tris (121.14 g/mol) 6.055g

dH20 to 1 Liter

pH to 8.5

Filter sterilize

Iodixanol

	Optiprep (60%)	5M NaCl	5xTD	dH20	Total Volume
15%	45mL	36mL	36mL	63mL	180mL
25%	50mL		24mL	46mL	120mL
40%	68mL		20mL	12mL	100mL
60%	100mL				100mL

5xTD (5x PBS, 5mM MgCl, 12.5mM KCL)

PBS 500mL of 10X stock

MgCl (203.3 g/mol) 1.0165g

KCl (74.56 g/mol) 0.932g

Alkaline Buffer (0.4M NaOH, 10mM EDTA pH 8.0)

20 mL 10M NaOH

10 mL 0.5M EDTA

Q.S to 500mL

Pre/Hybridization buffer (7% SDS, 0.25M NaHPO4 pH7.2, 1mM EDTA pH8.0)

700 mL 10% SDS

191 mL 1M Na2HPO4

79 mL 1M NaH2PO4

2mL 0.5M EDTA

Wash Buffer (1%SDS, 40mM NaHPO4 pH 7.2, 1mM EDTA pH 8.0)

100 mL 20x SSC

10 mL 10% SDS

890 mL H20

APPENDIX C
SUPPLEMENTAL MICROARRAY DATA

Table C-1. Cross validation of 8117/43 vs. mock arrays.

Array id	Class label	Genes/ classifier	CCP	DLD	1NN	3-NN	NC	SVM
040904A_18-R	81R	224	YES	YES	YES	YES	YES	YES
050404A_81-R	81R	214	YES	YES	YES	YES	YES	YES
050904A_81-R	81R	212	YES	YES	YES	YES	YES	YES
081404A_81-2d-R	81R	433	NO	NO	NO	NO	NO	NO
091504A-01_81R 2d	81R	241	YES	YES	YES	YES	YES	YES
092304A-01_812d-R	81R	260	YES	YES	YES	YES	YES	YES
081404A_M-2d-R	MR	272	YES	YES	YES	YES	YES	YES
081404A_M-3d-R	MR	265	YES	YES	YES	YES	YES	YES
100404A-01_M2dR-A	MR	222	YES	YES	YES	YES	YES	YES
100404A-01_M2dR-B	MR	219	YES	YES	YES	YES	YES	YES
100404A-01_M3dR-A	MR	220	YES	YES	YES	YES	YES	YES
100404A-01_M3dR-B	MR	221	YES	YES	YES	YES	YES	YES
Mean percentof correct classification:			92	92	92	92	92	92

BRB Array tools cross-validation anaysis identified one array (081404A_81-R) that failed all tests and was subsequently removed from the mock Vs. 8117/43 analysis. Classification method abbreviations: compound covariat predictor (CCP), diagonal linear discriminant (DLD), 1-nearest neighbor (1-NN), 3-nearest neighbors (3-NN), nearest centroid (NC), support vector machines (SVM).

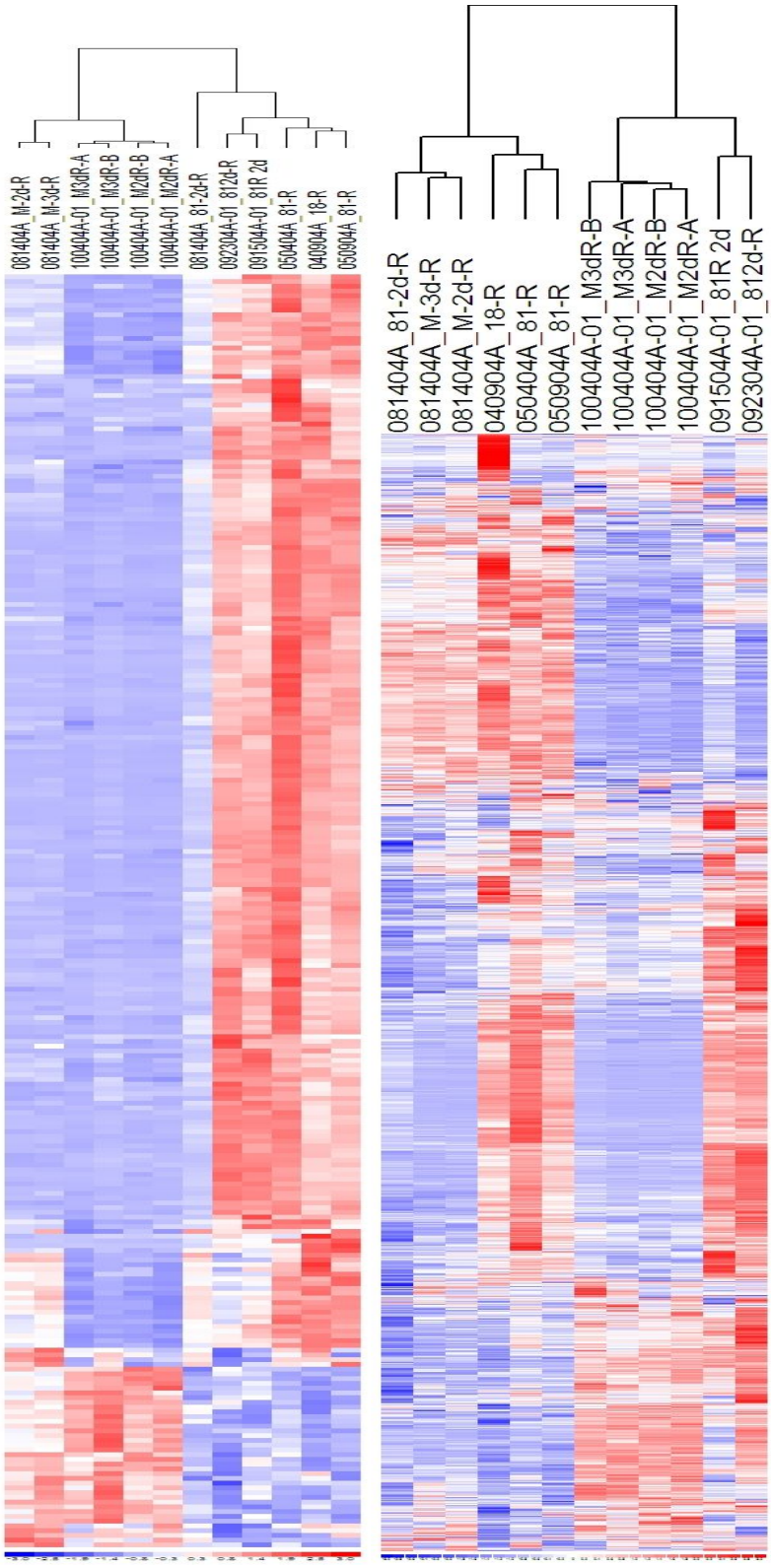

Figure C-1. Supervised (Left) and unsupervised (right) cluster analysis 8117/43, and mock injected arrays were performed using dChip.

A

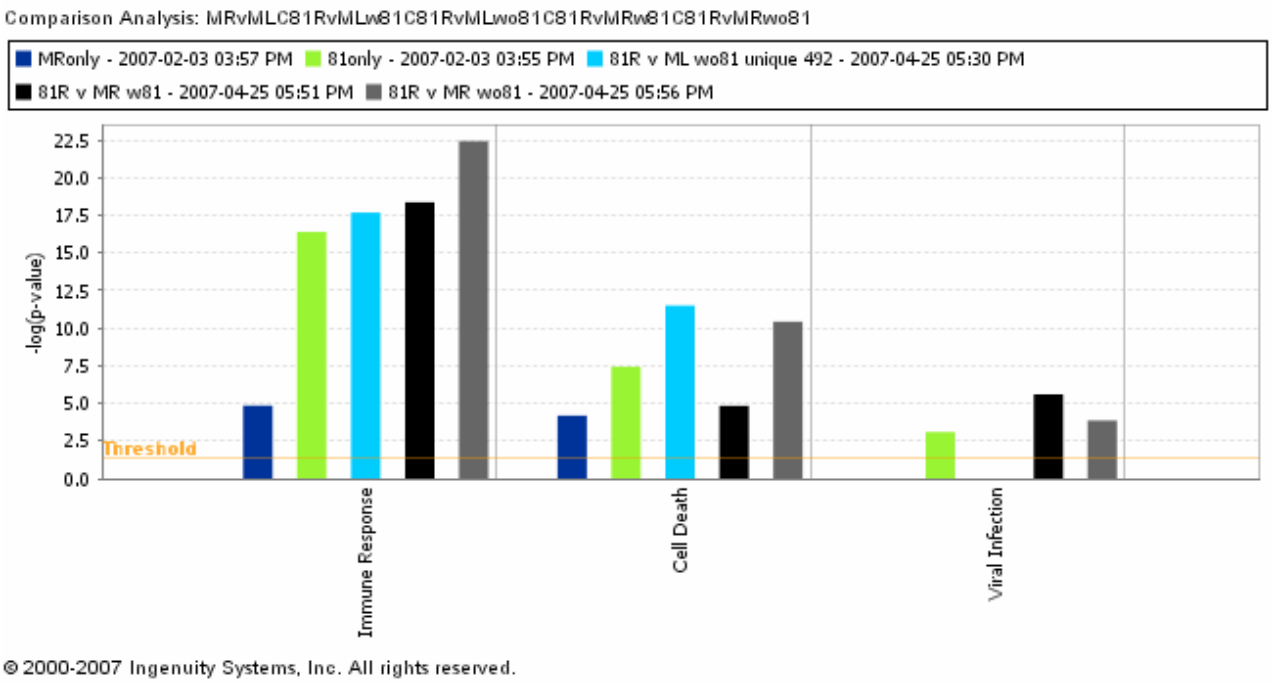

B

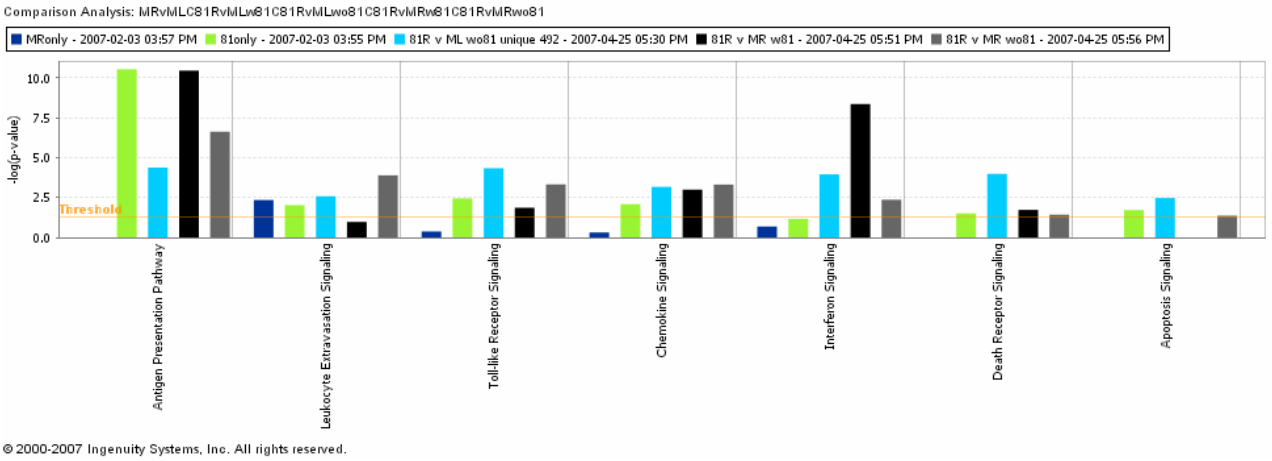

Figure C-2. Ingenuity pathway analysis of the putative 8117/43 outlier. Comparison of 8117/43 arrays controlled against mock injection, or uninjeted arrays with and without the putative outlier demonstrates, no major differences in biological functions as determined by IPA. However, antigen presentation pathway is more significant when the outlier is included. Cell death function is more significant when the outlier is excluded. In one case (8117/43 vs. mock) interferon signaling is somewhat represented when the outlier is included. A) IPA functions. Regardless of the inclusion of the outlier or whether it is compared to mock or un-injected control arrays, the major functions are consistent. B) IPA pathways. Pathways identified by IPA remain consistent regardless of control or outlier inclusion. Analysis and figure generation were performed using Ingenuity Pathway Analysis with permission (Ingenuity® Systems, www.ingenuity.com).

Table C-2. Cross validation of 8117/43 vs. un-injected arrays.

Array id	Class label	Genes/ classifier	CCP	DLD	1NN	3-NN	NC	SVM
040904A_18-R	81R	478	YES	YES	YES	YES	YES	YES
050404A_81-R	81R	434	YES	YES	YES	YES	YES	YES
050904A_81-R	81R	446	YES	YES	YES	YES	YES	YES
081404A_81-2d-R	81R	781	NO	NO	NO	NO	NO	NO
091504A-01_81R 2d	81R	493	YES	YES	YES	YES	YES	YES
092304A-01_812d-R	81R	511	YES	YES	YES	YES	YES	YES
081404A_M-2d-L	ML	573	YES	YES	YES	YES	YES	YES
081404A_M-3d-L	ML	590	YES	YES	YES	YES	YES	YES
100404A-01_M2dL-A	ML	461	YES	YES	YES	YES	YES	YES
100404A-01_M2dL-B	ML	458	YES	YES	YES	YES	YES	YES
100404A-01_M3dL-A	ML	461	YES	YES	YES	YES	YES	YES
100404A-01_M3dL-B	ML	450	YES	YES	YES	YES	YES	YES
Mean percent of correct classification:			92	92	92	92	92	92

The putative outlier reduced the number of significant genes identified in BRB array tools class comparison analysis and failed all cross validation tests but similar biological functions are observed whether or not it is included. For 8117/43 vs. mock it was included, for 8117/43 vs. un-injected it was removed. Classification method abbreviations: compound covariat predictor (CCP), diagonal linear discriminant (DLD), 1-nearest neighbor (1-NN), 3-nearest neighbors (3-NN), nearest centroid (NC), support vector machines (SVM).

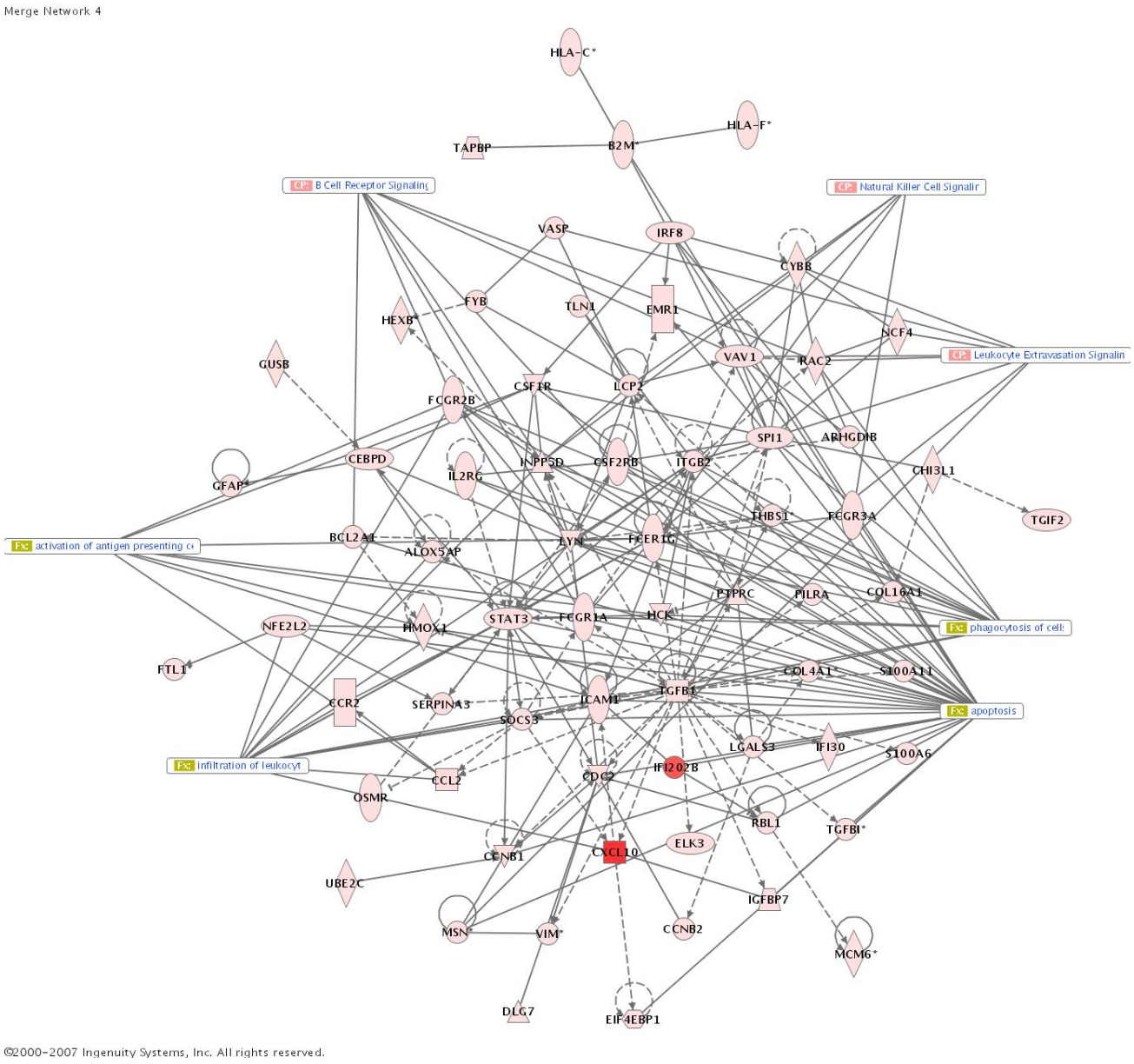

Figure C-3. Ingenuity pathway analysis network of significant genes common to both 8117/43 and mock. Analysis and figure generation were performed using Ingenuity Pathway Analysis with permission (Ingenuity® Systems, www.ingenuity.com).

Table C-3. Cross validation for UR v MR combine time-point comparison.

Array id	Class label	Genes/ classifier	CCP	DLD	1NN	3NN	NC	SVM
081404A_M-2d-R	MR	3016	YES	YES	YES	YES	YES	YES
081404A_M-3d-R	MR	3073	YES	YES	YES	YES	YES	YES
100404A-01_M2dR-A	MR	2381	YES	YES	YES	YES	YES	YES
100404A-01_M2dR-B	MR	2386	YES	YES	YES	YES	YES	YES
100404A-01_M3dR-A	MR	2339	YES	YES	YES	YES	YES	YES
100404A-01_M3dR-B	MR	2372	YES	YES	YES	YES	YES	YES
040904A_UTP-R	UR	2800	YES	YES	YES	YES	YES	YES
050404A_UTP-R	UR	2630	YES	YES	YES	YES	YES	YES
050904A_UTP-R	UR	2712	YES	YES	YES	YES	YES	YES
081404A_UTP-3d-R	UR	2398	YES	YES	YES	YES	YES	YES
091504A-01_UTPR3d	UR	2697	YES	YES	YES	YES	YES	YES
092304A-01_UTP3dR	UR	2777	YES	YES	YES	YES	YES	YES
Mean percentof correct classification:			100	100	100	100	100	100

BRB array tools cross validation identified no arrays that failed any of the prediction tests. Classification method abbreviations: compound covariat predictor (CCP), diagonal linear discriminant (DLD), 1-nearest neighbor (1-NN), 3-nearest neighbors (3-NN), nearest centroid (NC), support vector machines (SVM).

Table C-4. Cross validation of 8117/43 Vs mock at 2 days PI.

Array id	Class label	Genes/ classifier	CCP	DLD	1NN	3-NN	NC	SVM
081404A_81-2d-R	81 2d R	193	NO	NO	NO	NO	NO	NO
091504A-01_81R 2d	81 2d R	11	YES	NO	YES	YES	YES	YES
092304A-01_812d-R	81 2d R	16	YES	NO	YES	YES	YES	YES
081404A_M-2d-R	M 2d R	40	NO	NO	NO	NO	NO	NO
100404A-01_M2dR-A	M 2d R	8	YES	NO	YES	YES	YES	YES
100404A-01_M2dR-B	M 2d R	13	YES	YES	YES	YES	YES	YES
Mean percentof correct classification:			67	17	67	67	67	67

BRB array tools cross validation with the 081404A_81-2d-R outlier. Classification method abbreviations: compound covariat predictor (CCP), diagonal linear discriminant (DLD), 1-nearest neighbor (1-NN), 3-nearest neighbors (3-NN), nearest centroid (NC), support vector machines (SVM).

Table C-5. Cross validation of 8117/43 Vs mock at 2 days PI.

Array id	Class label	Genes/ classifier	CCP	DLD	1NN	3-NN	NC	SVM
091504A-01_81R 2d	81 2d R	169	YES	YES	YES	NO	YES	YES
092304A-01_812d-R	81 2d R	125	YES	YES	YES	NO	YES	YES
081404A_M-2d-R	M 2d R	169	YES	YES	YES	YES	YES	YES
100404A-01_M2dR-A	M 2d R	151	YES	YES	YES	YES	YES	YES
100404A-01_M2dR-B	M 2d R	141	YES	YES	YES	YES	YES	YES
Mean percentof correct classification			100	100	100	60	100	100

Cross validation without the outlier which was removed from the 8117/43 vs. mock analysis due to poor cross validation. Classification method abbreviations: compound covariat predictor (CCP), diagonal linear discriminant (DLD), 1-nearest neighbor (1-NN), 3-nearest neighbors (3-NN), nearest centroid (NC), support vector machines (SVM).

Table C-6. Cross validation of 8117/43 vs. mock at 3 days PI.

Array id	Class label	Genes/ classifier	CCP	DLD	1NN	3-NN	NC	SVM
040904A_18-R	81 3d R	954	YES	YES	YES	YES	YES	YES
050404A_81-R	81 3d R	1079	YES	YES	YES	YES	YES	YES
050904A_81-R	81 3d R	905	YES	YES	YES	YES	YES	YES
100404A-01_M3dR-A	M 3d R	815	YES	NO	YES	NO	YES	YES
100404A-01_M3dR-B	M 3d R	1021	YES	NO	YES	NO	YES	YES
Mean percentof correct classification			100	60	100	60	100	100

Removal of the mock outlier improves BRB array tools cross validation between the remaining arrays. Classification method abbreviations: compound covariat predictor (CCP), diagonal linear discriminant (DLD), 1-nearest neighbor (1-NN), 3-nearest neighbors (3-NN), nearest centroid (NC), support vector machines (SVM).arrays.

Table C-7. Molecular function (813dR v M3dR with mock outlier)

GO id	GO classification	Observed	Expected	Observed/Expected
30106	MHC class I receptor activity	16	0.40	39.87
42379	Chemokine receptor binding	8	0.36	22.00
8009	Chemokine activity	8	0.36	22.00
1664	G-protein-coupled receptor binding	8	0.46	17.24
3924	GTPase activity	8	0.88	9.11
4888	Transmembrane receptor activity	17	2.76	6.16
17111	Nucleoside-triphosphatase activity	9	1.86	4.85
5125	Cytokine activity	8	1.68	4.76
16462	Pyrophosphatase activity	9	1.91	4.72
16818	Hydrolase activity\, acting on acid anhydrides\, in phosphorus-containing anhydrides	9	1.96	4.60
16817	Hydrolase activity\, acting on acid anhydrides	9	1.97	4.57
4872	Receptor activity	35	9.38	3.73
4871	Signal transducer activity	45	14.48	3.11

Table C-8. Biological function (813dR v M3dR with mock outlier)

GO id	GO classification	Observed in	Expected in	Observed/Expected
19882	Antigen presentation	5	0.27	18.55
6955	Immune response	34	3.15	10.80
6952	Defense response	38	3.84	9.91
8285	Negative regulation of cell proliferation	5	0.55	9.07
9607	Response to biotic stimulus	39	4.37	8.92
50874	Organismal physiological process	38	7.00	5.43
50896	Response to stimulus	41	8.77	4.67
42127	Regulation of cell proliferation	5	1.42	3.52

Table C-9. Molecular Function (813dR v M3dR without mock outlier)

GO id	GO classification	Observed	Expected	Observed/Expected
30106	MHC class I receptor activity	20	3.03	6.60
4879	Ligand-dependent nuclear receptor activity	5	0.85	5.87
3707	Steroid hormone receptor activity	5	0.85	5.87
42379	Chemokine receptor binding	10	2.75	3.64
8009	Chemokine activity	10	2.75	3.64
1664	G-protein-coupled receptor binding	12	3.50	3.43
19955	Cytokine binding	6	1.80	3.34

Table C-10. Biological Process (813dR v M3dR without mock outlier)

GO id	GO classification	Observed	Expected	Observed/Expected
30316	Osteoclast differentiation	6	1.39	4.33
19882	Antigen presentation	8	2.03	3.93
45670	Regulation of osteoclast differentiation	5	1.29	3.86
30224	Monocyte differentiation	6	1.57	3.82
45655	Regulation of monocyte differentiation	5	1.39	3.61
6471	Protein amino acid ADP-ribosylation	8	2.22	3.61
6826	Iron ion transport	5	1.48	3.38

Molecular (Tables C-7,C-9) and biological functions (Tables C-8, C-10) are similar with (Tables C-8,C-9) or without (Tables C-9,C-10) the mock outlier being included. The array was not removed from any analysis.

Table C-11. Cross validation of HSVlacZgC Vs mock comparisons.

Array id	Class label	Genes/ classifier	CCP	DLD	1NN	3-NN	NC	SVM
081404A_M-2d-R	M 2d R	2215	YES	YES	YES	YES	YES	YES
100404A-01_M2dR-A	M 2d R	517	YES	YES	YES	YES	YES	YES
100404A-01_M2dR-B	M 2d R	540	YES	YES	YES	YES	YES	YES
040904A_UTP-R	U 2d R	604	YES	YES	YES	YES	YES	YES
050404A_UTP-R	U 2d R	556	YES	YES	YES	YES	YES	YES
050904A_UTP-R	U 2d R	636	YES	YES	YES	YES	YES	YES
Mean percent of correct classification			100	100	100	100	100	100

U2d v M2d had 930 significant genes and cross validation was perfect Classification method abbreviations: compound covariat predictor (CCP), diagonal linear discriminant (DLD), 1-nearest neighbor (1-NN), 3-nearest neighbors (3-NN), nearest centroid (NC), support vector machines (SVM)..

Table C-12. Cross validation of HSVlacZgC Vs mock comparisons.

Array id	Class label	Genes/ classifier	CCP	DLD	1NN	3-NN	NC	SVM
081404A_M-3d-R	M 3d R	1008	YES	YES	YES	YES	YES	YES
100404A-01_M3dR-A	M 3d R	711	YES	YES	YES	YES	YES	YES
100404A-01_M3dR-B	M 3d R	759	YES	YES	YES	YES	YES	YES
081404A_UTP-3d-R	U 3d R	822	YES	YES	YES	YES	YES	YES
091504A-01_UTPR 3d	U 3d R	764	YES	YES	YES	YES	YES	YES
092304A-01_UTP3d-R	U 3d R	714	YES	YES	YES	YES	YES	YES

Array id	Class label	Genes/ classifier	CCP	DLD	1NN	3-NN	NC	SVM
Mean percentof correct classification:			100	100	100	100	100	100

U3d v M3d had 1204 significant genes and cross validation was perfect. Classification method abbreviations: compound covariat predictor (CCP), diagonal linear discriminant (DLD), 1-nearest neighbor (1-NN), 3-nearest neighbors (3-NN), nearest centroid (NC), support vector machines (SVM).

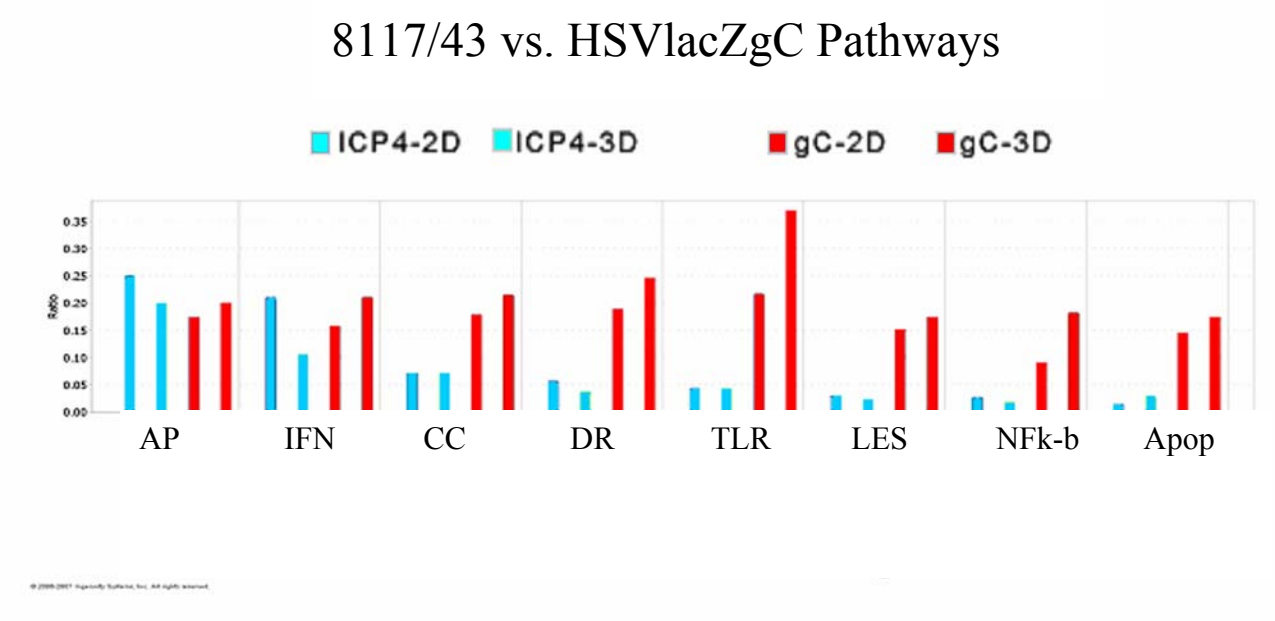

Figure C-4. Ratio of significant genes in the 8117/43 vs. HSVlacZgC comparison. The number of genes in the data set belonging to a pathway divided by the total number of genes in that pathway is represented as a ratio. Selected pathways are antigen presentation (AP), interferon signaling (IFN), chemokine signaling (CC), death receptor signaling (DR), toll-like receptor signaling (TLR), leukocyte extravasation (LES), NFk-b signaling (NFk-b), and apoptosis signaling (Apop). Analysis and figure generation were performed using Ingenuity Pathway Analysis with permission (Ingenuity® Systems, www.ingenuity.com).

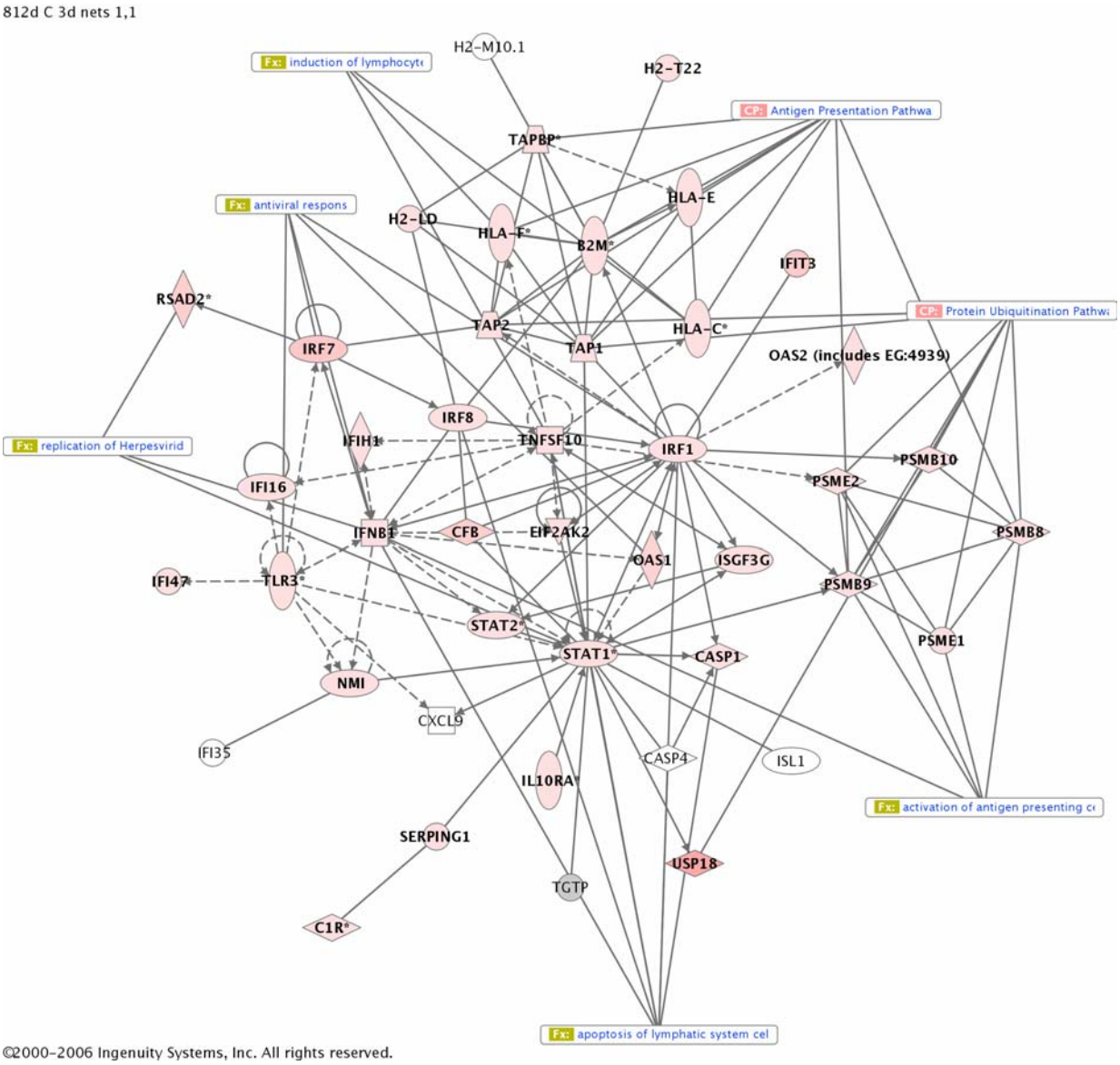

Figure C-5. Ingenuity pathway analysis networks from 2 day and 3 day time points for 8117/43 vs. mock were merged. Major nodes and selected biological functions and conical pathways are shown. Analysis and figure generation were performed using Ingenuity Pathway Analysis with permission (Ingenuity® Systems, www.ingenuity.com).

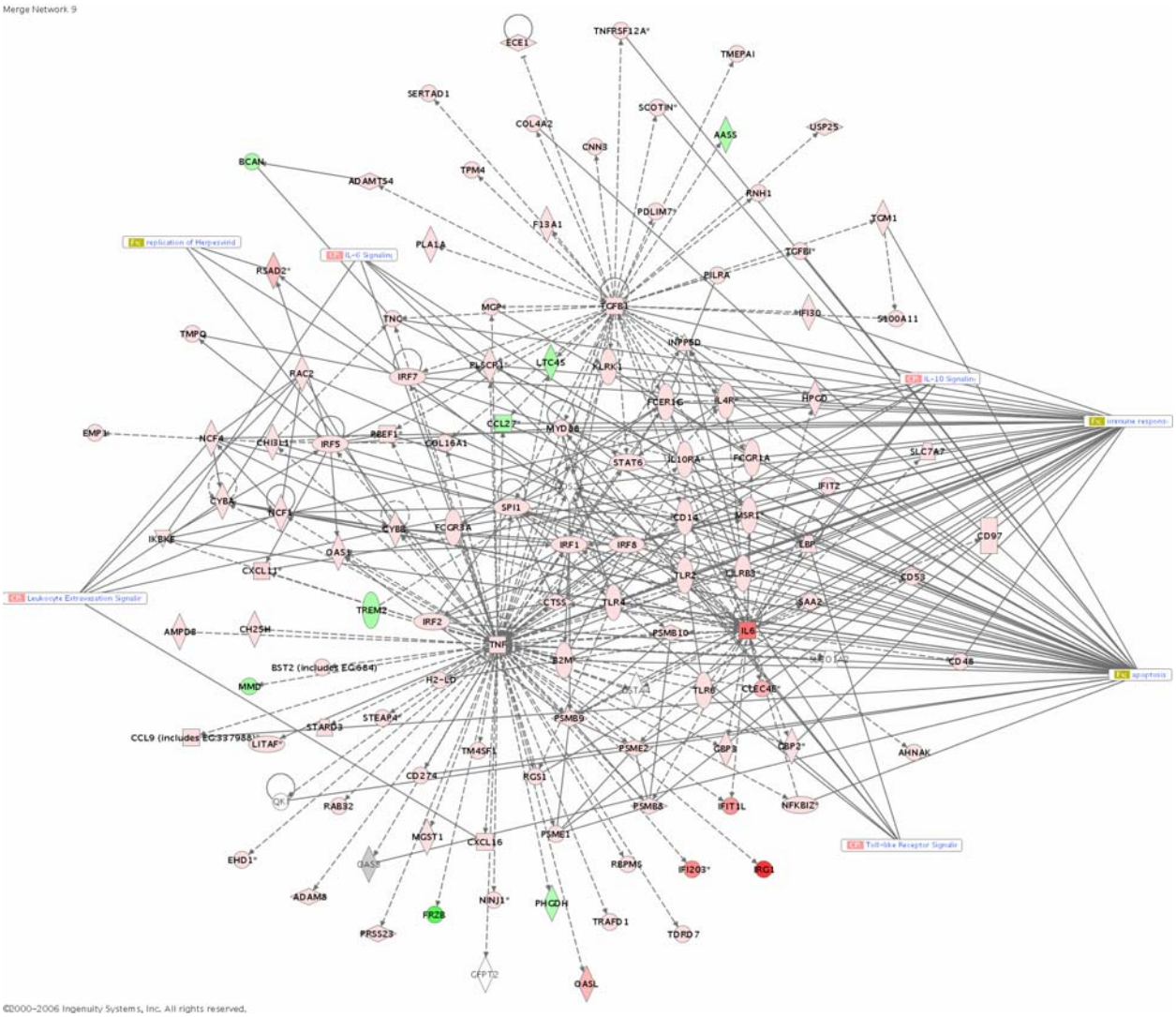

Figure C-6. Ingenuity pathway analysis networks from 2 day and 3 day time points for HSVlacZgC vs. mock were merged. Major nodes and selected biological functions and conical pathways are shown. Analysis and figure generation were performed using Ingenuity Pathway Analysis with permission (Ingenuity® Systems, www.ingenuity.com).

LIST OF REFERENCES

Aguilar JS, Ghazal P, Wagner EK (2005) Design of a herpes simplex virus type 2 long oligonucleotide-based microarray: global analysis of HSV-2 transcript abundance during productive infection. Methods Mol Biol 292:423-448.

Aguilar JS, Devi-Rao GV, Rice MK, Sunabe J, Ghazal P, Wagner EK (2006) Quantitative comparison of the HSV-1 and HSV-2 transcriptomes using DNA microarray analysis. Virology 348:233-241.

Amelio AL, McAnany PK, Bloom DC (2006a) A chromatin insulator-like element in the herpes simplex virus type 1 latency-associated transcript region binds CCCTC-binding factor and displays enhancer-blocking and silencing activities. J Virol 80:2358-2368.

Amelio AL, Giordani NV, Kubat NJ, O'Neil J E, Bloom DC (2006b) Deacetylation of the herpes simplex virus type 1 latency-associated transcript (LAT) enhancer and a decrease in LAT abundance precede an increase in ICP0 transcriptional permissiveness at early times postexplant. J Virol 80:2063-2068.

Amici C, Belardo G, Rossi A, Santoro MG (2001) Activation of I kappa b kinase by herpes simplex virus type 1. A novel target for anti-herpetic therapy. J Biol Chem 276:28759-28766.

Ashley CT, Jr., Wilkinson KD, Reines D, Warren ST (1993) FMR1 protein: conserved RNP family domains and selective RNA binding. Science 262:563-566.

Bagni C, Greenough WT (2005) From mRNP trafficking to spine dysmorphogenesis: the roots of fragile X syndrome. Nat Rev Neurosci 6:376-387.

Bear MF, Huber KM, Warren ST (2004) The mGluR theory of fragile X mental retardation. Trends Neurosci 27:370-377.

Berns KI, Giraud C (1996) Biology of adeno-associated virus. Curr Top Microbiol Immunol 218:1-23.

Bloom DC, Jarman RG (1998) Generation and use of recombinant reporter viruses for study of herpes simplex virus infections in vivo. Methods 16:117-125.

Bloom DC, Lokensgard JR, Maidment NT, Feldman LT, Stevens JG (1994) Long-term expression of genes in vivo using non-replicating HSV vectors. Gene Ther 1 Suppl 1:S36-38.

Bloom DC, Maidment NT, Tan A, Dissette VB, Feldman LT, Stevens JG (1995) Long-term expression of a reporter gene from latent herpes simplex virus in the rat hippocampus. Brain Res Mol Brain Res 31:48-60.

Bowers WJ, Olschowka JA, Federoff HJ (2003) Immune responses to replication-defective HSV-1 type vectors within the CNS: implications for gene therapy. Gene Ther 10:941-945.

Broberg EK, Hukkanen V (2005) Immune response to herpes simplex virus and gamma134.5 deleted HSV vectors. Curr Gene Ther 5:523-530.

Brown V, Small K, Lakkis L, Feng Y, Gunter C, Wilkinson KD, Warren ST (1998) Purified recombinant Fmrp exhibits selective RNA binding as an intrinsic property of the fragile X mental retardation protein. J Biol Chem 273:15521-15527.

Brown V, Jin P, Ceman S, Darnell JC, O'Donnell WT, Tenenbaum SA, Jin X, Feng Y, Wilkinson KD, Keene JD, Darnell RB, Warren ST (2001) Microarray identification of FMRP-associated brain mRNAs and altered mRNA translational profiles in fragile X syndrome. Cell 107:477-487.

Brukman A, Enquist LW (2006) Suppression of the interferon-mediated innate immune response by pseudorabies virus. J Virol 80:6345-6356.

Burger C, Nash K, Mandel RJ (2005a) Recombinant adeno-associated viral vectors in the nervous system. Hum Gene Ther 16:781-791.

Burger C, Nguyen FN, Deng J, Mandel RJ (2005b) Systemic mannitol-induced hyperosmolality amplifies rAAV2-mediated striatal transduction to a greater extent than local co-infusion. Mol Ther 11:327-331.

Burger C, Gorbatyuk OS, Velardo MJ, Peden CS, Williams P, Zolotukhin S, Reier PJ, Mandel RJ, Muzyczka N (2004) Recombinant AAV viral vectors pseudotyped with viral capsids from serotypes 1, 2, and 5 display differential efficiency and cell tropism after delivery to different regions of the central nervous system. Mol Ther 10:302-317.

Burton EA, Fink DJ, Glorioso JC (2002) Gene delivery using herpes simplex virus vectors. DNA Cell Biol 21:915-936.

Burton EA, Fink DJ, Glorioso JC (2005) Replication-defective genomic HSV gene therapy vectors: design, production and CNS applications. Curr Opin Mol Ther 7:326-336.

Calvano SE, Xiao W, Richards DR, Felciano RM, Baker HV, Cho RJ, Chen RO, Brownstein BH, Cobb JP, Tschoeke SK, Miller-Graziano C, Moldawer LL, Mindrinos MN, Davis RW, Tompkins RG, Lowry SF (2005) A network-based analysis of systemic inflammation in humans. Nature 437:1032-1037.

Chen L, Toth M (2001) Fragile X mice develop sensory hyperreactivity to auditory stimuli. Neuroscience 103:1043-1050.

Chou J, Kern ER, Whitley RJ, Roizman B (1990) Mapping of herpes simplex virus-1 neurovirulence to gamma 134.5, a gene nonessential for growth in culture. Science 250:1262-1266.

Coffee B, Zhang F, Warren ST, Reines D (1999) Acetylated histones are associated with FMR1 in normal but not fragile X-syndrome cells. Nat Genet 22:98-101.

Comery TA, Harris JB, Willems PJ, Oostra BA, Irwin SA, Weiler IJ, Greenough WT (1997) Abnormal dendritic spines in fragile X knockout mice: maturation and pruning deficits. Proc Natl Acad Sci U S A 94:5401-5404.

Costantini LC, Bakowska JC, Breakefield XO, Isacson O (2000) Gene therapy in the CNS. Gene Ther 7:93-109.

Crawford DC, Acuna JM, Sherman SL (2001) FMR1 and the fragile X syndrome: human genome epidemiology review. Genet Med 3:359-371.

D'Agata V, Warren ST, Zhao W, Torre ER, Alkon DL, Cavallaro S (2002) Gene expression profiles in a transgenic animal model of fragile X syndrome. Neurobiol Dis 10:211-218.

D-B-C (1994) Fmr1 knockout mice: a model to study fragile X mental retardation. The Dutch-Belgian Fragile X Consortium. Cell 78:23-33.

Darnell JC, Mostovetsky O, Darnell RB (2005) FMRP RNA targets: identification and validation. Genes Brain Behav 4:341-349.

Darnell JC, Jensen KB, Jin P, Brown V, Warren ST, Darnell RB (2001) Fragile X mental retardation protein targets G quartet mRNAs important for neuronal function. Cell 107:489-499.

De Boulle K, Verkerk AJ, Reyniers E, Vits L, Hendrickx J, Van Roy B, Van den Bos F, de Graaff E, Oostra BA, Willems PJ (1993) A point mutation in the FMR-1 gene associated with fragile X mental retardation. Nat Genet 3:31-35.

DeLuca NA, McCarthy AM, Schaffer PA (1985) Isolation and characterization of deletion mutants of herpes simplex virus type 1 in the gene encoding immediate-early regulatory protein ICP4. J Virol 56:558-570.

Denman RB, Sung YJ (2002) Species-specific and isoform-specific RNA binding of human and mouse fragile X mental retardation proteins. Biochem Biophys Res Commun 292:1063-1069.

Devys D, Lutz Y, Rouyer N, Bellocq JP, Mandel JL (1993) The FMR-1 protein is cytoplasmic, most abundant in neurons and appears normal in carriers of a fragile X premutation. Nat Genet 4:335-340.

Dobson AT, Margolis TP, Sedarati F, Stevens JG, Feldman LT (1990) A latent, nonpathogenic HSV-1-derived vector stably expresses beta-galactosidase in mouse neurons. Neuron 5:353-360.

Doll RF, Crandall JE, Dyer CA, Aucoin JM, Smith FI (1996) Comparison of promoter strengths on gene delivery into mammalian brain cells using AAV vectors. Gene Ther 3:437-447.

Dong JY, Fan PD, Frizzell RA (1996) Quantitative analysis of the packaging capacity of recombinant adeno-associated virus. Hum Gene Ther 7:2101-2112.

Dumas T, McLaughlin J, Ho D, Meier T, Sapolsky R (1999) Delivery of herpes simplex virus amplicon-based vectors to the dentate gyrus does not alter hippocampal synaptic transmission in vivo. Gene Ther 6:1679-1684.

Eidson KM, Hobbs WE, Manning BJ, Carlson P, DeLuca NA (2002) Expression of herpes simplex virus ICP0 inhibits the induction of interferon-stimulated genes by viral infection. J Virol 76:2180-2191.

El-Osta A (2002) FMR1 silencing and the signals to chromatin: a unified model of transcriptional regulation. Biochem Biophys Res Commun 295:575-581.

El Idrissi A, Ding XH, Scalia J, Trenkner E, Brown WT, Dobkin C (2005) Decreased GABA(A) receptor expression in the seizure-prone fragile X mouse. Neurosci Lett 377:141-146.

Faingold CL (2002) Role of GABA abnormalities in the inferior colliculus pathophysiology - audiogenic seizures. Hear Res 168:223-237.

Faingold CL, Marcinczyk MJ, Casebeer DJ, Randall ME, Arneric SP, Browning RA (1994) GABA in the inferior colliculus plays a critical role in control of audiogenic seizures. Brain Res 640:40-47.

Farrell MJ, Dobson AT, Feldman LT (1991) Herpes simplex virus latency-associated transcript is a stable intron. Proc Natl Acad Sci U S A 88:790-794.

Feng Y, Absher D, Eberhart DE, Brown V, Malter HE, Warren ST (1997a) FMRP associates with polyribosomes as an mRNP, and the I304N mutation of severe fragile X syndrome abolishes this association. Mol Cell 1:109-118.

Feng Y, Gutekunst CA, Eberhart DE, Yi H, Warren ST, Hersch SM (1997b) Fragile X mental retardation protein: nucleocytoplasmic shuttling and association with somatodendritic ribosomes. J Neurosci 17:1539-1547.

Fields BN, Knipe DM, Howley PM, Griffin DE (2001) Fields' virology, 4th Edition. Philadelphia: Lippincott Williams & Wilkins.

Frommer M, McDonald LE, Millar DS, Collis CM, Watt F, Grigg GW, Molloy PL, Paul CL (1992) A genomic sequencing protocol that yields a positive display of 5-methylcytosine residues in individual DNA strands. Proc Natl Acad Sci U S A 89:1827-1831.

Galvez R, Greenough WT (2005) Sequence of abnormal dendritic spine development in primary somatosensory cortex of a mouse model of the fragile X mental retardation syndrome. Am J Med Genet A 135:155-160.

Gantois I, Bakker CE, Reyniers E, Willemsen R, D'Hooge R, De Deyn PP, Oostra BA, Kooy RF (2001) Restoring the phenotype of fragile X syndrome: insight from the mouse model. Curr Mol Med 1:447-455.

Garcia-Cairasco N (2002) A critical review on the participation of inferior colliculus in acoustic-motor and acoustic-limbic networks involved in the expression of acute and kindled audiogenic seizures. Hear Res 168:208-222.

Goodkin ML, Ting AT, Blaho JA (2003) NF-kappaB is required for apoptosis prevention during herpes simplex virus type 1 infection. J Virol 77:7261-7280.

Goodkin ML, Morton ER, Blaho JA (2004) Herpes simplex virus infection and apoptosis. Int Rev Immunol 23:141-172.

Gordenin DA, Kunkel TA, Resnick MA (1997) Repeat expansion--all in a flap? Nat Genet 16:116-118.

Graham FL, Smiley J, Russell WC, Nairn R (1977) Characteristics of a human cell line transformed by DNA from human adenovirus type 5. J Gen Virol 36:59-74.

Greenough WT, Volkmar FR, Juraska JM (1973) Effects of rearing complexity on dendritic branching in frontolateral and temporal cortex of the rat. Exp Neurol 41:371-378.

Greenough WT, Klintsova AY, Irwin SA, Galvez R, Bates KE, Weiler IJ (2001) Synaptic regulation of protein synthesis and the fragile X protein. Proc Natl Acad Sci U S A 98:7101-7106.

Grimm D, Kern A, Rittner K, Kleinschmidt JA (1998) Novel tools for production and purification of recombinant adenoassociated virus vectors. Hum Gene Ther 9:2745-2760.

Grossman AW, Elisseou NM, McKinney BC, Greenough WT (2006) Hippocampal pyramidal cells in adult Fmr1 knockout mice exhibit an immature-appearing profile of dendritic spines. Brain Res 1084:158-164.

Hagerman RJ, Hagerman PJ (2002) The fragile X premutation: into the phenotypic fold. Curr Opin Genet Dev 12:278-283.

Hauswirth WW, Lewin AS, Zolotukhin S, Muzyczka N (2000) Production and purification of recombinant adeno-associated virus. Methods Enzymol 316:743-761.

Henricksen LA, Tom S, Liu Y, Bambara RA (2000) Inhibition of flap endonuclease 1 by flap secondary structure and relevance to repeat sequence expansion. J Biol Chem 275:16420-16427.

Higaki S, Gebhardt BM, Lukiw WJ, Thompson HW, Hill JM (2002) Effect of immunosuppression on gene expression in the HSV-1 latently infected mouse trigeminal ganglion. Invest Ophthalmol Vis Sci 43:1862-1869.

Hill JM, Lukiw WJ, Gebhardt BM, Higaki S, Loutsch JM, Myles ME, Thompson HW, Kwon BS, Bazan NG, Kaufman HE (2001) Gene expression analyzed by microarrays in HSV-1 latent mouse trigeminal ganglion following heat stress. Virus Genes 23:273-280.

Hinds HL, Ashley CT, Sutcliffe JS, Nelson DL, Warren ST, Housman DE, Schalling M (1993) Tissue specific expression of FMR-1 provides evidence for a functional role in fragile X syndrome. Nat Genet 3:36-43.

Ho DY, Fink SL, Lawrence MS, Meier TJ, Saydam TC, Dash R, Sapolsky RM (1995) Herpes simplex virus vector system: analysis of its in vivo and in vitro cytopathic effects. J Neurosci Methods 57:205-215.

Hou L, Antion MD, Hu D, Spencer CM, Paylor R, Klann E (2006) Dynamic translational and proteasomal regulation of fragile X mental retardation protein controls mGluR-dependent long-term depression. Neuron 51:441-454.

Huang T, Li LY, Shen Y, Qin XB, Pang ZL, Wu GY (1996) Alternative splicing of the FMR1 gene in human fetal brain neurons. Am J Med Genet 64:252-255.

Huber KM, Kayser MS, Bear MF (2000) Role for rapid dendritic protein synthesis in hippocampal mGluR-dependent long-term depression. Science 288:1254-1257.

Huber KM, Roder JC, Bear MF (2001) Chemical induction of mGluR5- and protein synthesis--dependent long-term depression in hippocampal area CA1. J Neurophysiol 86:321-325.

Huber KM, Gallagher SM, Warren ST, Bear MF (2002) Altered synaptic plasticity in a mouse model of fragile X mental retardation. Proc Natl Acad Sci U S A 99:7746-7750.

Irwin SA, Galvez R, Greenough WT (2000) Dendritic spine structural anomalies in fragile-X mental retardation syndrome. Cereb Cortex 10:1038-1044.

Irwin SA, Idupulapati M, Gilbert ME, Harris JB, Chakravarti AB, Rogers EJ, Crisostomo RA, Larsen BP, Mehta A, Alcantara CJ, Patel B, Swain RA, Weiler IJ, Oostra BA, Greenough WT (2002) Dendritic spine and dendritic field characteristics of layer V pyramidal neurons in the visual cortex of fragile-X knockout mice. Am J Med Genet 111:140-146.

Izumi KM, McKelvey AM, Devi-Rao G, Wagner EK, Stevens JG (1989) Molecular and biological characterization of a type 1 herpes simplex virus (HSV-1) specifically deleted for expression of the latency-associated transcript (LAT). Microb Pathog 7:121-134.

Jackson SA, DeLuca NA (2003) Relationship of herpes simplex virus genome configuration to productive and persistent infections. Proc Natl Acad Sci U S A 100:7871-7876.

Johnson PA, Wang MJ, Friedmann T (1994) Improved cell survival by the reduction of immediate-early gene expression in replication-defective mutants of herpes simplex virus type 1 but not by mutation of the virion host shutoff function. J Virol 68:6347-6362.

Johnson PA, Miyanohara A, Levine F, Cahill T, Friedmann T (1992) Cytotoxicity of a replication-defective mutant of herpes simplex virus type 1. J Virol 66:2952-2965.

Kaufmann WE, Reiss AL (1999) Molecular and cellular genetics of fragile X syndrome. Am J Med Genet 88:11-24.

Khodarev NN, Advani SJ, Gupta N, Roizman B, Weichselbaum RR (1999) Accumulation of specific RNAs encoding transcriptional factors and stress response proteins against a background of severe depletion of cellular RNAs in cells infected with herpes simplex virus 1. Proc Natl Acad Sci U S A 96:12062-12067.

Kijima H, Ishida H, Ohkawa T, Kashani-Sabet M, Scanlon KJ (1995) Therapeutic applications of ribozymes. Pharmacol Ther 68:247-267.

Kooy RF, Willemsen R, Oostra BA (2000) Fragile X syndrome at the turn of the century. Mol Med Today 6:193-198.

Kramer MF, Cook WJ, Roth FP, Zhu J, Holman H, Knipe DM, Coen DM (2003) Latent herpes simplex virus infection of sensory neurons alters neuronal gene expression. J Virol 77:9533-9541.

Kubat NJ, Tran RK, McAnany P, Bloom DC (2004) Specific histone tail modification and not DNA methylation is a determinant of herpes simplex virus type 1 latent gene expression. J Virol 78:1139-1149.

Kumari D, Usdin K (2001) Interaction of the transcription factors USF1, USF2, and alpha - Pal/Nrf-1 with the FMR1 promoter. Implications for Fragile X mental retardation syndrome. J Biol Chem 276:4357-4364.

Kurt-Jones EA, Chan M, Zhou S, Wang J, Reed G, Bronson R, Arnold MM, Knipe DM, Finberg RW (2004) Herpes simplex virus 1 interaction with Toll-like receptor 2 contributes to lethal encephalitis. Proc Natl Acad Sci U S A 101:1315-1320.

Li J, Samulski RJ, Xiao X (1997) Role for highly regulated rep gene expression in adeno-associated virus vector production. J Virol 71:5236-5243.

Li Z, Zhang Y, Ku L, Wilkinson KD, Warren ST, Feng Y (2001) The fragile X mental retardation protein inhibits translation via interacting with mRNA. Nucleic Acids Res 29:2276-2283.

Lilley CE, Groutsi F, Han Z, Palmer JA, Anderson PN, Latchman DS, Coffin RS (2001) Multiple immediate-early gene-deficient herpes simplex virus vectors allowing efficient gene delivery to neurons in culture and widespread gene delivery to the central nervous system in vivo. J Virol 75:4343-4356.

Lin R, Noyce RS, Collins SE, Everett RD, Mossman KL (2004) The herpes simplex virus ICP0 RING finger domain inhibits IRF3- and IRF7-mediated activation of interferon-stimulated genes. J Virol 78:1675-1684.

Lo WD, Qu G, Sferra TJ, Clark R, Chen R, Johnson PR (1999) Adeno-associated virus-mediated gene transfer to the brain: duration and modulation of expression. Hum Gene Ther 10:201-213.

Lokensgard JR, Berthomme H, Feldman LT (1997) The latency-associated promoter of herpes simplex virus type 1 requires a region downstream of the transcription start site for long-term expression during latency. J Virol 71:6714-6719.

Lokensgard JR, Bloom DC, Dobson AT, Feldman LT (1994) Long-term promoter activity during herpes simplex virus latency. J Virol 68:7148-7158.

Lowenstein PR (2002) Immunology of viral-vector-mediated gene transfer into the brain: an evolutionary and developmental perspective. Trends Immunol 23:23-30.

Lu R, Wang H, Liang Z, Ku L, O'Donnell W T, Li W, Warren ST, Feng Y (2004) The fragile X protein controls microtubule-associated protein 1B translation and microtubule stability in brain neuron development. Proc Natl Acad Sci U S A 101:15201-15206.

Mandel RJ, Burger C (2004) Clinical trials in neurological disorders using AAV vectors: promises and challenges. Curr Opin Mol Ther 6:482-490.

Mandel RJ, Manfredsson FP, Foust KD, Rising A, Reimsnider S, Nash K, Burger C (2006) Recombinant adeno-associated viral vectors as therapeutic agents to treat neurological disorders. Mol Ther 13:463-483.

Marconi P, Tamura M, Moriuchi S, Krisky DM, Niranjan A, Goins WF, Cohen JB, Glorioso JC (2000) Connexin 43-enhanced suicide gene therapy using herpesviral vectors. Mol Ther 1:71-81.

Markovitz NS, Baunoch D, Roizman B (1997) The range and distribution of murine central nervous system cells infected with the gamma(1)34.5- mutant of herpes simplex virus 1. J Virol 71:5560-5569.

Marques CP, Hu S, Sheng W, Lokensgard JR (2006) Microglial cells initiate vigorous yet non-protective immune responses during HSV-1 brain infection. Virus Res 121:1-10.

Marques CP, Hu S, Sheng W, Cheeran MC, Cox D, Lokensgard JR (2004) Interleukin-10 attenuates production of HSV-induced inflammatory mediators by human microglia. Glia 47:358-366.

Miyashiro KY, Beckel-Mitchener A, Purk TP, Becker KG, Barret T, Liu L, Carbonetto S, Weiler IJ, Greenough WT, Eberwine J (2003) RNA cargoes associating with FMRP reveal deficits in cellular functioning in Fmr1 null mice. Neuron 37:417-431.

Morris R (1984) Developments of a water-maze procedure for studying spatial learning in the rat. J Neurosci Methods 11:47-60.

Morris RG, Anderson E, Lynch GS, Baudry M (1986) Selective impairment of learning and blockade of long-term potentiation by an N-methyl-D-aspartate receptor antagonist, AP5. Nature 319:774-776.

Morrison LA (2004) The Toll of herpes simplex virus infection. Trends Microbiol 12:353-356.

Mossman K (2005) Analysis of anti-interferon properties of the herpes simplex virus type I ICP0 protein. Methods Mol Med 116:195-205.

Mossman KL, Ashkar AA (2005) Herpesviruses and the innate immune response. Viral Immunol 18:267-281.

Mossman KL, Macgregor PF, Rozmus JJ, Goryachev AB, Edwards AM, Smiley JR (2001) Herpes simplex virus triggers and then disarms a host antiviral response. J Virol 75:750-758.

Moutou C, Vincent MC, Biancalana V, Mandel JL (1997) Transition from premutation to full mutation in fragile X syndrome is likely to be prezygotic. Hum Mol Genet 6:971-979.

Musumeci SA, Hagerman RJ, Ferri R, Bosco P, Dalla Bernardina B, Tassinari CA, De Sarro GB, Elia M (1999) Epilepsy and EEG findings in males with fragile X syndrome. Epilepsia 40:1092-1099.

Musumeci SA, Bosco P, Calabrese G, Bakker C, De Sarro GB, Elia M, Ferri R, Oostra BA (2000) Audiogenic seizures susceptibility in transgenic mice with fragile X syndrome. Epilepsia 41:19-23.

Musumeci SA, Calabrese G, Bonaccorso CM, D'Antoni S, Brouwer JR, Bakker CE, Elia M, Ferri R, Nelson DL, Oostra BA, Catania MV (2007) Audiogenic seizure susceptibility is reduced in fragile X knockout mice after introduction of FMR1 transgenes. Exp Neurol 203:233-240.

Nielsen DM, Derber WJ, McClellan DA, Crnic LS (2002) Alterations in the auditory startle response in Fmr1 targeted mutant mouse models of fragile X syndrome. Brain Res 927:8-17.

Nimchinsky EA, Oberlander AM, Svoboda K (2001) Abnormal development of dendritic spines in FMR1 knock-out mice. J Neurosci 21:5139-5146.

Nosyreva ED, Huber KM (2005) Developmental switch in synaptic mechanisms of hippocampal metabotropic glutamate receptor-dependent long-term depression. J Neurosci 25:2992-3001.

Nosyreva ED, Huber KM (2006) Metabotropic receptor-dependent long-term depression persists in the absence of protein synthesis in the mouse model of fragile X syndrome. J Neurophysiol 95:3291-3295.

O'Donnell WT, Warren ST (2002) A decade of molecular studies of fragile X syndrome. Annu Rev Neurosci 25:315-338.

Olschowka JA, Bowers WJ, Hurley SD, Mastrangelo MA, Federoff HJ (2003) Helper-free HSV-1 amplicons elicit a markedly less robust innate immune response in the CNS. Mol Ther 7:218-227.

Oostra BA, Willemsen R (2001) Diagnostic tests for fragile X syndrome. Expert Rev Mol Diagn 1:226-232.

Oostra BA, Willemsen R (2003) A fragile balance: FMR1 expression levels. Hum Mol Genet 12 Spec No 2:R249-257.

Pasieka TJ, Baas T, Carter VS, Proll SC, Katze MG, Leib DA (2006) Functional genomic analysis of herpes simplex virus type 1 counteraction of the host innate response. J Virol 80:7600-7612.

Paulus C, Sollars PJ, Pickard GE, Enquist LW (2006) Transcriptome signature of virulent and attenuated pseudorabies virus-infected rodent brain. J Virol 80:1773-1786.

Peden CS, Burger C, Muzyczka N, Mandel RJ (2004) Circulating anti-wild-type adeno-associated virus type 2 (AAV2) antibodies inhibit recombinant AAV2 (rAAV2)-mediated, but not rAAV5-mediated, gene transfer in the brain. J Virol 78:6344-6359.

Peier AM, McIlwain KL, Kenneson A, Warren ST, Paylor R, Nelson DL (2000) (Over)correction of FMR1 deficiency with YAC transgenics: behavioral and physical features. Hum Mol Genet 9:1145-1159.

Peterson PK, Remington JS (2000) New concepts in the immunopathogenesis of CNS infections. Malden, Mass.: Blackwell Science.

Pfeiffer BE, Huber KM (2006) Current advances in local protein synthesis and synaptic plasticity. J Neurosci 26:7147-7150.

Pieretti M, Zhang FP, Fu YH, Warren ST, Oostra BA, Caskey CT, Nelson DL (1991) Absence of expression of the FMR-1 gene in fragile X syndrome. Cell 66:817-822.

Premont RT, Gainetdinov RR (2007) Physiological roles of G protein-coupled receptor kinases and arrestins. Annu Rev Physiol 69:511-534.

Price J, Turner D, Cepko C (1987) Lineage analysis in the vertebrate nervous system by retrovirus-mediated gene transfer. Proc Natl Acad Sci U S A 84:156-160.

Puskovic V, Wolfe D, Goss J, Huang S, Mata M, Glorioso JC, Fink DJ (2004) Prolonged biologically active transgene expression driven by HSV LAP2 in brain in vivo. Mol Ther 10:67-75.

Rattazzi MC, LaFauci G, Brown WT (2004) Prospects for gene therapy in the fragile X syndrome. Ment Retard Dev Disabil Res Rev 10:75-81.

Restivo L, Ferrari F, Passino E, Sgobio C, Bock J, Oostra BA, Bagni C, Ammassari-Teule M (2005) Enriched environment promotes behavioral and morphological recovery in a mouse model for the fragile X syndrome. Proc Natl Acad Sci U S A 102:11557-11562.

Ross KC, Coleman JR (2000) Developmental and genetic audiogenic seizure models: behavior and biological substrates. Neurosci Biobehav Rev 24:639-653.

Rousseau F, Heitz D, Biancalana V, Blumenfeld S, Kretz C, Boue J, Tommerup N, Van Der Hagen C, DeLozier-Blanchet C, Croquette MF, et al. (1991) Direct diagnosis by DNA analysis of the fragile X syndrome of mental retardation. N Engl J Med 325:1673-1681.

Rudelli RD, Brown WT, Wisniewski K, Jenkins EC, Laure-Kamionowska M, Connell F, Wisniewski HM (1985) Adult fragile X syndrome. Clinico-neuropathologic findings. Acta Neuropathol (Berl) 67:289-295.

Ryther RC, Flynt AS, Phillips JA, 3rd, Patton JG (2005) siRNA therapeutics: big potential from small RNAs. Gene Ther 12:5-11.

Samaniego LA, Neiderhiser L, DeLuca NA (1998) Persistence and expression of the herpes simplex virus genome in the absence of immediate-early proteins. J Virol 72:3307-3320.

Samulski RJ, Chang LS, Shenk T (1987) A recombinant plasmid from which an infectious adeno-associated virus genome can be excised in vitro and its use to study viral replication. J Virol 61:3096-3101.

Sandri-Goldin RM (2006) Alpha herpesviruses : molecular and cellular biology. Wymondham: Caister Academic.

Scarpini CG, May J, Lachmann RH, Preston CM, Dunnett SB, Torres EM, Efstathiou S (2001) Latency associated promoter transgene expression in the central nervous system after stereotaxic delivery of replication-defective HSV-1-based vectors. Gene Ther 8:1057-1071.

Schaeffer C, Bardoni B, Mandel JL, Ehresmann B, Ehresmann C, Moine H (2001) The fragile X mental retardation protein binds specifically to its mRNA via a purine quartet motif. Embo J 20:4803-4813.

Singh J, Wagner EK (1995) Herpes simplex virus recombination vectors designed to allow insertion of modified promoters into transcriptionally "neutral" segments of the viral genome. Virus Genes 10:127-136.

Snyder EM, Philpot BD, Huber KM, Dong X, Fallon JR, Bear MF (2001) Internalization of ionotropic glutamate receptors in response to mGluR activation. Nat Neurosci 4:1079-1085.

Spencer CA, Dahmus ME, Rice SA (1997) Repression of host RNA polymerase II transcription by herpes simplex virus type 1. J Virol 71:2031-2040.

Stevens JG, Wagner EK, Devi-Rao GB, Cook ML, Feldman LT (1987) RNA complementary to a herpesvirus alpha gene mRNA is prominent in latently infected neurons. Science 235:1056-1059.

Steward O, Schuman EM (2001) Protein synthesis at synaptic sites on dendrites. Annu Rev Neurosci 24:299-325.

Stingley SW, Ramirez JJ, Aguilar SA, Simmen K, Sandri-Goldin RM, Ghazal P, Wagner EK (2000) Global analysis of herpes simplex virus type 1 transcription using an oligonucleotide-based DNA microarray. J Virol 74:9916-9927.

Sun A, Devi-Rao GV, Rice MK, Gary LW, Bloom DC, Sandri-Goldin RM, Ghazal P, Wagner EK (2004) Immediate-early expression of the herpes simplex virus type 1 ICP27 transcript is not critical for efficient replication in vitro or in vivo. J Virol 78:10470-10478.

Sutton MA, Schuman EM (2005) Local translational control in dendrites and its role in long-term synaptic plasticity. J Neurobiol 64:116-131.

Tabbaa S, Corso TD, Jenkins L, Tran RK, Bloom DC, Stachowiak MK (2005) In vivo gene transfer to the brain cortex using a single injection of HSV-1 vector into the medial septum. Folia Morphol (Warsz) 64:273-281.

Taddeo B, Esclatine A, Roizman B (2002) The patterns of accumulation of cellular RNAs in cells infected with a wild-type and a mutant herpes simplex virus 1 lacking the virion host shutoff gene. Proc Natl Acad Sci U S A 99:17031-17036.

Taddeo B, Luo TR, Zhang W, Roizman B (2003) Activation of NF-kappaB in cells productively infected with HSV-1 depends on activated protein kinase R and plays no apparent role in blocking apoptosis. Proc Natl Acad Sci U S A 100:12408-12413.

Taddeo B, Zhang W, Lakeman F, Roizman B (2004) Cells lacking NF-kappaB or in which NF-kappaB is not activated vary with respect to ability to sustain herpes simplex virus 1 replication and are not susceptible to apoptosis induced by a replication-incompetent mutant virus. J Virol 78:11615-11621.

Tamanini F, Bontekoe C, Bakker CE, van Unen L, Anar B, Willemsen R, Yoshida M, Galjaard H, Oostra BA, Hoogeveen AT (1999) Different targets for the fragile X-related proteins revealed by their distinct nuclear localizations. Hum Mol Genet 8:863-869.

Teng J, Takei Y, Harada A, Nakata T, Chen J, Hirokawa N (2001) Synergistic effects of MAP2 and MAP1B knockout in neuronal migration, dendritic outgrowth, and microtubule organization. J Cell Biol 155:65-76.

Thomas SK, Lilley CE, Latchman DS, Coffin RS (2002) A protein encoded by the herpes simplex virus (HSV) type 1 2-kilobase latency-associated transcript is phosphorylated, localized to the nucleus, and overcomes the repression of expression from exogenous promoters when inserted into the quiescent HSV genome. J Virol 76:4056-4067.

Tsavachidou D, Podrzucki W, Seykora J, Berger SL (2001) Gene array analysis reveals changes in peripheral nervous system gene expression following stimuli that result in reactivation of latent herpes simplex virus type 1: induction of transcription factor Bcl-3. J Virol 75:9909-9917.

Turner AM, Greenough WT (1985) Differential rearing effects on rat visual cortex synapses. I. Synaptic and neuronal density and synapses per neuron. Brain Res 329:195-203.

Verkerk AJ, Pieretti M, Sutcliffe JS, Fu YH, Kuhl DP, Pizzuti A, Reiner O, Richards S, Victoria MF, Zhang FP, et al. (1991) Identification of a gene (FMR-1) containing a CGG repeat coincident with a breakpoint cluster region exhibiting length variation in fragile X syndrome. Cell 65:905-914.

Wagner EK, Bloom DC (1997) Experimental investigation of herpes simplex virus latency. Clin Microbiol Rev 10:419-443.

Wagner EK, Ramirez JJ, Stingley SW, Aguilar SA, Buehler L, Devi-Rao GB, Ghazal P (2002) Practical approaches to long oligonucleotide-based DNA microarray: lessons from herpesviruses. Prog Nucleic Acid Res Mol Biol 71:445-491.

Weiler IJ, Greenough WT (1993) Metabotropic glutamate receptors trigger postsynaptic protein synthesis. Proc Natl Acad Sci U S A 90:7168-7171.

Weiler IJ, Greenough WT (1999) Synaptic synthesis of the Fragile X protein: possible involvement in synapse maturation and elimination. Am J Med Genet 83:248-252.

Weiler IJ, Irwin SA, Klintsova AY, Spencer CM, Brazelton AD, Miyashiro K, Comery TA, Patel B, Eberwine J, Greenough WT (1997) Fragile X mental retardation protein is translated near synapses in response to neurotransmitter activation. Proc Natl Acad Sci U S A 94:5395-5400.

Wolfe D, Goins WF, Yamada M, Moriuchi S, Krisky DM, Oligino TJ, Marconi PC, Fink DJ, Glorioso JC (1999) Engineering herpes simplex virus vectors for CNS applications. Exp Neurol 159:34-46.

Wood MJ, Byrnes AP, Kaplitt MG, Pfaff DW, Rabkin SD, Charlton HM (1994) Specific patterns of defective HSV-1 gene transfer in the adult central nervous system: implications for gene targeting. Exp Neurol 130:127-140.

Xu R, Janson CG, Mastakov M, Lawlor P, Young D, Mouravlev A, Fitzsimons H, Choi KL, Ma H, Dragunow M, Leone P, Chen Q, Dicker B, During MJ (2001) Quantitative comparison of expression with adeno-associated virus (AAV-2) brain-specific gene cassettes. Gene Ther 8:1323-1332.

Yan QJ, Rammal M, Tranfaglia M, Bauchwitz RP (2005) Suppression of two major Fragile X Syndrome mouse model phenotypes by the mGluR5 antagonist MPEP. Neuropharmacology 49:1053-1066.

Yan QJ, Asafo-Adjei PK, Arnold HM, Brown RE, Bauchwitz RP (2004) A phenotypic and molecular characterization of the fmr1-tm1Cgr fragile X mouse. Genes Brain Behav 3:337-359.

Yang WC, Devi-Rao GV, Ghazal P, Wagner EK, Triezenberg SJ (2002) General and specific alterations in programming of global viral gene expression during infection by VP16 activation-deficient mutants of herpes simplex virus type 1. J Virol 76:12758-12774.

Zhang YQ, Bailey AM, Matthies HJ, Renden RB, Smith MA, Speese SD, Rubin GM, Broadie K (2001) Drosophila fragile X-related gene regulates the MAP1B homolog Futsch to control synaptic structure and function. Cell 107:591-603.

Zolotukhin S, Potter M, Hauswirth WW, Guy J, Muzyczka N (1996) A "humanized" green fluorescent protein cDNA adapted for high-level expression in mammalian cells. J Virol 70:4646-4654.

Zolotukhin S, Byrne BJ, Mason E, Zolotukhin I, Potter M, Chesnut K, Summerford C, Samulski RJ, Muzyczka N (1999) Recombinant adeno-associated virus purification using novel methods improves infectious titer and yield. Gene Ther 6:973-985.

Zolotukhin S, Potter M, Zolotukhin I, Sakai Y, Loiler S, Fraites TJ, Jr., Chiodo VA, Phillipsberg T, Muzyczka N, Hauswirth WW, Flotte TR, Byrne BJ, Snyder RO (2002) Production and purification of serotype 1, 2, and 5 recombinant adeno-associated viral vectors. Methods 28:158-167.

BIOGRAPHICAL SKETCH

Zane Zeier was born in 1976 in Billings, Montana. Most of his childhood was spent working on his familie's ranch near the small agricultural town of Ryegate where he graduated high school in 1995 with only 5 classmates. During his secondary education Zane was an honor student and was bestowed academic awards in physics and chemistry, strongly influenced by his teacher in those subjects, Mr. David Bruner. Zane also received many athletic accolades and was captain of the track-and-field, basketball, and football teams, and was an avid band member. Capitalizing on academic scholarship and opportunity to participate in football and track-and-field, Zane attended the University of Mary, maintaining a high GPA. The following year he attended Montana State University-Bozeman to concentrate on academic achievement. His undergraduate research project examined the role of calcium-calmodulin kinase II in ischemic stroke, under the mentorship of Dr. Mike Babcock, department head of psychology. In 1999 Zane participated in a study abroad program attending the University of Lancaster in Lancashire, England. In 2000 Zane received two B.S. degrees for biochemistry and psychology from Montana State University-Bozeman. In the fall of the same year Zane enrolled at the University of Florida to pursue a Ph.D. in neuroscience, supported by an Alumni Fellowship Award. Under the mentorship of Dr. David C. Bloom, Zane has investigated the potential for gene therapy vectors to treat Fragile X syndrome. During his graduate career and in the spirit of interdisciplinary biomedical research, Zane met elective requirements for the department of Molecular Genetics and Microbiology and Neuroscience. Zane placed first in the department of Neuroscience Medical Guild research competition, and was a silver medalist in interdepartmental competition. In addition to his graduate work at the University of Florida, Zane has received awards for extreme sport film production, and motorcycle stunt riding.